PEOPLE'S DEMOCRATIC REPUBLIC OF ALGERIA

Ministry of Higher Education and Scientific Research

University of Amar Telidji – Laghouat

Faculty of Technology

Department of Electrical Engineering

PhD Thesis in Electrical Engineering

Discipline: Electrotechincal

Option: Modeling, Control and Identification of Electrical Machines

BENHAMIDA ISLAM

Predictive Control of a Permanent Magnet Synchronous Motor Supplied by a Three-Phase Inverter

Thesis defended on: 01/07/2021

Mrs	CHETTIH Saliha	*Jury President*	Prof	University of Amar Telidji – Laghouat
Mr	AMEUR Aissa	*Supervisor*	Prof	University of Amar Telidji – Laghouat
Mrs	KOUZI Katia	*Co-supervisor*	Prof	University of Amar Telidji – Laghouat
Mr	BENALIA Atallah	*Examiner*	Prof	University of Amar Telidji – Laghouat
Mr	ALLAOUI Tayeb	*Examiner*	Prof	University of Ibn Khaldoun – Tiaret
Mr	TOUAL Belkacem	*Examiner*	M.C.A	University of Ziane Achour – Djelfa

Dedication

I dedicate this thesis first and foremost to the memory of my dear brother "Oussama" who passed away; and what a terrible emptiness he left for us.

I dedicate also this modest work to: my dear parents, my wife and my beautiful daughter,for their deep tenderness, patience and encouragement. My dearest brothers and sisters, all my large family. To all my friends.

Happiness comes not from having much to live on
but having much to live for.

Success never resides in the world of weak wishes,
but in the palace of purposeful plans and prayerful .

William Arthur Ward

Acknowledgments

First of all, i would like to thank God “Allah” the almighty who gave me the strength and courage to carry out this modest work.

I would also like to express my gratitude and thanks to

Mr. Ameur Aissa

Mrs. kouzi Katia

Professors at the university of Laghouat, Departement of Electrical Engineering, For supervising, encouraging and leading me with their recommendations.

My sincere thanks also go to the members of the jury for the honour they have bestowed on me for having accepted to value this work and also for taking the time to review the thesis.

I would also like to thank all the teachers who have contributed in one way or another to my work.

I would also like to thank the teachers in the Department of Electrical Engineering at Laghouat University who have contributed confidently in my educational training during the doctorate cycle.

I thank, my parents for their contribution, support and patience.

To all those who contributed in any way to our development, we say thank you.

Abstract

Variable speed electric drive systems have been widely adopted in many technological and industrial applications. The recent period has seen the development and success of various control methods based mainly on mathematical models of systems.

The advent of vector control (FOC) technology allowed the development of an alternative control technique in the mid-1980s called Direct Torque Control (DTC), which is characterized by its simplicity and ability to cope with non-linear systems and restrictions. However, despite its simplicity and its fast dynamic response, a number of challenges must be addressed in order to be used effectively in electrical control applications. One of them is the variable switching frequency that causes undulations in the magnetic flux and torque, which makes noise and therefore adversely affects the machine's performances.

In this context, an emerging predictive control method has proven its superiority over conventional equivalent strategies through numerous distinctive features, including its simplicity and its compatibility of the discrete nature property of the power converters.

This thesis consists in evaluating and improving the different torque control strategies of a permanent magnet synchronous motor according to several criteria. The integrated space vector modulation (SVM) technique was found to be promising for addressing the main challenges of DTC strategy. In addition, we have continued our efforts to improve the finite control set predictive direct torque control FCS-MPDTC method by using fuzzy logic modulator (FLM) or a duty cycle space vector modulation based on fuzzy logic, which effectively reduces torque fluctuations and maintained a constant switching frequency. In order to reduce the calculation load, a simple and efficient method based on the use of two voltage vectors was proposed. Furthermore, a Kalman filter estimator is used to improve the predictive behavior in the one hand and to increase the reliability of the control system and reduce its cost in the other. Finally, we re-examined the use of the fuzzy logic space vector modulaion technique using a neural network technology to achieve neural predictive control. The proposed improved methods were verified by numerical simulation using MATLAB software. The obtained results highlight the success of improved techniques in controlling torque and magnetic flux in an efficient and separate way. It also confirms the reduction of undesirable current harmonics in the motor.

Keys-words: Permanent magnets synchronous motor, Direct torque control, Space vector modulation, Model predictive control, Dutty cycle controller, Fuzzy logic controller, Kalman filter estimator, Neural network.

Résumé

Les systèmes d'entraînement électrique à vitesse variable ont été largement adoptés dans de nombreuses applications technologiques et industrielles. La période récente a vu le développement et le succès de diverses méthodes de contrôle basées principalement sur des modèles mathématiques de systèmes.

L'avènement de la technologie de contrôle vectorielle (FOC) a permis le développement d'une technique de contrôle alternative au milieu des années 1980 appelée Contrôle direct de couple (DTC), qui se caractérise par sa simplicité et sa capacité à faire face aux systèmes non linéaires et aux contraints. Cependant, malgré sa simplicité et sa réponse dynamique rapide, un certain nombre de défis doivent être traités pour être utilisés efficacement dans les applications de contrôle électrique. L'une d'entre elles est la fréquence de commutation variable qui provoque des ondulations dans le flux magnétique et le couple, ce qui fait du bruit et donc affecte négativement les performances de la machine.

Dans ce contexte, une méthode de contrôle prédictif émergente a prouvé sa supériorité par rapport aux stratégies équivalentes conventionnelles grâce à de nombreuses caractéristiques distinctives, notamment sa simplicité et sa compatibilité avec la nature discrète des convertisseurs de puissance.

Cette thèse consiste à évaluer et améliorer les différentes stratégies de contrôle du couple d'un moteur synchrone à aimants permanents en fonction de divers critères. La technique de modulation vectorielle (SVM) intégré est apparue prometteuse pour faire face aux principaux défis de la stratégie DTC. De plus, nous avons poursuivi nos efforts pour améliorer la méthode de contrôle direct prédictif a ensemble (état) de commande fini FCS-MPDTC en utilisant un modulateur à logique floue (FLM) ou une modulation vectorielle d'espace de cycle de service basée sur la logique floue, ce qui réduit efficacement les fluctuations de couple et maintient une fréquence de commutation constante. Dans le bute de réduire la charge de calcul, une méthode simple et efficace basée sur l'utilisation de deux vecteurs tension a été proposée. De plus, un estimateur de filtre de Kalman est utilisé pour améliorer le comportement prédictif d'une part, augmenter la fiabilité du système de contrôle

et réduire son coût d'autre part. Enfin, nous avons réexaminé l'utilisation de la technique de modulation de vecteur d'espace floue en utilisant une technologie de réseau neuronal pour obtenir un contrôle prédictif neuronal. Les méthodes améliorées proposées ont été vérifiées par simulation numérique à l'aide du logiciel MATLAB. Les résultats obtenus mettent en évidence le succès de techniques améliorées dans le contrôle du couple et du flux magnétique d'une manière efficace et séparée. Il confirme également la réduction des harmoniques de courant indésirables dans le moteur.

Mots-clés : Moteur synchrone à aimants permanents, Commande direct de couple, Modulation vectorielle, Commande predictive, Controlleur a cycle de service, Controlleur a logic floue, Estimateur de filtre de kalman, Reseaux de neurone.

ملخص

لقد تم تبني أنظمة القيادة الكهربائية المتغيرة السرعة على نطاق واسع في العديد من التطبيقات التكنولوجية والصناعية. وقد شهدت الفترة الأخيرة تطورا ونجاحا واسعا لطرق التحكم المختلفة المعتمدة أساسا على النماذج الرياضية للأنظمة.

سمح ظهور تقنية التحكم الشعاعي (FOC) بنشأت تقنية بديلة للتحكم في منتصف الثمانينيات أطلق عليها التحكم المباشر في العزم (DTC) التي تميزت ببساطتها وقدرتها على التعامل مع الأنظمة غير الخطية والقيود. ولكن على الرغم من بساطة وسرعة الاستجابة الديناميكية لهذا النوع من التحكم إلا أن هناك عدد من التحديات التي يجب مواجهتها كي تستخدم بشكل فعال في تطبيقات التحكم الكهربائي. منها تواتر التبديل المتغير الذي يسبب ظهور تموجات على مستوى التدفق المغناطيسي والعزم مما يحدث ضجيج والذي يأثر على الأداء العام للماكنة سلبا.

في هذا السياق، أثبتت طريقة التحكم التنبئي الناشئة تفوقها على الاستراتيجيات التقليدية المكافئة الأخرى بفضل العديد من من الخصائص المميزة، بما في ذلك بساطتها وتوافقها مع الطبيعة المتقطعة لمحولات الطاقة.

تتضمن هذه الأطروحة تقييم وتحسين طرق التحكم في العزم المختلفة للماكنة المتزامنة وذلك وفقا لعدة معايير. أثبتت تقنية تعديل طول النبضة الشعاعي المدمجة أنها واعدة في مواجهة التحديات الرئيسية لاستراتيجية DTC. وبالإضافة لذلك واصلنا جهودنا لتحسين أسلوب التحكم في العزم المباشر التنبؤي ذات مجموعة التحكم المحددة (FCS-MPDTC) باستخدام تقنية تعديل طول النبضة الشعاعي ذو دورة العمل المعتمد أساسا على الذكاء الاصطناعي (FLM) والتي أدت إلى تقليل تذبذب العزم بشكل فعال وضمان تطبيق تواتر تبديل ثابت. وبهدف تقليل العبئ الحسابي فقد تم اقتراح طريقة بسيطة وفعالة تعتمد على استخدام متجهين للجهد فقط .علاوة على هذا، تم استخدام مرشح كالمان لتحسين السلوك التنبؤي من جهة و الزيادة من موثوقية نظام التحكم وتخفيض تكلفته من جهة أخرى. وفي الأخير تطرقنا من جديد الى استخدام تقنية تعديل طول النبضة الشعاعي الضبابي وذلك بالاعتماد على تقنية الشبكة العصبية الذكية من أجل الحصول على تحكم تنبؤي عصبي. تم التحقق من صحة الطرق المقترحة المعززة باستخدام المحاكاة الرقمية

باستعمال برنامج ماتلاب. حيث أظهرت النتائج المتحصل عليها نجاح التقنيات المحسنة في التحكم في كل من العزم و التدفق المغناطيسي بشكل فعال و منفصل. كما أوضحت تقليل توافقيات التيار الغير مرغوب بها في المحرك.

كلمات-مفتاحية : محرك متزامن ذو مغانط دائمة، التحكم المباشر في العزم، تعديل طول النبضة الشعاعي، التحكم التنبئي، وحدة تحكم ذو دورة العمل، وحدة تحكم ذو المنطق الضبابي، مقدر مرشح كالمان، شبكة عصبية .

List of Publications

Journal Publications

- ✓ Benhamida, I., Ameur, A., Kouzi, K., & Gaoui, B. (2019). Torque Ripple Minimization in Predictive Torque Control Method of PMSM Drive Using Adaptive Fuzzy Logic Modulator and EKF Estimator. Journal of Control, Automation and Electrical Systems, 30(6), 1007-1018.

- ✓ Benhamida, I., Ameur, A., Kouzi, K (2020). Torque ripple mitigation in FCS-MPDTC of PMSM Drive using an Adaptive Fuzzy Logic Modulator. International Journal of Industrial and Systems Engineering, 1(1), 1-18.

Conference Proceedings

- ✓ Benhamida, I., Ameur, A., Kouzi, K, I., Sayaf, H. (2018, October). Predictive Direct Torque Control Based on New Formulation and Fuzzy Logic for Permanent Magnet Synchronous Machine. In 2018 International Conference on Electrical Sciences and Technologies in Maghreb (CISTEM) (pp. 1-6). IEEE.

- ✓ Benhamida, I., Ameur, A., Kouzi, K, I., Sayaf, H. (2018, November). Online Selection of Weighting Factor in Model Predictive Direct Torque Control of PMSM Using FuzzyAdjustment Process. International Conference on Electronics and Electrical Engineering (IC3E'18), University of Bouira, Algeria. IEEE.

- ✓ Benhamida, I., Ameur, A., Kouzi, K, I., Sayaf, H. (2018). Predictive DTC-SVM of a Permanent Magnet Synchronous Motor. Fifth Doctoral Day of the Faculty of Technology (5JDFT), University of Laghouat, Algeria.

- ✓ Cheknane, A., Kouzi, K., Sayaf, H., & **Benhamida, I**. (2019, November). Robust Speed Sensorless Fuzzy DTC Using Simplified Extended Kalman Filter for Dual-Star Asynchronous Motor (DSIM) with Stator Resistance Estimation. In International Conference in Artificial Intelligence in Renewable Energetic Systems (pp. 598-609). Springer, Cham.

- ✓ Sayaf, H., Kouzi, K., **Benhamida, I**., Cheknane, A. (2020). On the improvement of Vector Control of PMSM drive: robust Backstepping control approach. The First International Conference on Communications, Control Systems and Signal Processing (CCSSP 2020), University El Oued, Algeria. IEEE.

List of Figures

CHAPTER I State of The Art in a Variety of Control Paradigms for Electrical Machines

CHAPTER II Implementation and Improvement of Direct Torque Control for a Permanent Magnet Synchronous Motor.

CHAPTER III Finite State_Model Predictive based Control Methods for a Permanent Magnet Synchronous Motor Drive (PMSM)

CHAPTER IV Improved FS_MPDTC For PMSM_Drive using Fuzzy Logic System and EKF

CHAPTER V Supervised Imitation Learning of a Fuzzy Logic Duty Cycle Controller Based on the FS_MPDTC of PMSM Drive

Appendix A

Appendix C

List of Tables

CHAPTER II Implementation and Improvement of Direct Torque Control for a Permanent Magnet Synchronous Motor.

CHAPTER III Finite State_Model Predictive based Control Methods for a Permanent Magnet Synchronous Motor Drive (PMSM).

CHAPTER IV Improved FS_MPDTC For PMSM_Drive using Fuzzy Logic System and EKF.

CHAPTER V Supervised Imitation Learning of a Fuzzy Logic Duty Cycle Controller Based on the FS_MPDTC of PMSM Drive

Appendix B

List of Abbreviations

CO2	Carbon dioxide.
DC	Direct Current.
AC	Alternative Current.
VFD	Variable Frequency Drive
VC	Voltage Control.
DTC	Direct Torque Control.
SVM	Space Vector Modulation
FOC	Field Oriented Control.
MPDTC	Model Predictive Direct Torque Control.
FCS	Finite Control Set .
FPGA	Field Programable Gate Array.
DSP	Digital Signal Processor.
IM	Induction Motor/Machine.
MPC	Model Predictive Control
CCS	Continous Control Set.
EMF	Electro-Motive Force.
DCC	Duty Cycle Controller.
PD	Proportional Derivative.
GPC	Generalized Predictive Control.
MRAS	Model Reference Adaptive System.
EKF	Extended Kalman Filter.
PI	Proportional-Integral.
PMSM	Permanent Magnet Synchronous Motor/Machine.
PWM	Pulse Width Modulation.
ANN	Artificial Neural Network
ANNI	Artificial Neural Network Imitator .
NN	Neural Network
FLM	Fuzzy Logic Modulator.
FLC	Fuzzy Logic Controller.
SMC	Sliding Mode Control.
DSO	Disturbance Speed Observer.
SMO	Alternative Current.
PCC	Predictive Current Control.
PTC	Predictive Torque Control.
PDTC	Precictive Direct Torque Control.
VSI	Voltage Source Inverter.
UPS	Uninterruptible Power Source .
VSC	Voltage Source Converter.
MLP	Multi Layer Perceptrons
THD	Total Harmonics Distortion.
LPF	Low Pass Filter.

List of Symbols

Reference axes:

a, b, c	Axes linked to three-phase windings
d, q	Axes of the Park reference system
θ	Angle between stator and rotor

Electrical quantities at the stator:

i_a, i_b, i_c	Stator phase currents a, b, and c
i_s, i_{abc}	Vector of the stator currents
i_d, i_q	Vector of the stator currents in d and q rotating frame
u_s, u_{abc}	Vector of the stator voltage in *a*, *b* and *c* three-phase frame
u_{dq}	Vector of the stator voltage in d and q rotating frame

Electrical quantities of the power supply system:

$S_{a,b \text{ and } c}$	Inverter control switches
f	Power source frequency
u_a, u_b, u_c	Power source voltages in *a*,*b* and *c* three-phase frame
u_a^*, u_b^*, u_c^*	Reference power source voltages in *a*,*b* and *c* three-phase frame
u_α^*, u_β^*	Reference power source voltages in alpha-beta (α , β) frame
u_d, u_q	Power source voltages in *d*, *q* rotating frame

Magnetic quantities at the stator:

ψ_s^*	Reference value of stator flux

$\psi_\alpha, \psi_b, \psi_c$	Flux of the stator phases *a*, *b* et *c*
ψ_d, ψ_q	Stator flux in the *d*-axis and *q*-axis
ψ_s, ψ_{abc}	Stator flux vector

Magnetic quantities at the rotor:

ψ_{rm}	PM flux linkage

Mechanical quantities :

T_e	Electromagnetic torque
T_e^*	Reference electromagnetic torque
T_L	Load torque.
f_r	Coefficient of viscous friction
J	Motor moment of inertia
ω_r	Mechanical rotational speed of the rotor
ω_r^*	Reference rotational speed

Parameters of the machine, feeding system and control techniques:

T_s	Sampling time.
T_1, T_2	Durations of the applied voltage space vecors
l_d	Inductance on the d-axis
l_q	Inductance on the q-axis
p	Number of pole pairs
R_s	Stator phase resistance

δ	Load angle between the stator and rotor flux vectors.
Δd	Duty cycle
$x\ (k)$	Control variable
$u\ (k)$	Control action
$x\ (k+1)$	Predicted variable
λ	wgheting factor
η	Learning step gain.
K_p	Proportional gain
K_i	Integral gain
K	The Kalman gain matrix.
R	Covariance matrix of the measurement noise vector.
P	Covariance matrix of the state vector.
Q	Covariance matrix of the system noise vector.

Table of Contents

General Introduction

General Introduction

Overview:

Nowadays, the permanent magnet synchronous motors PMSMs have become the most targeted machines to fulfil the growing demands of modern technologies. Accordingly, they are widely used in various industrial traction systems and automotive applications such as hybrid vehicles (HVs), electric vehicles (EVs) and fuel cell (FCVs) vehicles [1]. In fact, due to the inserted magnetic materials alloy inside the rotor core as well to the inherent magnetic saliency (i.e. interior PMSM) , the PMSMs possess an exceptional physical properties over other types of motors (DC motors, AC induction motors) [2], [3]. As a result, the PMSMs provide interesting merits such as high power and torque density, robust rotor structure, low acoustic noise and operating capability in a wide speed range [2], [3]. In fact, the progressive development of modern semiconductor devices and power electronic converters, allows these motors to operate with variable frequency/speed by powering them through a static converter of variable frequency such as the voltage source inverter. However, in contrast to the applications which do not require a control system, it is difficult to realize a precise control of the PMSM due to its nonlinear characteristics (i.e. the magnetic saturation and strict coupling between the state variables) and also due to the fact that the dynamic model of PMSM is very sensitive to physical constraints and uncertainties [4]. Furthermore, one of the main difficulties for the control of the PMSM is the detection of the initial position of the rotor in order to control it in the direction of rotation imposed by the control, otherwise there is a risk of loss of control and stall of the machine [5].

Besides, some industrial applications require certain control aspects , that must be fulfilled by the controlled drive. For this reson, Several interesting control techniques have been developed for the objective to guarantee the high efficiency and the better exploitation of PMSMs during the last few decades, and the most established control methods are stator flux or field oriented control (FOC) and direct torque control (DTC) [6-8]. The voltage-frequency v/f control is also one of the first control strategys developed for the speed regulation of asynchronous motors. However, its slow dynamic response make it suitable only for low performance applications [9].

FOC, that called also vector control has been widely employed in PMSM control due to the advantages of a simple algorithm, good robustness, and high reliability. Compared to this control technique the DTC scheme is relatively simple because it does not need any current regulators, axes transformations, or a pulse width modulator (PWM). Moreover, DTC features fast dynamic response and robustness against machine parameters variation (except stator resistance) [4], [10]. Nevertheless, the basic DTC scheme employs two hysteresis controllers for torque and flux magnitudes control in order to select the inverter switching states according to a predefined switching table. Consequently, high torque and flux ripples are the main drawbacks of DTC method [4], [10], [11].

Otherwise, a suitable design of space vector modulation can be integrated to make the control's law more effective versus the undesired torque and flux undilations. Space vector modulation (SVM) based DTC (DTC-SVM) is a good solution for alleviating torque and flux ripples, reducing current harmonics and maintaining a constant commutation frequency[12], [13]. Two major structures of DTC-SVM have been studied in literature such that the closed-loop torque control or also known as load angle control with SVM [12] and the stator flux vector control (SFVC) based SVM-DTC [13]. However, the high complexity of both control laws negatively affects the simplicity of DTC.

Generally, a control pradigme aims to control a given electromechanical system in order to obtain a correct functioning of the latter. The control permits the system to track a desired response for a given input while rejecting the effects of disturbances. Unfortunately, when system modeling is difficult, the design of the control system can be very complex. This difficulty is due to high non-linearities, strict coupling betwwen states and inaccuracies of internal variables. These difficulties have led in recent years to the development of innovative control techniques [14-18].

Model predictive control (MPC) has lately gained considerable importance in research and industry [19]. The basic principle of model predictive-based control approach is to use a model of the system to predict its future behavior for series of control decision over a receding prediction horizon [20], [21]. During the last decade, many MPC approaches have been presented to overcome the limitation such as design simplicity and explicit inclusion of constraints that stem from the controlled drive [22]. A well-known model based approach is the so-called predictive direct torque control (PDTC) or predictive torque control [23-27], which is a strategy based on DTC, but the design process

is more straightforward and simpler. The main control objectives are the same, i.e. the regulation of the torque and stator flux magnitude to their reference values, and captured in an objective function. Thus, the use of hysteresis bounds and look-up tables is omitted.

Recently, and thanks to the progress made in microprocessor technology, model predictive control (MPC) has become a promising and an extensive control approach in the areas of power electronics and electric drive systems [19]. MPC has several features, such as the explicit inclusion of constraints and non-linearities, absence of modulator, and intuitive concept. Another significant merit of MPC can be synthesised through the optimization capability, which is a vital key factor of this approach. In fact, with the MPC, the optimal control action is selected through optimizing a designed quality (cost) function. Additionaly, MPC can be mainly classified into two main groups [28]: continuous control set (CCS-MPC) and Finite control set (FCS-MPC). In the first group, due to the use of a modulator stage the controller can generate the reference voltage vector (VV) under a constant switching frequency, this is also the case of GPC [29]. However, its control algorithm involves high calculation burden and remain complicated.

Contrariwise, instead of using a modulator; FCS-MPC suits the discrete nature property of the inverter model and uses all available voltage vectors to determine the optimal VV by optimizing a designed criterion [30]. In fact, model based predictive control methods have been successfully applied to induction machine drive control [31] as well as to synchronous motor drive control [29], [30], [32], [33] and control of other types of ac electric drives [34], [35]. They have also been used to extend the performance of the drive control to additional objectives like: current limitation of the drive [36] and improving switching losses [37]. The criterion quality contains several control objectives and constraints, and the weighting factors can tune the importance among these different control goals [38].

The main advantage of FCS-MPC lies in the direct application of the control action to the converter [28],[39]. Moreover, the key components of a successful FCS-MPC controller resides straightforwardly in the appropriate selection of the control variables and/ or in the judicious determination of the weighting factors. If tuned well FCS-MPC can successfully compete with conventional PWM based control mechanisms [28 -39]. Nevertheless, the FCS-MPC also has its weak points, such as variable switching frequency resulting in spread frequency spectrum of the converter currents, and operation at lower

switching frequencies resulting in higher current ripple [40]. These can be mitigated by smart techniques or using PWM as a modulator for control designed by the FCS-MPC [41], [42]. Aditionally, One of the main drawbacks or challenges in FCS-MPTC is the heavy calculation burden, which requires a very fast digital processor for practical implementation and engineering application. In particular, for the application of multilevel or multiphase inverters, the calculation effort rises exponentially [29].For this reason we interest in this thesis with the two level voltage source inverter which offers only egiht distinct voltage vectors. On the other hand, artificial intelligence methodologies have emerged recently as promising ways to solve nonlinear control problems. In particular, the fuzzy logic control and neural network can handle complexes, uncertainties and weakdefined control plants [43], [44].

Within the contents of this thesis , different control strategies are studied and developed for the PMSM drive, so that a detailed survey about this control strategies have been carried out through numerical simulation and discussed.

Thesis Objectives :

In view of the foregoing general introduction, the main objectives of the thesis are summarized as follows:

- Enhancing the basic DTC strategy used for controlled our PMSM drive, with the well dominated space vector modulation technique, through which high steady-state and dynamic performances can be achieved.

- Designing and implementing of the recent emerged predictive control techniques namely, Model predictive current control (MPCC) and Model predictive direct torque control (MPDTC) with efficient predictive aspects. Thus, high dynamic performance can be obtained.

- Addressing the main issues associated with the FCS-MPDTC namely, the relative torque/flux ripples, current harmonics and the variable switching freaquency, by inserting the concept of the fuzzy logic duty-cycle vector modulation .

- As an alternative to the use of very expensive speed sensors and improve the prediction behavior, a well-established stochastic control algorithm for sensorless variable speed operation is developed.

- Finally, we re-examine the concept of the Duty-Cycle-Controller for the FCS-MPTDC but with the integration of a neural network imitator to chek and analysis the neural network prediction behavior.

In summary, it can be said that the work on advanced torque control in variables speed drives, especially for permanent magnet synchronous motor has resulted an innovative and powrfull strategies. Thus, the introduction of a novel concept or structure has graetly improve the model predictive torque control method, the concept of artificial intellegence-based duty-cycle vector modulation in particular. Moreover, this structure results in the implementation of simple and robuste algorithms, which can be applied with either synchronous machines or the induction ones by using any power converter topology as interface between the machine and the predictive controller.

Thesis Outlines :

In order to meet the objectives mentioned above, the manuscript of the thesis will be organized into six chapters as follows:

- Chapter 1: The first chapter presents an overview about electrical machines and the different control strategies, such as scalar control , vector control and DTC. Thereafter, advanced control techniques (i.e. nonlinear , artificial) and sensorless control approaches are discussed.

- Chapter 2: The second chapter presents a comprehensive study of the well established conventional DTC and its aimplementation. The chapter presents also the designe and the implementation of improved DTC by using space vector modulation technique. So, the main advantages of these control methods are discussed, and their major drawbacks are outlined. Simulation tests were carried out aiming to verified the theoretical backgrounds.

- Chapter 3 presents a review of the MPC approach, which has been selected as an effective control tool for the PMSM drive system. The past, present and future use of predictive controllers in power electronics and machine drives is summarised. Furthermore, the chapter provides also the designe and the implementation of the two most widely used predictive controller schemes. So a comparative assesement for both predictive-controllers is illustrated, for which the strengths and weaknesses points of each one of which are specifyed, while the control that take our interest in the present thesis is identifyed.

- Chapter 4 proposes an anhanced model predictive direct torque control approach based on an adaptive fuzzy logic modulator for PMSM drive. The chapter presents a detailed analysis of the proposed fyzzy logic vector modulation and its implementation procedure. The proposed technique capable to reduce effectively the ripple contents in the controlled flux and torque. On the other hand, this work focuses on sensorless control techniques used to improve the control performance in terms of improving the prediction model and decreasees the cost of the overall control system.

- Chapter 5 presents the designe and the development of another intelegent control technique for Duty-Cycle-modulated voltage vector technology of MPDTC based on neural network imitator . Simulation tests were caried out aiming to chek and disply the neural prediction performances.

- Chapter 6 provides general conclusion, for which the findings of the previous chapters are summarized, and the essential contributions are outlined. Also, further perspectives and topics for future research are identified for being the new available trends both in the scientific literature and in the industry oriented research.

ChapterI

State of The Art in a Variety of Control Paradigms for Electrical Machines

In this chapter, we present first an overview of electrical machines, considering their benefits, drawbacks, field of application and the different types of synchronous motors, while specifying the type to be studied in this thesis. Next, we will describe in more detail the different control technologies. Thereafter, advanced control techniques (i.e. nonlinear , artificial) and sensorless control approaches are discussed.

I.1. Introduction

As the industrial and energy sectors are the main emitters of CO2, research towards the development and integration of electric motors in vehicles and renewable energy conversion has greatly increased [45]. The development of new electric motors and generators constitutes an important factor in ecology. Studies have shown that new targeted machine topologies are better qualified to fulfill the present-day requirements than the classical ones. An example of such candidates machines topology are the induction and synchronous machines, which the later one is very suitable for electric vehicles and small to medium power range wind energy systems.

Scientists have been interested for a long time in studies concerning variable speed electrical drives (for industrial or domestic needs). This difficult task can only be properly carried out when there is a good knowledge of the dynamic model of the system to be controlled to predict its behavior for different operating modes.

From the beginning, Direct Current (DC) machine played an important role in variable speed applications [5]. On the one hand, it guarantees the operation in several industrial equipments and on the other hand it is easily controllable. However, the DC has several disadvantages mainly related to the mechanical commutator [46]. To overcome these problems related to the DC motor, researchers have turned to the use of alternative current (AC) electrical machines in order to benefit from their advantages such as speed variation, high torque density and reliability. Among these machines the Permanent Magnet Synchronous Motor (PMSM), which remains a good choice in variable speed electric drives and expert researchers expect that this motor will occupy a prominent place in the future and impressively outperform the asynchronous motors.

I.2. Electrical Machine

I.2.1. Direct Current Motor (DC Motor)

Over the past 10 decades, the internal combustion engine has dominated the individual/public road transport market [47], while electric vehicles (EVs) have always existed. During these years, researchers have been interested in studies concerning variable speed electrical drive systems (for industrial, accademic and domestic needs).

In the meantime, Direct current (DC) machines was gained a huge importance in industriel applications, particularly in conveyors, robots and others for which adjustable speed and constant or low-speed torque are required [48], [49]. In fact, they were primarily used in automobiles for the marketing of first generation of electric vehicles. A DC motor has separate field and armature windings. Thus, the torque and flux can be controlled separately by the field and armature currents. A DC motor characterized mainly by its simplicity of control. However, there are several disadvantages related mainly to its inherent mechanical collector. The latter inherently limites the speed of the DC motor. The large size and weight of a DC motor is also undesirable due to the mechanical commutator brush system [50]. As a result, the collector brush system limits the DC-motor robustness, reliability, capacity and its application environment.

I.2.2. Induction motor (IM)

In 1831 Faraday published the electromagnetic law of induction and around 1860 Maxwell formulated the equations for electricity,‘‘Maxwell's equations’’ [51]. In fact, this knowledge was essential for the invention of the first induction motor (IM). **Fig I.1** illustarte the first induction motor from Tesla (1886) [52]. In a simple operating principle, a rotating magnetic field in the stator induces currents in rotor bars or windings that produces the torque of the motor. Squirrel cage induction motor, for example, is widely used due to its straightforward operation, reasonable cost, and low maintenance requirement, meaning that it can be connected to the grid without external starting device, and thus benefit from a low cost [53]. The IM has been known to be called "the work horse" of the industry [54]. Moreover, the performance of IM has been significantly improved in terms of efficiency and power density through the development of modern technology. However, the currents that are induced in the rotor windings cause unnecessary losses. These losses are called rotor copper losses, which is the main downside of this candidate machine [55].

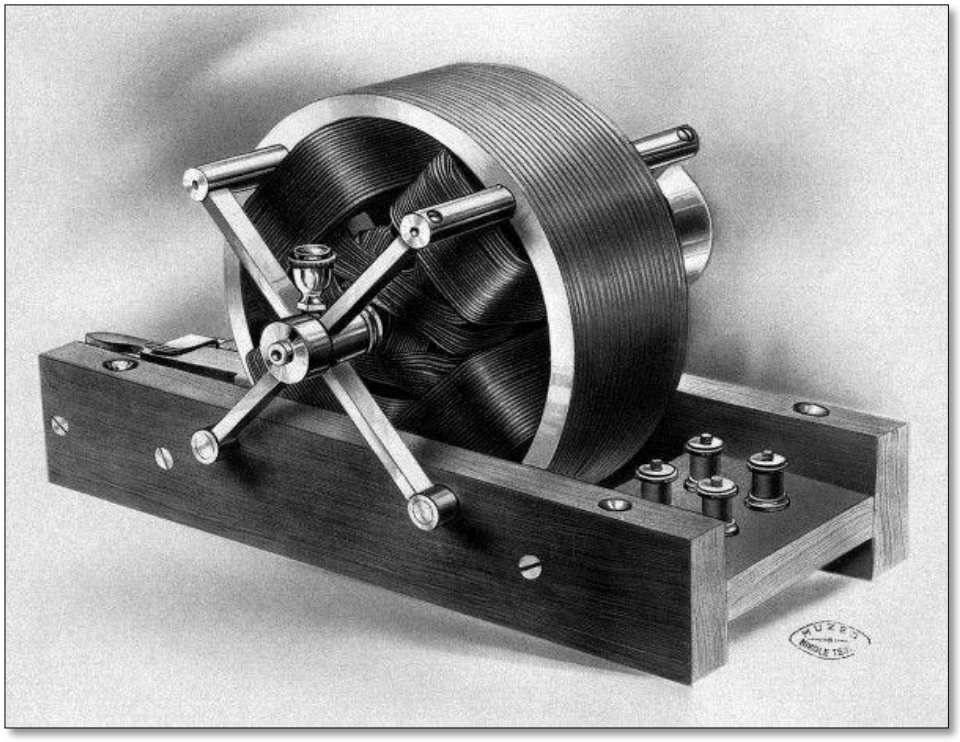

Figure I.1 Tesla's First Induction Motor.

I.2.3. Synchronous Machine (SM)

I.2.3.1. Wound-Rotor Synchronous Machines

Originally, synchronous machines, which are essentially alternators excited by direct current (DC), are the major producers of the electrical energy consumed in the worldwide. They are mainly composed of stator, rotor and amortisseur windings. Conventional synchronous motors require an AC power supply for stator windings and a DC power supply for the rotor windings [5].

The motor speed is determined by the AC power supply frequency and the number of poles of the synchronous motor, the rotor rotates at the speed of the stator rotating field at synchronous speed, which is constant. Any changes in mechanical load within the rated capacity of the machine will not affect the synchronous speed of the motor. The interaction between the rotating field created by the stator and the field due to the inductor gives rise to the electromagnetic torque and causes a rotation of the rotor.

One of the types of these electromechanical machines is the permanent-magnet synchronous motor (PMSM). Compared to the conventional synchronous motor, the PMSM consists of conventional three-phase windings in the stator and permanent magnets in the rotor core. Consequently, the objective of the field windings in the conventional synchronous machine is achieved by permanent magnets in PMSM. Additionally, the conventional synchronous machine requires an AC and DC power supply, while the PMSM only requires an AC power supply for its operation. So it's evident to notice that one of the greatest advantages of the PMSM over its counterpart is the elimination of DC power supply for field excitation. The main components of wound-rotor synchronous motor are shown in **Fig I.2**.

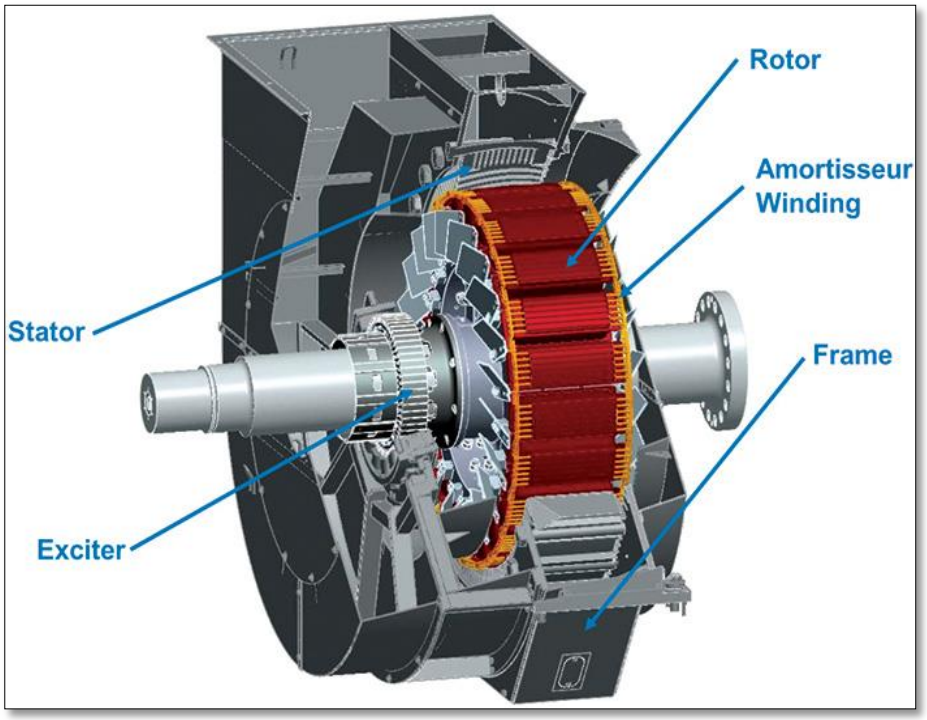

Figure I.2 The main components of wound-rotor synchronous motor.

Note:

A squirrel cage winding or rotor damper (amortisseur) is placed near the surface of the pole faces of a synchronous motor. The main role of amortisseur winding is to dampen any speed fluctuation or oscillations that may occurs as a result to sudden load changes. It is also used to accelerate the motor during starting.

I.2.3.2. Types of Synchronous Machine with Permanent Magnets

The development of PMSM has happened due to the invention of novel magnetic materials and rare earth materials. As illustrated in **Fig I.3**, the PMSMs are classified mainly based on the placing of the permanent magnets in two types[56], [57]:

1. Surface mount PMSMs

2. Interior PMSMs

The first type of arrangement provides the highest air gap flux density, but it has the drawback of lower structural integrity and mechanical robustness. This rotor configuration is the most commonly used. The main advantage of the machine with surface magnets is its simplicity of manufacturing. Thus, low manufacturing costs compared to other magnet machines. Their main drawback is that the magnets are subjected to centrifugal forces that can cause their detachment from the rotor. Sometimes a non-ferromagnetic outer cylinder of high conductivity is used; this gender referred as ''surface inset permanent magnets''. This cylinder can additionally provide asynchronous starting torque and act as a damper. For the surface rotor configuration, the synchronous reactance in the d-axis and the q-axis are practically the same. Technically, this type is devoted to the novel investigations and recent control algorithms due to the absence of magnetic saliency, which gives more simplicity of modeling and implementation than that of other types. So, the type with this arrangement of magnets (Surface mount PMSMs) will take our interest in the present thesis.

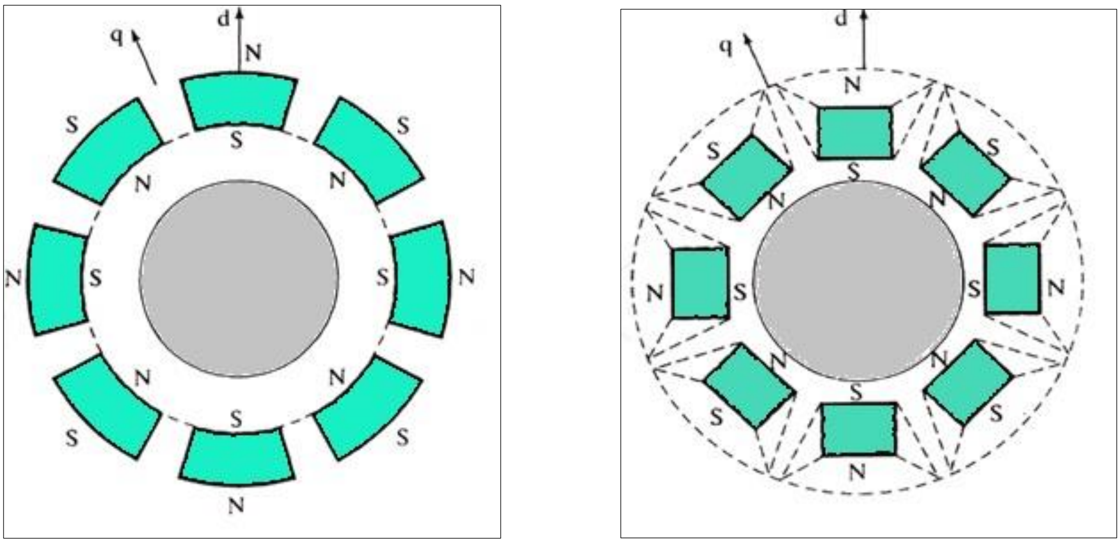

Figure I.3 Surface PMSM to the left and interior PMSM to the right.

In general mode working, for both types (i.e. surface and interior PMSMs), a stator current externally imposed gives rise to a magnetic field which interacts with the magnetic field generated by the permanent magnets. The result is a rotation of the rotor disc. The electrical power is thus transformed into mechanical power, which is available on the machine shaft. One of the most important advantages of PMSMs in general is the fact that they have a good energy efficiency. Usually permanent magnets with a high energy density, such as neodymium (NdFeB) magnets, are used to generate the magnetic field. As a result, no field excitation current is necessary and the corresponding copper losses are absent. Large torque-ampere ratios are obtained [58].

I.2.4. Safe and Functional PMSM Operation

A synchronous motor operating without synchronized mode is extremely unstable [5]. Independently of the type of machine and associated power supply, the mechanism of synchronization requires the synchronization of the electrical power supply quantities with the rotation speed. A first way to adjust the speed of a synchronous motor is to operate it with variable frequency currents. This is provided by a variable frequency power converter [59]. In this case it is essential to control not only amplitude but also frequency and/or phase [5], [59], [60]. However, for such control paradigm the position information of the rotor is essential for high performance operation especially for the PMSM drive [61]. There are different methods to keep track of the rotor position; for this end the position can be measured with a sensor or estimated by using some specific sensorless control algorithme. In this section we will interesse by the first method (i.e. measured position). In the following, two major position sensor technologies are presented in order to understand their advantages and disadvantages.

I.2.4.1.Resolver

The resolver is a sensor that can be used to obtain information on the absolute position of the rotor. Its structure consists of three windings, as illustrated in **Fig I.4**. The principal, also called the excitation winding, is wound on the rotor. The two other 'secondary' coils are identical and are wound on the stator. The principal winding is supplied with a high-frequency reference signal which in turn induces a voltage in the other two placed 90± secondary windings which in turns delivred two outputs (sine and cosine signal) [5], [62], [63]. Consequently, the rotor angle can be derived as the arctangent of the sine and cosine signal [62-64].

The two secondary (output) terminal voltages can be expressed in the time domain by [5] :

$$U_{\sin} = U_0 k\left[\sin\theta\cos(\omega t) + \frac{1}{\omega}\frac{d\theta}{dt}\cos\theta\sin(\omega t)\right] \quad (1.1)$$

$$U_{\cos} = U_0 k\left[\cos\theta\cos(\omega t) + \frac{1}{\omega}\frac{d\theta}{dt}\sin\theta\sin(\omega t)\right] \quad (1.2)$$

With,

K : The rotor/stator transformation ratio.

U_0: The amplitude of the excitation signal.

θ : The absolute angular position of the rotor.

ω : Excitation signal pulsation.

From a practical point of view, a resolver equipped with a digital converter is characterized by the absence of sliding friction, its simple structure, its robustness against temperature variations and its high reliability.

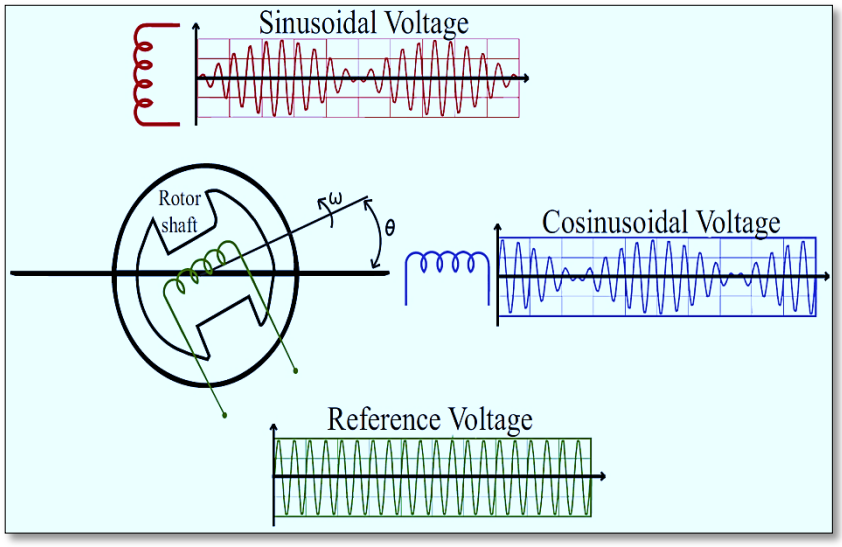

Figure I.4 The working concept of resolver.

I.2.4.2. Absolute Optical Encoder

An encoded disc is divided into multiple tracks. Each track has alternating reflective and non-reflective sectors, as illustrated in **Fig I.5**. A transmitter-receiver per track provides the information. The number of tracks determines the number of discrete positions that can be defined: 1 track = 2 positions, 2 tracks = 4 positions, 3 tracks = 6 positions, ... n tracks = 2n positions [5].

A high-precision absolute encoder can accurately determine the tracking position. However, it has some weaknesses that need to be taken into account, such as it cannot cope with harsh environments that subject the sensor to shock and vibration. The encoder is also sensitive to external materials such as dust particles, making it unreliable in such environments. The sensor could give erroneous readings if objects such as dust particles become attached to the disc [65].

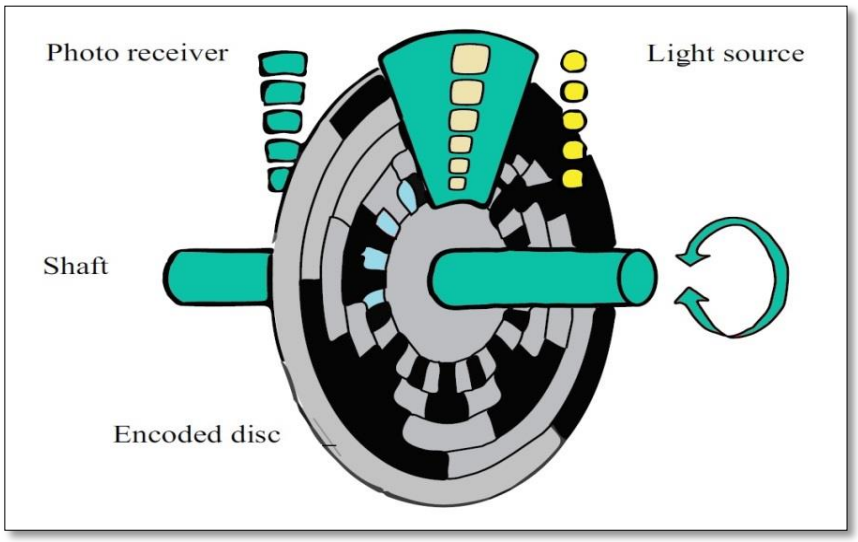

Figure I.5 An absolute optical encoder.

I.3. Background on Adjustable Speed Drives

The drive systems based on AC machines integrate the power supply, the power converter, the actuator and the control package essential for the operation of the whole assembly. This means that a model of the studied system is necessary for the smooth running of the drive process, both for the study of its behaviour and for the implementation of the control system functionality.

The development of different control methods for a such non linear system is justified by the need to take into account its non-linear structure. For this reason, and despite its evolutive design and small size, the industry has preferred the use of the synchronous actuator. This is mainly due to the fact that its non-linear structure is relatively easier than others. One modality of AC motor control for variable speed applications is the open-loop scalar control [66], which is the most popular control strategy for squirrel-cage AC motors. It is generally used in applications where information about the angular speed need not be known. Unfortunately, this modality suffers from significant drawbacks namely, the speed dependence on external load torque, and the reduced dynamic performance [67].

A control method for the synchronous motor, which was reduced to a linear control structure by the so-called flux orientation assumption, was proposed by Blaschke in 1972. Although this method remained little used until the early 1980s, advances in semiconductor technology and microelectronics made it possible to use it in today's industrial drives. However, the experiment has proven the weaknesses of this method regarding the uncertainties of parameters, whether they are measured, such as motor speed, or vary during operation, such as stator resistance [5], [68],[69].

In other respects, the control of electric motors has proved to be a field of application for the non-linear automatic control methodologies developed since the 1970s. Indeed, the modeling of AC motors is well mastered, and it results in non-linear models characterized by a limited number of state variables. At the same time, the rapid development of digital electronics allows the realisation of increasingly sophisticated controls such as direct torque control [12], [69], linearised input-output control [70], and the predictive control which is the focus of our work.

I.3.1. Scalar Control

Scalar control is the most traditional control method for AC machines, its structure is very simple, it is based on the imposition of a constant ratio between the supply voltage module and its frequency (V/f). The general control scheme is illustrated in **Fig I.6**. This control strategy provides good results for relatively constant speed setpoints [66]. The main advantage of this simple approach lies in the possibility of operating in sensorless mode (i.e without closed loop of speed control). On the other hand, for a start-up or for a speed sense reversing, the flux oscillates strongly with large amplitudes and its module is variable during transient state[67] .This explains why the relationships used to calculate this command are only valid in the steady state. Moreover, these oscillations effects seriously the expected responses, particularly in transient state, and hence, degrading the dynamic performances of machine. Therefore, this type of control is only used for applications where the speed variation is not very high like in application of pumping or ventilation [5].Depending on the power actuator used to supply the machine, the authors divide the scalar control into two types, one called "current control", for machines driven by current inverters and the other, which is most commonly used, called "voltage control", also knows about the name "voltage control (V/f), for machines driven by voltage inverters.

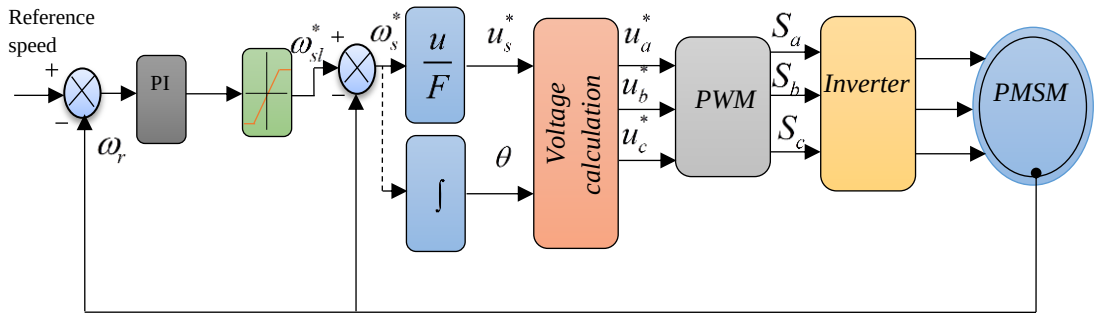

Figure I.6 Closed loop scalar control.

I.3.2. Field Oriented Control

Introduced by Blaschke in 1972, the objective of vector orientation controlled PMSM is to achieve a model equivalent to that of a DC machine, i.e. a linear and decoupled model, which improves its dynamic behavior [5], [6]. Thus, by orienting or aligning the reference frame on a rotating *d,q* coordinate system, the decoupling of the components of the variables forming the flux and torque in the AC machine is achieved. The general block diagram of the FOC for a PMSM is shown in **Fig I.7**.

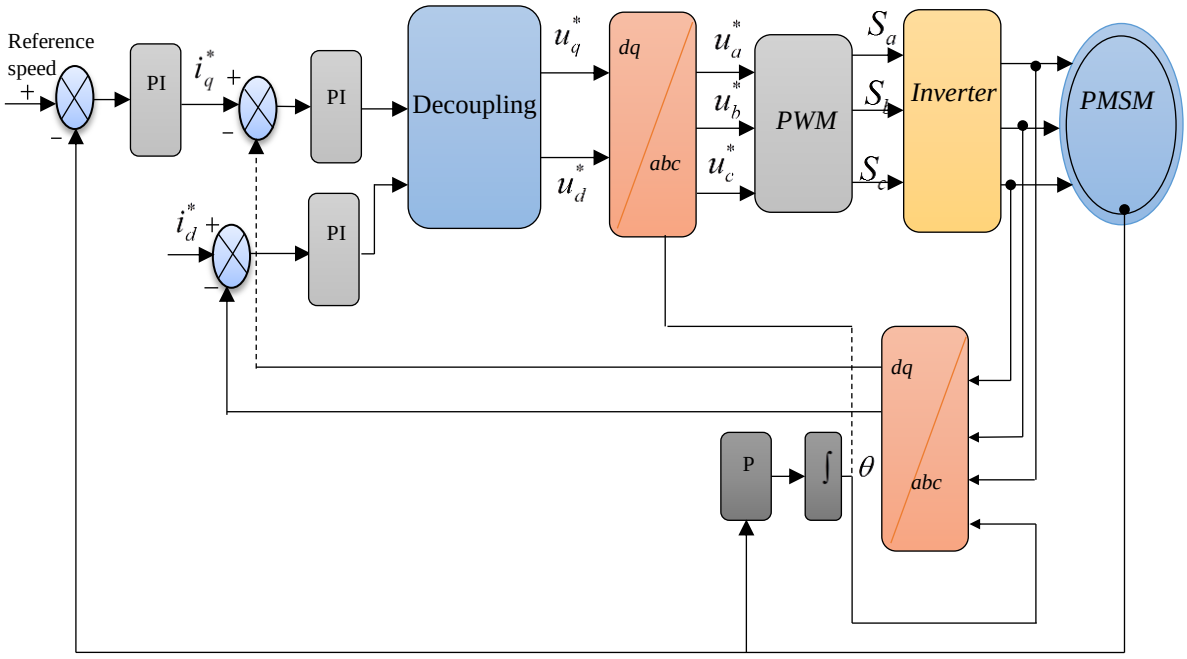

Figure I.7 Field oriented control scheme (FOC) of PMSM.

However, although it gives high performance for both asynchronous and synchronous motors, field or vector orientation control has a number of disadvantages such as: low

robustness against parameter changes, presence of coordinate transformations and using of linear controllers. Moreover, the linear torque control, obtained by the effective decoupling of the machine, is no longer valid when such key parameter changes with external envirenement. This parameter can vary extremely with temperature and can induce errors on the amplitude and orientation of the flux in the machine [5],[6],[69]. To ensure good performance in dynamic and steady state vector control, it is necessary to design a robust control that is insensitive to parametric variations, especially those of the stator resistance, which remains the key parameter in the FOC pradigme.

I.3.3. Direct Torque Control

I.3.3.1. Switching table based direct torque control

The general block diagram of direct torque and flux control (Takahashi & Noguchi, 1986) is depicted in **Fig I.8**. The command values (references) of stator flux and electromagnetic torque are compared with estimated values of flux and torque respectively. The result of this comparison can create the flux error and torque error. These results should be transferred to two independent hysteresis control units to determine the appropriate switching combinaions[4], [8], [10], [11]. The general block diagram of the DTC for a PMSM is shown in **Fig.1.8**.

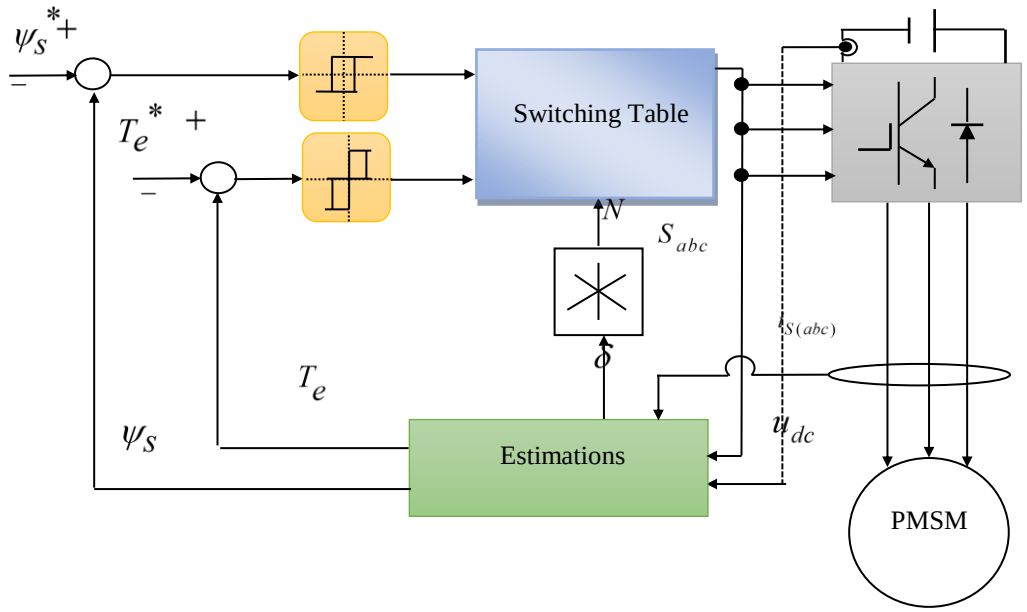

Figure I.8 Direct Torque Control Scheme (DTC) of PMSM.

In fact, the use of this type of hysteresis controller in DTC assumes the existence of a variable switching frequency in the converter due to the inherent discrete nature of this type of controller. So, it is preferable to operate the DTC with a high computing frequency in order to reduce the torque oscillations caused by hysteresis controllers [5].

I.3.3.2. Direct torque control with fixed switching comutation

In 1992, Habetler introduced for the first time the integration of the SVM into the DTC paradigms for the induction motor [71], then further research and efforts were made to integrate it for the PMSM drive [12],[72]. Distincts SVM-DTC structures have been proposed [12], [69], [71-73] and impressive results are achieved.

Space vector modulation (SVM) is a non-linear control algorithm based on the modulation of the average voltage vector to control the electromagnetic torque of the PMSM. This technique offers a fixed switching frequency, it improves the dynamic response and static behavior of the DTC. In this improved DTC structure, the predefined switching table and the hysteresis controllers are replaced by modulation stage for actuating the switches of the voltage converter.The purpose of this improved control structure is to reduce the ripple of torque/flux and speed fluctuations, which results a reduction in acoustic noise.

Despite its efficiency and superiority, the main disadvantage of this controlled technique is the high complexity of its design. The general block diagram of the improved DTC (DTC with fixed switching comutation) using SVM for a PMSM is illustrated in **Fig I.9**.

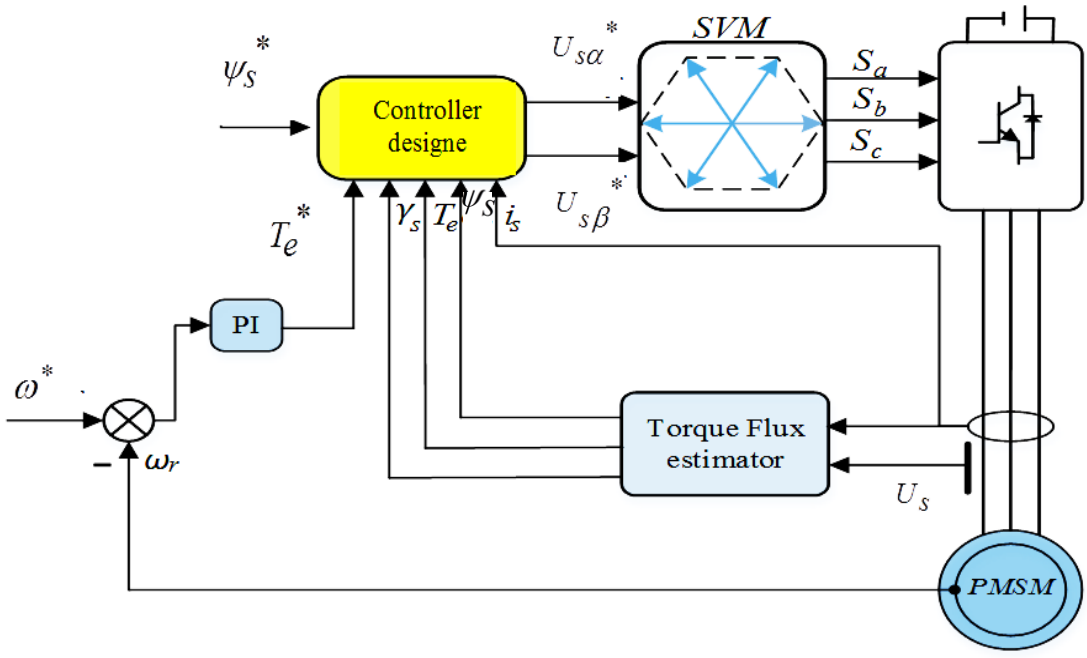

Figure I.9 Direct torque control with fixed switching comutation of PMSM.

I.4. Advanced Nonlinear Control Techniques

Well-dominated conventional proportional-integral (PI), proportional-derivative (PD), and proportional-integral-derivative (PID) controllers fail to accurately understand the behavior of most controlled nonlinear systems, especially through analytical techniques [74]. Despite the available mathematical modeling tools, there are existence of mismatches between the actual model and the model developed for the design of controls, resulting in a high level of uncertainty. This has led to an intense interest in the development of the so-called Advenced nonlinear control theory that seeks to solve this problem [75], [76].

For the development of nonlinear control, modern mathematical tools and algorithms have been introduced and successfully applied to the strict coupling non linear system, contributing significantly to the development of advenced nonlinear control aproaches. Significant progress has been made for that aim. Among the most important nonlinear control strategies developed in recent decades are: Model predictive control [77], Fuzzy system [43], Sliding mode control [3] and Backstepping control [15].

I.4.1. Model Predictive based Control (MPC)

The principle of model-based predictive control, abbreviated to MPC, was first introduced in the 1970s for industrial control applications [78]. Subsequently, MPC gained importance in the academic field because of its advantage in including multi-variable constraints [77]. MPC does not identify a particular control algorithm, but a family of controller types. The common characteristic of all these controllers is the principle of determining an optimal value for the control variable using an explicit model of the system to be controlled and minimizing a cost function.

The main distinction between the MPC design used to control AC drives and the well dominated feedback control schemes based on Pl controllers is the pre-calculation of the behavior of the controlled system and the inclusion of this behavior in the control signal before a difference between the actual value and the reference value by means of an optimization procedure, whereas the feedback control only reacts and tries to correct a control difference when it has already occurred. The general block diagram of MPC is illustrated in **Fig I.10**.

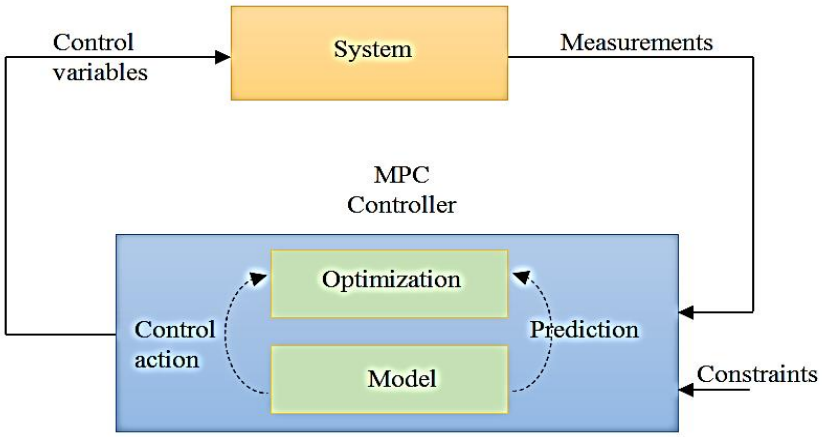

Figure I.10 General block diagram of MPC.

I.4.2. Generalized Predictive based Control (GPC)

Generalized Predictive Control (GPC), which emerged as an advanced control technology in the mid-1980s, has been developed in two main directions [79]:

- From D.W. Clarke 1985: Generalized Predictive Control (GPC).
- From J. Richalet 1987: Predictive Functional Control (PFC).

Clarke's GPC control, is considered the most popular prediction method, especially for industrial processes. It combines prediction of future process behavior with feedback control. A simplified general block diagram of GPC is illustrated in **Fig I.11**.

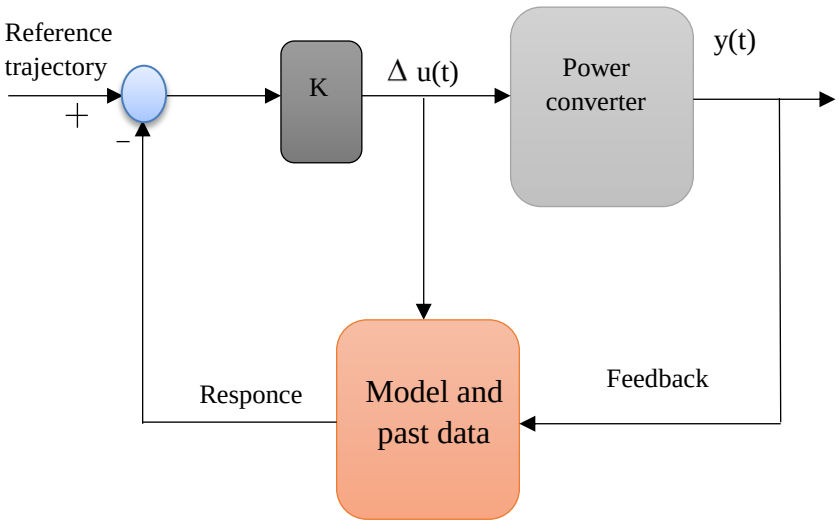

Figure I.11 General block diagram of GPC.

The philosophy of GPC is based on four main ideas reproducing the basic decision-making mechanisms of human behavior: creation of an anticipatory effect by exploiting the trajectory to be followed in the future, definition of a numerical prediction model, minimization of a quadratic criterion with a finite horizon, and the principle of the receding horizon. However, GPC has certain restriction. For example, the formulation algorithm is much more complex when applied to such nonlinear systems and it does not include the system constraints.The main problem associated with GPC when applied to power converters is that it presents a complex formulation of the GPC problem. In summary, GPC is useful for both linear and unconstrained problems [19].

I.4.3. Finite Control Set-MPC (FCS-MPC)

Appearing in 2004, through the impressive work of the Chilean J. Rodriguez and his team [80]. Finite Control Set-MPC (FS-MPC) has received a lot of attention from industrialists and academics. Broadly stated, FCS-MPC is a very interesting alternative for the numerical control of power supply systems integrating converters [77]. A simplified general block diagram of the FCS-MPC is illustrated in **Fig I.12**.

In contrast to the generalized predictive control GPC with several parameters of tuning and using expensive calculation times and complex algorithms to take into account constraints. The FCS-MPC uses a model of the system to predict its future behavior at only one or two prediction steps. This prediction is used by the control algorithm to obtain the optimal control, according to a predefined optimization criterion.

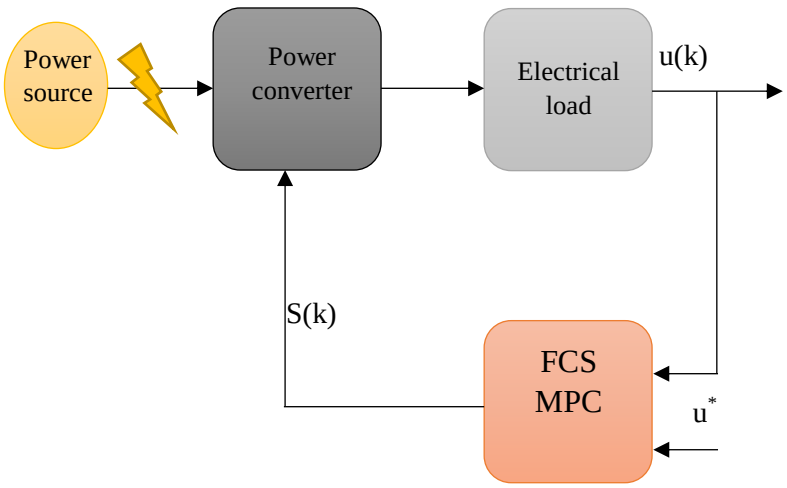

Figure I.12 Simplified control diagrame of FCS-MPC.

The main advantage of the FCS-MPC method is that:

- The simplicity of implementation.
- The process does not need linear or non-linear controllers in the inner loops.
- No need for a modulator as in the case of most linear controller.
- The constraints are taken into account thanks to its flexibility which significantly reduces the overall cost of the drive system.

The basic fundamentals of this control strategy will take most of our interest in this thesis.

I.4.4. Continous Control Set-MPC (CCS-MPC)

The continuous control set also called dead-beat control is a subclass of MPC, where the control actions are continuous time signals with a modulation stage. Unlike the FCS-MPC, the CCS does not determine the optimal candidate for the control action; it is based on voltage calculation ; and of corse the steady-state errors are lower. The most developed method is the generalized predictive control (GPC), which has been proven to be fast enough for drive control [79],[81]. However, the main distinctions between CCS-MPC and GPC reside mainly in their numerical design phase. Therefore, each one has its own design and formulated algorithm.

With GPC, both designed control algorithme and calculation are rmore complicated thant that of CCS-MPC [77]. The computation time of CCS-MPC is not much different for the FCS-MPC scheme. In general, the CCS-MPC can cope with a less powerful Digital Signal Processor (DSP) than for the FCS-MPC. A simplified general block diagram of the CCS-MPC is illustrated in **Fig I.13**.

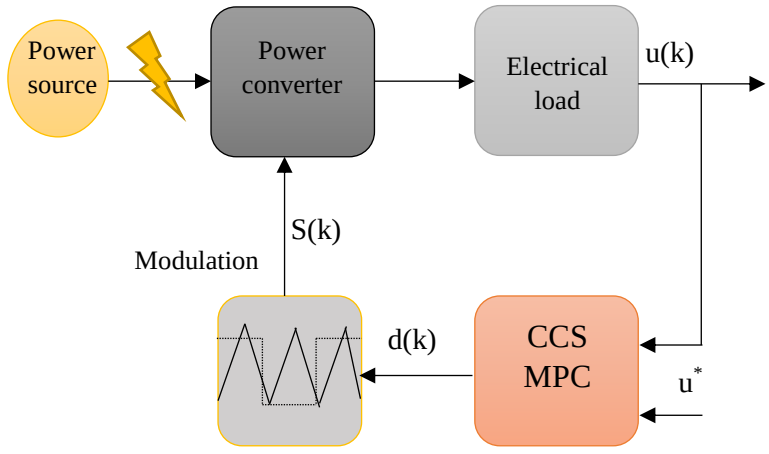

Figure I.13 Simplified control diagrame of CCS-MPC.

I.5. Survey on the Application of Artificial Intellegence Techniques for Electrical Machines

Artificial intelligence (AI) techniques such as fuzzy logic (FL), artificial neural network (ANN) and genetic algorithm (GA) have recently been extensively applied in power electronics and machinery [5]. The meaning of intelligence in brief is "the ability to acquire and apply knowledge and skills." It is also meaning "the ability to learn or under-stand or to deal with new or trying situations"[82].

The objective of AI is to implant human or natural intelligence into a high-performance smart system (computer) so that the computer can think intelligently like a human being (perceiving). A system equipped with integrated artificial intelligence is often defined as " a smart technological system " that has a capacity for " learning ", " auto-organization " or " auto-adaptation ".

Computer intelligence has long been the subject of debate, and may be forever. As John Mc.Carthy defines it is "The science and engineering of making intelligent machines,especially intelligent computer programs" [83]. Thus, it is a fact that computers can have adequate intelligence to help solve our problems that are difficult to solve by traditional methods. It is therefore true that AI techniques are now widely used in industrial process control, image processing, diagnostics, medicine, space technology and information management systems [5].

In fact, experts in fuzzy logic system attempt to construct fuzzy rules based on a specific design to mimic the behavioral nature of the human brain, while experts interested with ANN system tends to directly emulate the biological neural network.

The history of NN dates back to the 1943s, but its development has been camouflaged by the growth of modern digital computers. By the early 1990s, NN technology had captured the attention of a large segment of the scientific community [84],[85]. Ever since then, the technology has progressed rapidly and its applications are developing for power electronics and electric drive systems.

The major aspects that motivate the use of artificial intelligence are the following:

- The availability of large data; the enormous amount of data generated in accordance with the digital cards.
- The machine learning algorithms are improved continuously and extensive algorithms are updated.
- Software packages and high-performance computing systems become inexpensive.

In the literatures [14], [30], [41], [43] and [54] various AI techniques in combined with conventional and advanced control strategies are devloped. Technically, the combination of these intelligent techniques results in imprecise aspects to improve the response and robustness of well-disciplined control techniques while eliminating torque and flux ripples through artificial systems [86-90].

I.6. Sensorless Control Techniques for PMSM

High performance control of electrical machines depends mainly on the direct and/or indirect measurement of the variables and states (i.e. current, speed, torque and flux) of the system to be controlled. Generally, the specific development of such control technology implies a precise knowledge of all acquired data (i.e. states and variables), which are mainly classified in two categories : Data acquired from physical equipments and data acquired from digital tools (algorithms).

In the first group, there are some drawbacks related mainly with the use of physical equipments or sensors, such as the high cost, fragility and the limited cabling space. In addition, sensors require frequent maintenance and, in some situations, it is not easy to install sensors due to some physical or environmental constraints [91], [92].

To disuse the disadvantages associated with the first groupe and achieve a precise control with high performance control system, several researchers are moving towards the use of software sensors or also known by sensorless control methodologies [67], [91], [92]. The objective of sensorless control operation for AC drives is to estimate the state vector components such as mechanical speed, current, torque, flux and position. The speed sensorless control for electrical machines has taken a lot of attention by proffissionel comunities in the few past years, since it can reduce the cost by eliminating the traditional mechanical equipments and cabling systems and thus avoid the difficulty of theirs installation.

Recently, several sensorless control techniques have been introduced for PMSM [93]. For medium and high speed operations, those techniques can be classified into two categories [94]:

- open-loop techniques .
- closed-loop techniques.

Open-loop techniques are not encouraged because their performance depends entirely on the accuracy of the measurements and parameters of the controlled system.

The closed-loop techniques are: Disturbance speed observers (DSO) [95], Sliding-mode observers (SMOs) [96], Model reference adaptive system (MRAS) observers [97] and extended Kalman filters (EKFs) [98]. Disturbance and MRAS observers are sensitive to variations of the PMSM parameters [99]. However, due to the simplicity, ease of implementation and algorithmic modernization, both disturbance and MRAS-based observers have received increased interest from researchers and engineers.

SMO is an attractive/promising technique for estimating state vector components of the PMSM due to its robustness against parameters variations. However, a well-tuned low-pass filter is crucial to attenuates the chatering phenomenon due to the used switching function [99]. The EKF is apromising and robust non-linear state observer for estimating state vector componenrs of AC machines [98],[100]

A variety of speed and position estimation methods have been proposed for permanent-magnet synchronous machines (PMSMs) and induction machines (IMs), and recently they were applied successfully to other types of machine [101], [102].

The Extended Kalman filter (EKF) is considered one of the most popular method for sensorless control. it considered the optimal recursive estimator for nonlinear systems and it is very suitable for the system with noisy measurement and parameter changes [98]. However, tuning and design of the covariance matrices is considered the main weakness. The general block diagram of EKF is illustrated in **Fig I.14**.

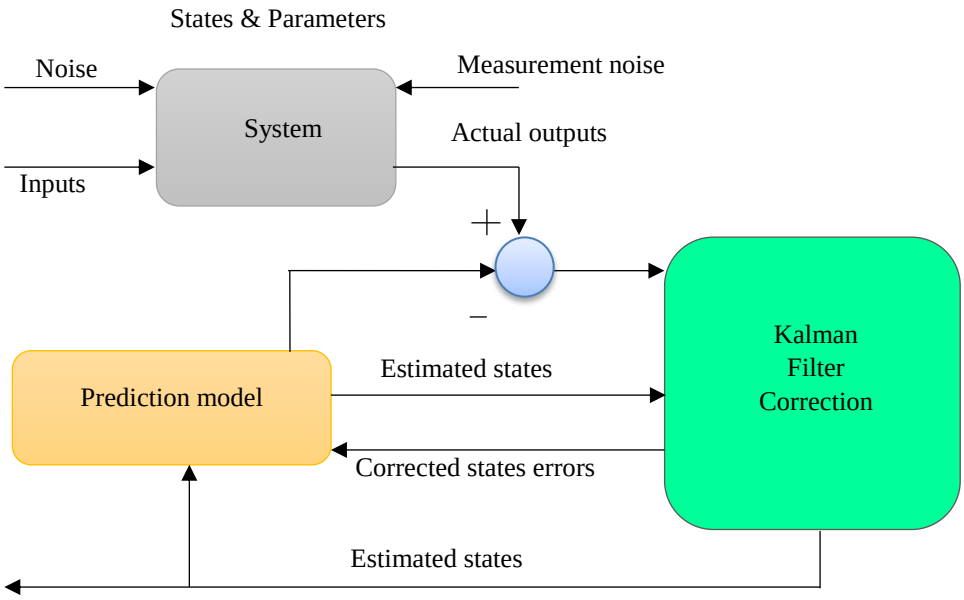

Figure I.14 General block diagram of Kalman filter.

I.7. Conclusion

In this first chapter, we have tried to highlight certain overviews about the different types of electrical machines and their progressive control techniques (conventional and advenced). Indeed, both conventional and advenced variable speed drive techniques have been presented and compared. The insights discussed in the presented chapter focus mainly on the problems specifically related to the use of VC, FOC and DTC controls, such as parametric variations and undesirable ripples. In this context of studies, non-linear control techniques such as space vector modulation and artificial intelligence are commonly inserted to improve basic control schemes. Next, we turned our attention to the emerging MPC paradigms for AC motor control. As a matter of fact, the FCS-MPC has retained most of our interest, where we have highlighted its advantages and disadvantages. The last part of our work focuses on sensorless control techniques used to improve the control performance in terms of increasing the reliability and decreasees the cost of the overall control system.

ChapterII

Implementation and Improvement of Direct Torque Control for a Permanent Magnet Synchronous Motor

This chapter is dedicated to the implementation and the improvement of the direct torque control (DTC) strategy to operate our PMSM. First, the principle of conventional DTC is presented. Then, the effects of voltage space vectors (VSVs) application are analysed and discussed in order to control the electromagnetic torque and stator flux. Finally, an elegant and efficient control technique called ‘space vector modulation’ (SVM) is integrated for the improvement of the DTC startegy.

II.1. Introduction

For the first time, direct torque control (DTC) was initially proposed by Takahashi and Depenbrock in the mid-1980s [8]. This strategy became an alternative to field-oriented control (FOC) [75]. Through this type of control strategy, it is possible to control the magnitude and angle of the resulting flux phasor by appropriately selecting one of the eight possible voltage space vectors (VSVs) for actuating the voltage source inverter (VSI). As the classical DTC strategy has its own constraints, especially with regard to the high torque and flux ripples, various control structures are proposed to improve its control performance [5]. The modified DTC sectors based on an extended switching states and the constant switching frequency based DTC using space vector modulation (SVM-DTC) are the most possible solutions [4], [5], [12], [13]. This chapter presents a comprehensive descriptive study of the basic and enhanced DTC pradigme including the PMSM model, conventional DTC and enhanced DTC design using SVM-based constant switching frequency. The proposed DTC control solutions will be analyzed and the appropriate control scheme will be used for a comparative numerical simulation study using MATLAB/Simulink software.

II.2. Model of PMSM Dedicated for Direct Torque Control

The mathematical model of PMSM in the stationary reference frame (α–β) are as follows [103]:

$$\begin{cases} \dfrac{di_{s\alpha}}{dt} = \dfrac{-R_s i_{s\alpha} + \omega_e \psi_{rm} \sin(\theta) + u_{s\alpha}}{L_s} \\ \dfrac{di_{s\beta}}{dt} = \dfrac{-R_s i_{s\beta} - \omega_e \psi_{rm} \cos(\theta) + u_{s\beta}}{L_s} \end{cases} \tag{2-1}$$

$$\begin{cases} \dfrac{d\psi_{s\alpha}}{dt} = u_{s\alpha} - R_s i_{s\alpha} \\ \dfrac{d\psi_{s\beta}}{dt} = u_{s\beta} - R_s i_{s\beta} \end{cases} \tag{2-2}$$

Where $i_{s\alpha}$, $i_{s\beta}$ and $u_{s\alpha}$, $u_{s\beta}$ are, respectively, stator currents and voltages. $\psi_{sa}, \psi_{s\beta}$ are separate magnetic flux linkage generated by stator currents. ψ_{rm} is the permanent magnet rotor flux. θ is the electrical rotor position angle and ω_e is the rotor electrical speed. R_s is armature winding resistance, and L_s denotes the total inductance for each phase.

The mechanical equation for the motor dynamics, on the other hand, is

$$T_e - T_L - f_r\omega_r = J\frac{d\omega_r}{dt} \tag{2-3}$$

Where ω_r is the rotor speed, J is the total moment of inertia of the rotor and f_r is the friction coefficient. T_L is the load torque and T_e is the electromagnetic torque.

The electromagnetic torque is given by:

$$T_e = \frac{3}{2}p\left(\psi_{s\alpha}i_{s\beta} - \psi_{s\beta}i_{s\alpha}\right) \tag{2-4}$$

II.3. Two-Level Voltage Source Inverter (VSI) Model

Before proceeding to the basic DTC algorithm, we need to represent our uninterruptible power supply device model, which is a two-level voltage source inverter (2-LVSI).**Fig II.1** below shows a simplified scheme of 2-LVSI topology. In the most applications, IGBT transistors with anti-parallel diodes are the most existed configuration. The switching devices in the voltage source inverter must be capable of being turned off and on. For this purpose , Insulated gate bipolar transistors (IGBT) are used; because they have this capability and also offer high switching capacity with sufficient power rating. Each IGBT has an inverse parallel-connected diode. This diode provides alternate path for the motor current after the IGBT is turned off [104]. We supposes that the stator of the synchronous machine is coupled in a star configuration. The DC link voltage u_{dc} is provided by a rectifier or another DC source.

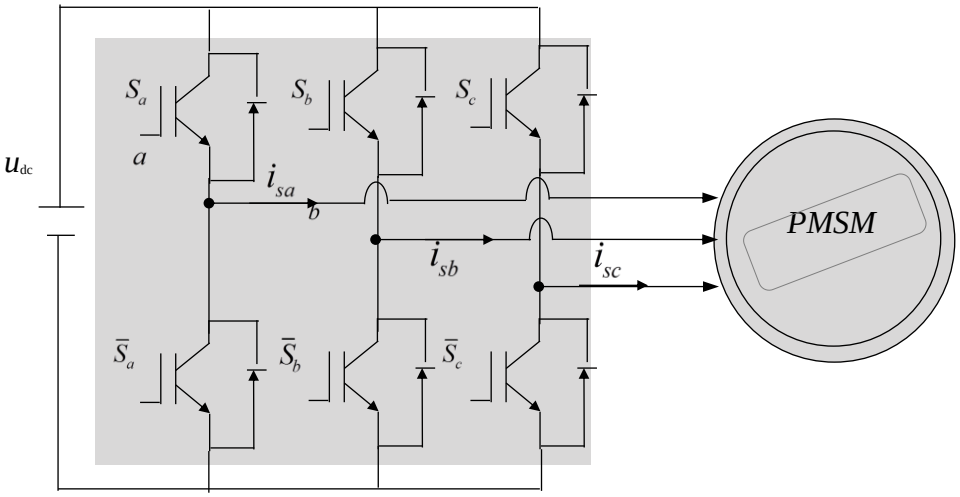

Figure II.1 A simplified scheme of 2-LVSI fed PMSM.

The states of the supposed perfect switches can be defined by :

- S_{abc} = 1 : The situation where the upper switch is closed and the lower switch is open.
- $\overline{S}_{abc}$ = 0 : The situation where the upper switch is open and the lower switch is closed.

The switches of the same leg must be controlled in a complementary way to ensure the continuous operation of the alternating currents through the load on the one hand and to avoid the so-called shoot-through of the source on the other hand.

A set of voltage space vectors $u_{s,abc}$ at *K*th instant is defined as [30]:

$$u_{s,abc}(k) = \frac{1}{3} u_{dc} m_{abc} S_{abc} \tag{2-5}$$

where $S_{abc} = (S_a, S_b, S_c)^T \in \{0, 1\}^3$ is the switching state of the voltage source inverter (VSI), and (m_{abc}) is expressed as:

$$m_{abc} = \begin{bmatrix} 2 & -1 & -1 \\ -1 & 2 & -1 \\ -1 & -1 & 2 \end{bmatrix} \tag{2-6}$$

Consequently, eight VVs are possible to be obtained from the combination of switching states S_{abc}. Six of them are active VVs ($u_1 \ldots u_6$), and two are zero voltage vectors (u_0, u_7). These eight space voltage vectors are shown in **Fig II.2**.

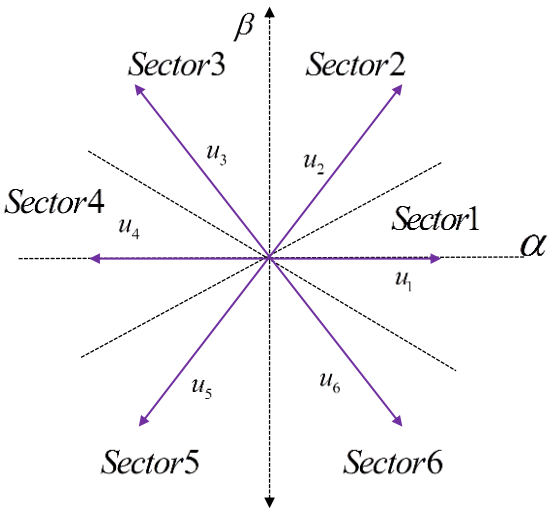

Figure II.2 Space voltage vectors reprensentation in (α,β) plane .

According to the eight authorized switching states of S_a, S_b and S_c. **Table II.1** shows all possible combinations.

Table II.1 The components of the stator voltage vectors in (α, β) plane

Voltage Space Vectors (VSVs)	S_a	S_b	S_c	u_α	u_β
u_0	0	0	0	0	0
u_5	0	0	1	$\frac{-u_{dc}}{3}$	$\frac{-u_{dc}}{\sqrt{3}}$
u_3	0	1	0	$\frac{-u_{dc}}{3}$	$\frac{u_{dc}}{\sqrt{3}}$
u_4	0	1	1	$\frac{-2u_{dc}}{3}$	0
u_1	1	0	0	$\frac{2u_{dc}}{3}$	0
u_6	1	0	1	$\frac{u_{dc}}{3}$	$\frac{-u_{dc}}{\sqrt{3}}$
u_2	1	1	0	$\frac{u_{dc}}{3}$	$\frac{u_{dc}}{\sqrt{3}}$
u_7	1	1	1	0	0

II.4. Direct Torque Control Paradigm

The classical DTC paradigm is based on the control of the generator's electromagnetic torque and stator flux directly by selecting an optimal voltage vector to actuates the VSI. Based on the discreet nature of the inverter, the original DTC was developed for bang-bang control (all or nothing control) of the electromagnetic torque and stator flux. The difference between the referential stator flux (ψ_s^*) and the estimated stator flux ($\psi_{s,est}$) (i.e the resulting flux error e_ψ) is introduced into a two level hysteresis controller that indicates whether the flux needs to be increased or decreased in order to control the stator flux vector and keep its vector rotating in a circular path. While the difference between the referential torque (T_e^*) and the estimated electromagnetic torque ($T_{e,est}$) (i.e the resulting torque error e_{Te}) is processed through a three level hysteresis controller that indicates whether the torque should be increased ,maintained constant, or decreased [4], [5], [10], [12], [69].

II.4.1. Principle of Direct Torque Control

The principle of the DTC is to appropriately select a such given voltage space vector (VSV) from the eight possible generated by the VSI to maintain the torque and the stator flux magnitude of the PMSM in the bandwidth of the hysteresis commands which adjust their amplitudes. The selection of the VSV is based on the evaluation of the torque and the flux response, while an optimum switching table is used to generate the switches commands to be applied to the VSI. As soon as the appropriate voltage vector is selected, the control strategy directly generates the pulses for the converter, without using any modulation scheme [4], [5], [10], [12]. The general control scheme of basic direct torque control strategy is illustrated in **Fig II.3**.

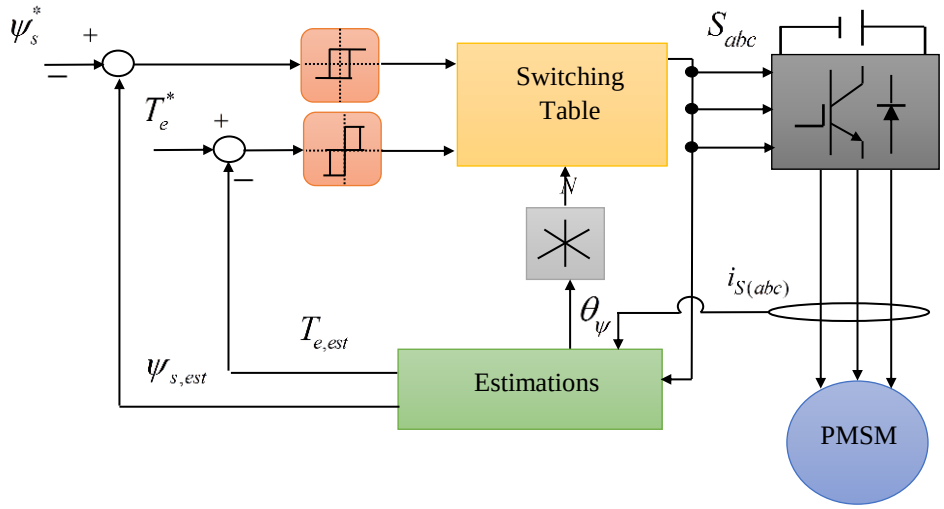

Figure II.3 Simplified control scheme of basic DTC.

II.4.2. The Effects of VSVs Application On Stator Flux

To understand the effect of applying one of the eight possible voltage space vector VSV on the stator flux variable, it is necessary to analyze the equation that defines the stator flux vector (2.2). For this, the integral voltage model provides a better explanation of the effects of VSVs in PMSM variables:

$$\psi_s = \psi_{so} + \int_0^t \left(u_s - R_s \cdot i_s\right) dt \qquad (2.7)$$

It can be noted from (2.7) the relationship between the voltage applied to the PMSM and the magnitude of the stator flux vector. In this sense, if a certain active voltage space vector (AVSV) is applied to the machine for a period of time Δt, the magnitude of stator flux can be modified (increased or decreased). Moreover, for high speed regions, the voltage

drop at the stator resistor is neglected and hence, the relationship between the applied voltage and the generated flux is given by (2.8).

$$\psi_s = \psi_{so} + \int_0^{\Delta t} (u_s)\, dt \tag{2.8}$$

With ψ_{so} : is the stator flux vector at the instant *t=0*.

So, the application of the VSV is done discreetly, if the VSV is applied during a sufficiently small period of time Δt, the voltage vector is considered as constant, therefore:

$$\psi_s(k+1) = \psi_s(k) + u_s\ \Delta t \tag{2.9}$$

The change in the stator flux vector became apparent in terms of the applied VSVs:

$$\Delta t\ \psi_s \approx u_s\ \Delta t \tag{2.10}$$

By applying one of the VSV's of the VSI, the magnitude and angle of displacement of the stator flux can be controlled in an almost continuous and uniform manner [105]. Each of the VSV has a different effect on the flux of the PMSM, for example, in **Fig II.4** we can see the effect of applying the VSV (u_2) or (u_3) for the instant of time (k+1). On the one hand, by applying the VSV (u_2) an increase in flux is obtained, while for (u_3) the opposite effect is obtained.

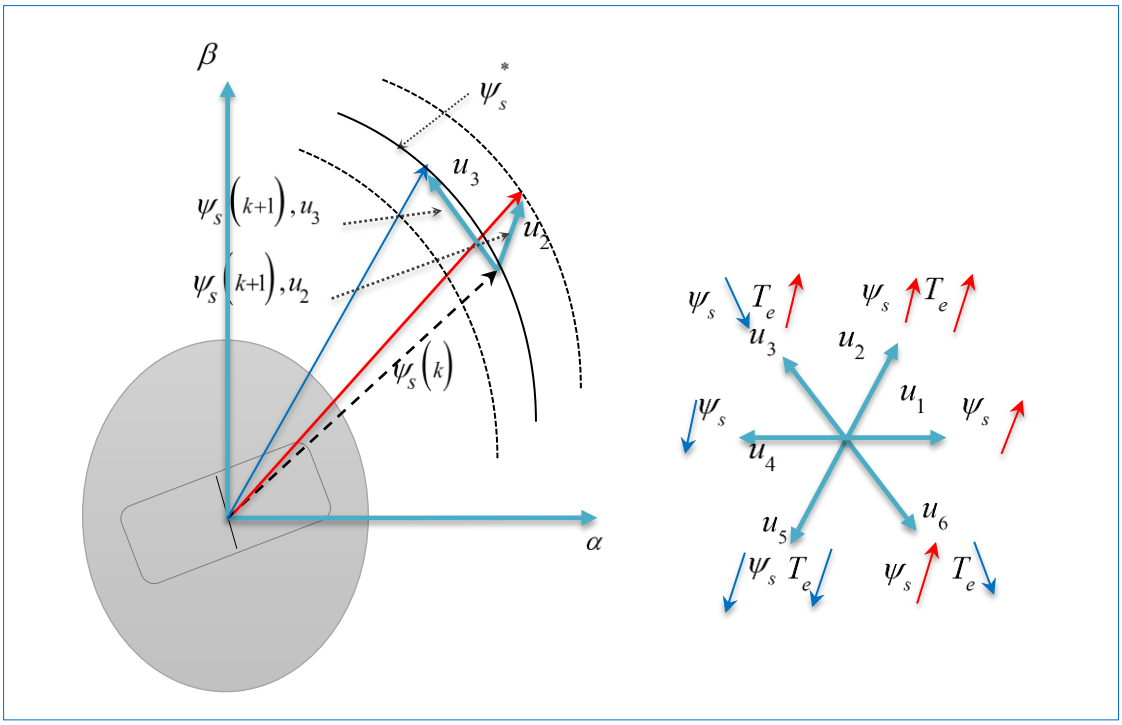

Figure II.4 Effects of the application of spatial voltage vectors generated by the VSI to the PMSM stator flux.

II.4.3. Flux and Torque Control

In the conventional DTC scheme, the stator voltage is controlled so that the amplitude of the flux developed by the PMSM constantly follows the reference. Thus, the torque is controlled by an on-off logic that works as follows: if the torque developed by the PMSM is below the reference, it is necessary to apply one of the six AVSV to achieve an increase in it; in the opposite case, that is, when the torque of the PMSM is greater the reference it is necessary to apply one of the zero voltage space vector (ZVSV), thus, the torque will decrease but not as much as when the AVSV's are selected [106]. Therefore, by applying one of the AVSV and one of the ZVSV, a direct control of the torque is obtained, and since applying a VSV directly modifies the magnitude of the torque and the stator flux angle, a very fast dynamic response of the torque is obtained. The selection of possible AVSV or ZVSV is limited by six sectors (**Fig II.5**). Generally, in order to increase the torque, the stator flux vector should be rotated as much as possible counterclockwise. If the torque is to be decreased, the stator flux vector should be rotated in clockwise direction (see **Fig II.4** right side) [14].

For example, in **Fig II.5** we assume that the stator flux vector is in the first sector on its superior limit (A). In addition, we want to increase the torque, and we want to keep the flux at the superior limit. For this, the vector (u_3) is applied to move the top of the rotor flux vector towards (B). If we want to increase the torque again and decrease the flux, in this case, the vector (u_4) is applied, and the top of the vector is shifted to (C)... and so on.

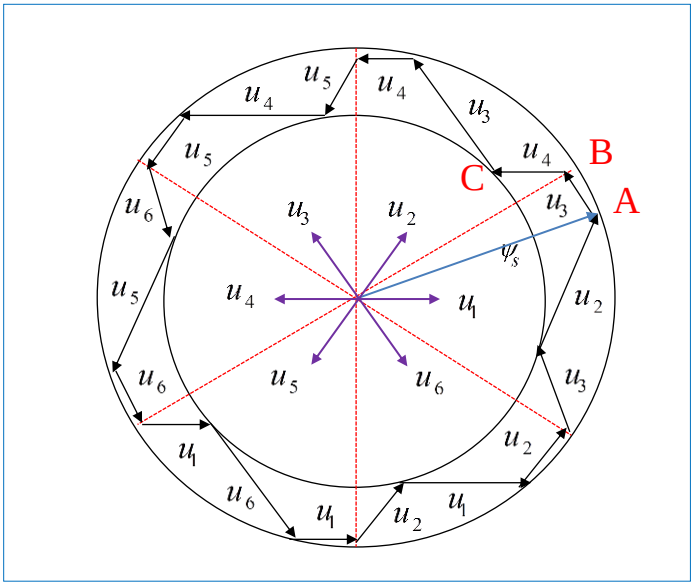

Figure II.5 Trajectory of the stator flux vector according to the applications of differents stator voltage space vectors.

A perfect control of the stator flux vector (ψ_s) from VSV in module and position allows us to control both control variables(torque/flux) in a decoupled way [4], [5] ,[10].

The torque regulation can be realized using three-level hysteresis comparator. It allows to control the motor in both rotation senses. The tow-level comparator can be used for one rotation sense which is the case of flux regulation.

By injecting different stator voltage vectors among the eight possibilities, in general, only some of them are allowed. This is for seeking to keep the stator flux within the width of the allowed hysteresis band.

The torque of PMSM can be expressed in terms of stator and rotor flux vectors as follows [5], [12], [69]:

$$T_e = \frac{3p}{2l_q}\left(\psi_s \times \psi_r\right) \tag{2.11}$$

$$\left|T_e\right| = \frac{3p}{2l_q}\left|\psi_s\right|\left|\psi_r\right|\sin\left(\delta\right) \tag{2.12}$$

where:

p: is the number of poles pairs

ψ_s, ψ_r : are stator and rotor flux vectors

δ : angle between the stator and rotor flux vectors

From expression (2.12), the electromagnetic torque depends on the amplitude of (stator / rotor) flux vectors and their relative position. If we can perfectly control the stator flux (from theVSVs) in module and position, we can therefore control the amplitude of stator flux, and the electromagnetic torque in a decoupled way.

Depending on the location of the stator flux vector, the amplitude of the stator flux is controlled only by the stator voltage vector (u_s). By means of (2.10) the direct relationship between the application of the VSV and its response in the stator flux, so that for an AVSV the response flux will cause a rapid change of the space phasor (increment or decrement); (i.e. depending to its effect on stator flux) while for in ZVSV the Space phasor (i.e. stator flux space vector) almost stopped.

The objective of flux control in the DTC consists of maintain a circular trajectory of the stator space flux phasor by the discreet control of the VSVs applied. This principle is observed in **Fig II.6**, where it is assumed that the space vector ψ_s (k) is in sector 1. Initially ψ_s (k) is located at the lowest lımit of the hysteresis band, therefore a VSV is applied to

increase the stator vector ψ_s (k) until reaching the superior lımit of the hysteresis band at ψ_s(k +2); once the superior lımit is reached, the control selects a VSV so that the phasor ψ_s (k+3) decreases its magnitude until reaching the lower lımit of the hysteresis band at ψ_s (k +4). This process is repeated in a cyclic manner maintaining a circular path of the stator vector ψ_s [105].

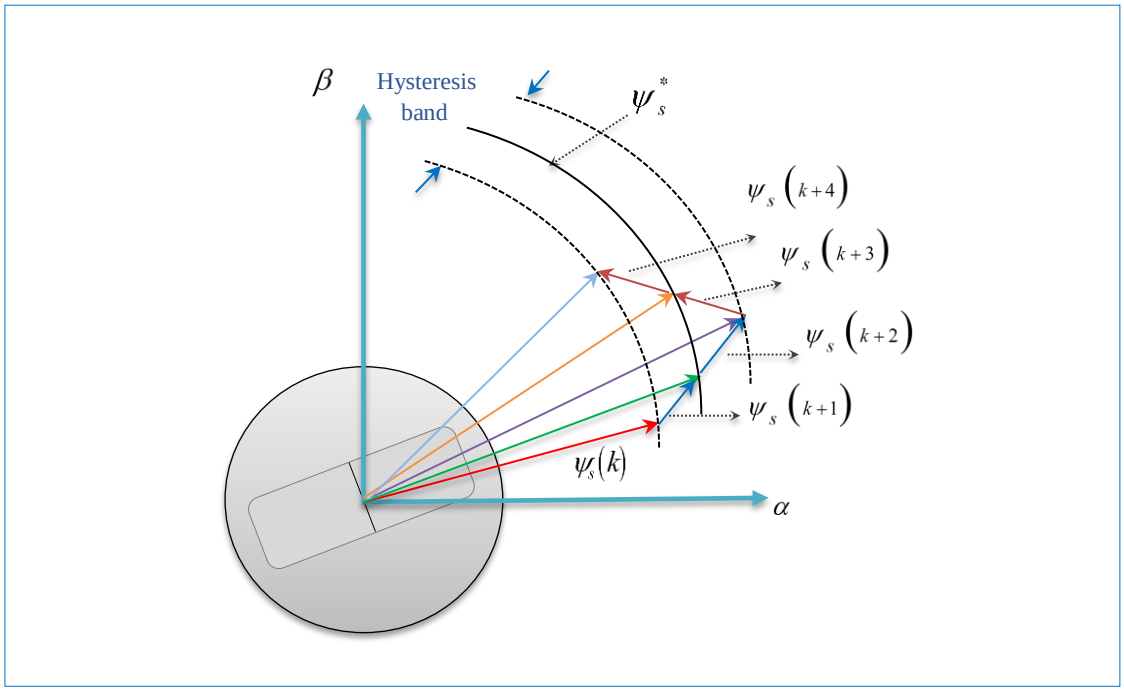

Figure II.6 Principle of DTC (flux control).

II.4.4. Stator Flx and Electromagnetic Torque Estimations

The estimation of the stator flux is usually done by (2-7), thus the estimation of stator flux components are as follow:

$$\psi_{s\alpha} = \int_0^t \left(u_{s\alpha} - R_s i_{s\alpha}\right) dt \tag{2.13}$$

$$\psi_{s\beta} = \int_0^t \left(u_{s\beta} - R_s i_{s\beta}\right) dt \tag{2.14}$$

the stator flux magnitude and flux angle can be expressed as:

$$|\psi_s| = \sqrt{\psi_{s\alpha}^2 + \psi_{s\beta}^2} \tag{2.15}$$

$$\theta_\psi = \tan^{-1}\left(\frac{\psi_{s\beta}}{\psi_{s\alpha}}\right) \tag{2.16}$$

II.4.5. Optimum Switching Table

The Optimum Switching Table (OST) was developed considering the effects that each VSV causes on the torque and flux of the stator [4], [5], [10], [12], [41], [69]. For example, when the stator flux vector ψs is in sector 1 of the plane α-β and a reference VSV is applied for a positive rotation ($\boldsymbol{\omega_e} > 0$, $E_{Te} = 1$) ‘‘with E_{Te} the output of the torque hysteresis comparator’’, the most favorable AVSVs to generate an increase in the torque angle δ are (u_2) and (u_3) (see **Fig II.4**.). To make the selection between both vectors the magnitude of flux is considered. First, by applying the VSV (u_2) the magnitude of flux is increased ($E\psi s = 1$) ‘‘with Eψs the output of the flux hysteresis comparator’’. Then, by applying the VSV (u_3) the magnitude of flux is reduced ($E\psi_s = 0$) as shown in **Fig II.4**. On the other hand, when a ZVSV is applied the spatial phasor ψs stops and the PMSM torque decreases ($\delta M = 0$) according to the direction of rotation. The same principle can be applied to deduce the VSV when a negative rotation is required ($\boldsymbol{\omega_e} < 0$, $E_{Te} = -1$). In this way, the optimal switching table given by **Table II.2** is determined.

Table II.2 Optimum Switching Table

$E\psi_s$	E_{Te}	sector 1	sector 2	sector 3	sector 4	sector 5	sector 6
1	1	u_2	u_3	u_4	u_5	u_6	u_1
	0	u_7	u_0	u_7	u_0	u_7	u_0
	-1	u_6	u_1	u_2	u_3	u_4	u_5
0	1	u_3	u_4	u_5	u_6	u_1	u_2
	0	u_0	u_7	u_0	u_7	u_0	u_7
	-1	u_5	u_6	u_1	u_2	u_3	u_4

II.5. Improved Direct Torque Control Based On Space Vector Modulation

Various control methods have been developed to generate a sinusoidal voltage waveform at the inverter output with reduced ripple . To improve the performance of conventional DTC, the concept of Space Vector Modulation (SVM) is integrated in the overal DTC control scheme [12], [71-73]. As a matter of fact, the SVM maintains a constant switching frequency, which reduces significant torque/flux ripples and optimises current harmonic distortion. Several SVM based DTC pradigms have been proposed according to their distinct control schemes, the well widespread control structures are: The closed loop torque control based space vector modulation (CLTC-SVM) [5], [12] and The imitated stator flux vector oriented control concept based space vector modulation (ISFVOC-SVM) [73]. The latter one method combines the concept of both FOC and DTC and benefits from their advantageous.

In this section, the closed-loop torque control structure is integrated in DTC control scheme, which can not only enhance the DTC strategy, but also eliminate the tedious setting of the additional PI controller used in the ISFVOC structure for stator flux control. Moreover, as an alternative to the traditional DTC, the proposed control technique (i.e. CLTC-SVM) employ only one PI controller instead of two hysteresis controllers to achieve a decoupled control of stator flux and electromagnetic torque, and replaces the switching table by SVM unit for actuating the switches of the VSI. It is based on a predictive controller, where a pre-calculation of the stator voltage vector components is done for each sampling time.

II.5.1. Schematic Diagram of CLTC-SVM for PMSM

The block diagram of the Closed-Loop Torque Control-Space Vector Modulation for a PMSM supplied by a two level voltage source inverter is shown in **Fig II.7** [12], [5], [69].

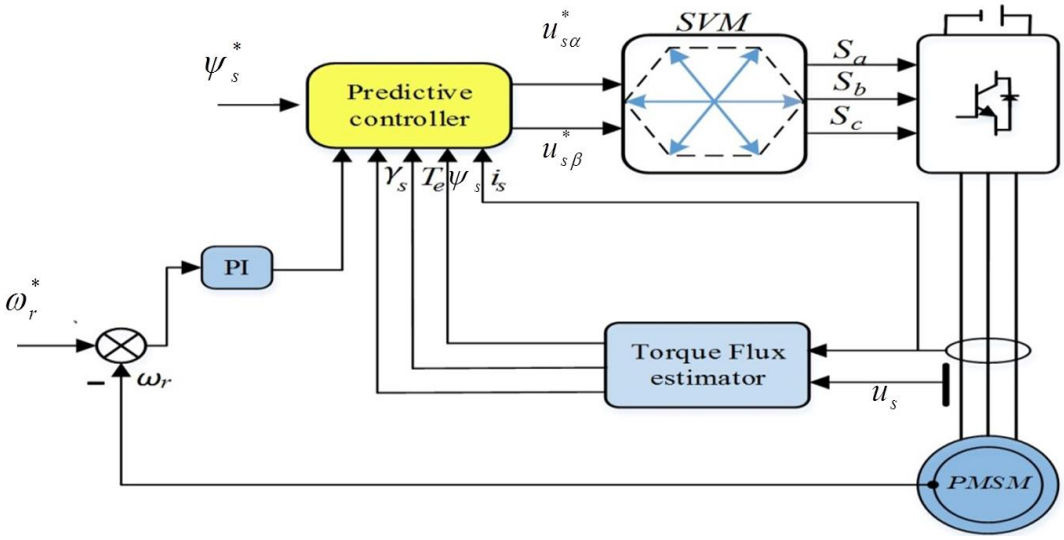

Figure II.7 Closed-loop torque control-SVM for PMSM.

The design of the torque and flux predictive controller is shown in **Fig II.8**.

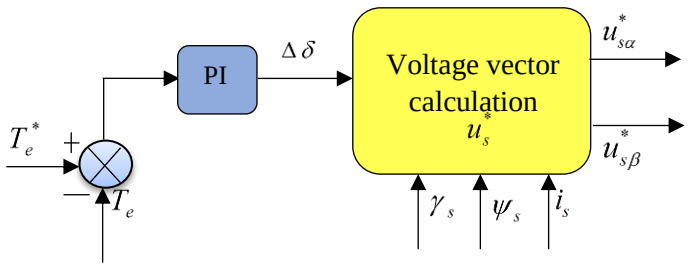

Figure II.8 Predictive voltage vector calculator.

According to the CLTC-SVM technique (**Fig II.7**), the generation of control pulses (S_a, S_b, S_c) applied to the inverter switches is mainly based on the use of a predictive controller (**Fig II.8**), which receives information about increment of load angle $\Delta\delta$, reference stator flux ψ_s^*, estimated stator flux $\psi_{s,est}$, the position of the estimated stator flux vector γ_s and the value of the measured currents i_s. Then, the predictive controller determine online the Reference of Stator Voltage Vector (RSVV) components, which are delivered then to the modulation stage (i.e. space vector modulation stage), which in turns generates the switching signals (S_a, S_b, S_c) to actuates the inverter. Therefore, the reference stator voltage vector components ($u_{s\alpha}^*$), ($u_{s\beta}^*$) in stationnary coordinate system are calculated as [5],[12],[69]:

$$u_{s\alpha}^* = \frac{\left|\psi_s^*\right|\cos\left(\gamma_s + \Delta\delta\right) - \left|\psi_s\right|\cos\gamma_s}{T_s} + R_s i_{s\alpha} \tag{2.17}$$

$$u_{s\beta}^* = \frac{\left|\psi_s^*\right|\sin\left(\gamma_s + \Delta\delta\right) - \left|\psi_s\right|\sin\gamma_s}{T_s} + R_s i_{s\alpha} \tag{2.18}$$

The stator voltage vector magnitude and angle can be computed as:

$$\left|u_s^*\right| = \sqrt{u_{s\alpha}^* + u_{s\beta}^*} \tag{2.19}$$

$$\theta_{u_s^*} = \tan^{-1}\left(\frac{u_{s\beta}^*}{u_{s\alpha}^*}\right) \tag{2.20}$$

II.5.2. Space Vector Modulation Algorithme

The main principle of SVM algorithm consists in using two adjacent vectors (two active voltage space vectors) and a null voltage vector, to determine the average stator voltage space vector (u_s), which is necessary to control the electromagnetic torque and the stator flux of the controlled system [5], [12], [69]. Then, in an instantaneous manner the reference voltage space vector (u_s^*) is approximately calculated by combining the switching states according to the basic space vector provided by the VSI. Meanwhile, it is recognized that the two-level voltage source inverter can be represented as a space vector by a hexagon divided into six sectors, each of which is expanded by 60° as shown in **Fig II.9.** Thus, the corresponding voltage vector located in sector one is expressed by :

$$u_s^*.T_s = u_0.T_0 + u_1.T_1 + u_2.T_2 \tag{2.21}$$

When (u_s^*) is located in sector one, u_1, u_2 and u_0 are the vectors that define the triangle region. T_1 , T_2 and T_0 are the corresponding time durations. T_s , is the sampling time.

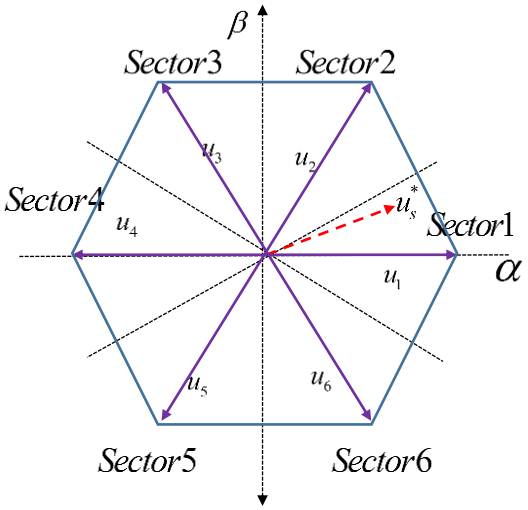

Figure II.9 Space voltage vectors.

II.5.3. Impulse series generation S_a, S_b and S_c

Before broceding to the pulses generation process, the application times of the adjacent vectors for each sector are determined according to the values of the following X, Y and Z variables, **Table II.3** summarize all the possible actuation times [4], [5], [12], [69]:

$$\begin{cases} X = \dfrac{T_s}{u_{dc}}\sqrt{3}\cdot u_{s\beta}^* \\ Y = \dfrac{T_s}{u_{dc}}\left(\dfrac{\sqrt{3}}{2}\cdot u_{s\beta}^* + \dfrac{\sqrt{6}}{2}\cdot u_{s\alpha}^*\right) \\ Z = \dfrac{T_s}{u_{dc}}\left(\dfrac{\sqrt{3}}{2}\cdot u_{s\beta}^* - \dfrac{\sqrt{6}}{2}\cdot u_{s\alpha}^*\right) \end{cases} \tag{2.22}$$

Table II.3 Corresponding actuation times.

Sector (S_i)	1	2	3	4	5	6
T_i	-Z	Y	X	Z	-Y	-X
T_{i+1}	X	Z	-Y	-X	-Z	Y

The pulses that are generated according to the given sector and their appropriate duration times for voltage vectors application are summarized in **Table II.4** [12], [69]**.**

Table II.4 Impulse series generation S_a, S_b and S_c

Sector	pulses	Duty cycles
1	S_a	$T_{aon}=T_1+T_2+T_0/2$
	S_b	$T_{bon}=T_2+ T_0/2$
	S_c	$T_{con}= T_0/2$
2	S_a	$T_{aon}=T_1+ T_0/2$
	S_b	$T_{bon}=T_1+T_2+ T_0/2$
	S_c	$T_{con}= T_0/2$
3	S_a	$T_{aon}= T_0/2$
	S_b	$T_{bon}=T_1+T_2+ T_0/2$
	S_c	$T_{con}=T_2+ T_0/2$
4	S_a	$T_{aon}= T_0/2$
	S_b	$T_{bon}=T_1+ T_0/2$
	S_c	$T_{con}=T_1+T_2+T_0/2$
5	S_a	$T_{aon}=T_2+ T_0/2$
	S_b	$T_{bon}= T_0/2$
	S_c	$T_{con}=T_1+T_2+T_0/2$
6	S_a	$T_{aon}=T_1+T_2+T_0/2$
	S_b	$T_{bon}= T_0/2$
	S_c	$T_{con}=T_1+ T_0/2$

II.6. Simulation Results

The direct torque control (DTC) and the improved DTC based on the modulated space voltage vector technique (SVM) of a PMSM are tested by numerical simulation using MATLAB/SIMULINK software. The parameters used for the simulation are given in **Appendix B** [107].

At first, a unified monitoring scenario is employed for both control methods. The monitoring scenario include: the starting up and the steady states at rated speed with rated load torque introduction are presented. After that, a maneuver of speed sense reversing of

1000 rpm at t=0.15 is applied. For the classical DTC, the chosen bandwidths of the hysteresis controllers are ± 0.005Wb for flux and ±0. 05N.m for torque.

II.6.1. Starting, steady state at rated speed, application of rated load torque and rated speed sense reversing operation

In this part, both control techniques (DTC and DTC-SVM) was tested for a target rated speed of 1000 rpm with a rated load of torque insertion at t=0.1 s followed by a speed sense reversing operation at t=0.15. The Starting up situation and steady states with load torque application and the speed sense reversal are depicted. For that, **Figs II.10** to **II.15** show the rotor speed, torque, stator phases current, stator flux evolution respectively. As there are extremely limited references and thesis for the detailled THD analysis especially for the PMSM drive, a detailed THD analysis of the stator phase current for the complete monitoring scenario is presented in **Appendix C**. The figures are mentioned by **(a)** for the conventional DTC, and **(b)** for the SVM-DTC.

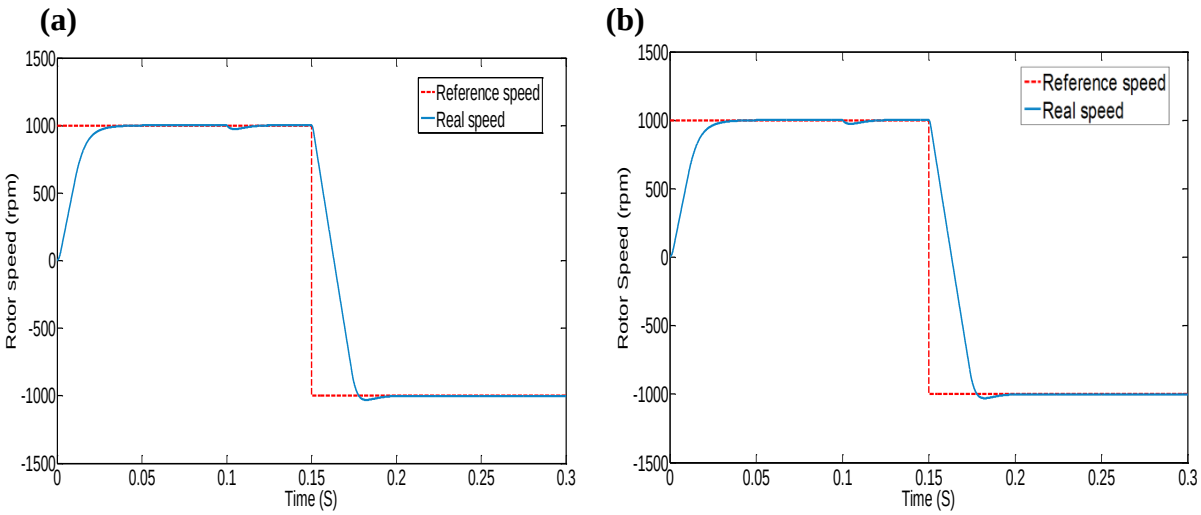

Figure II.10 Rotor speed (rpm)

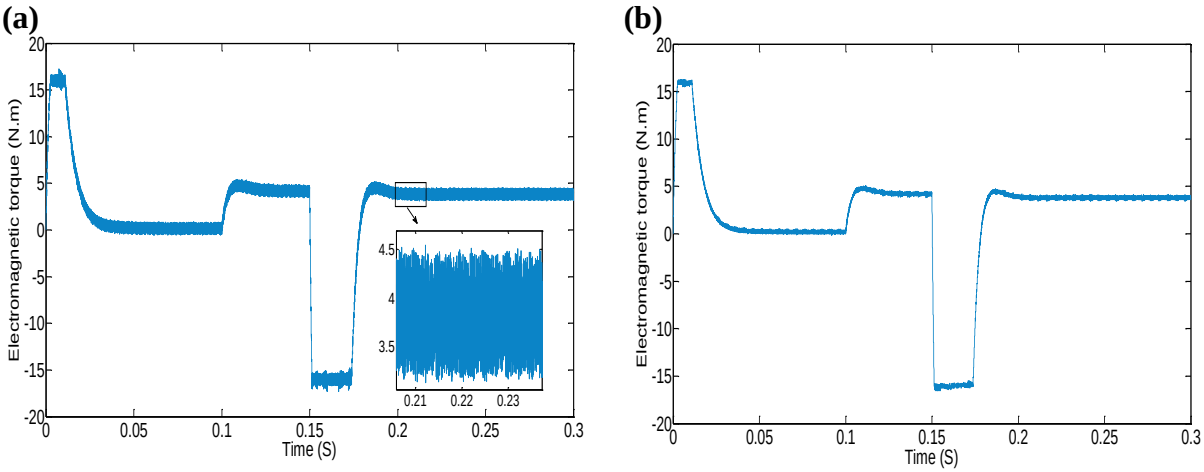

Figure II.11 Electromagnetic torque (N m).

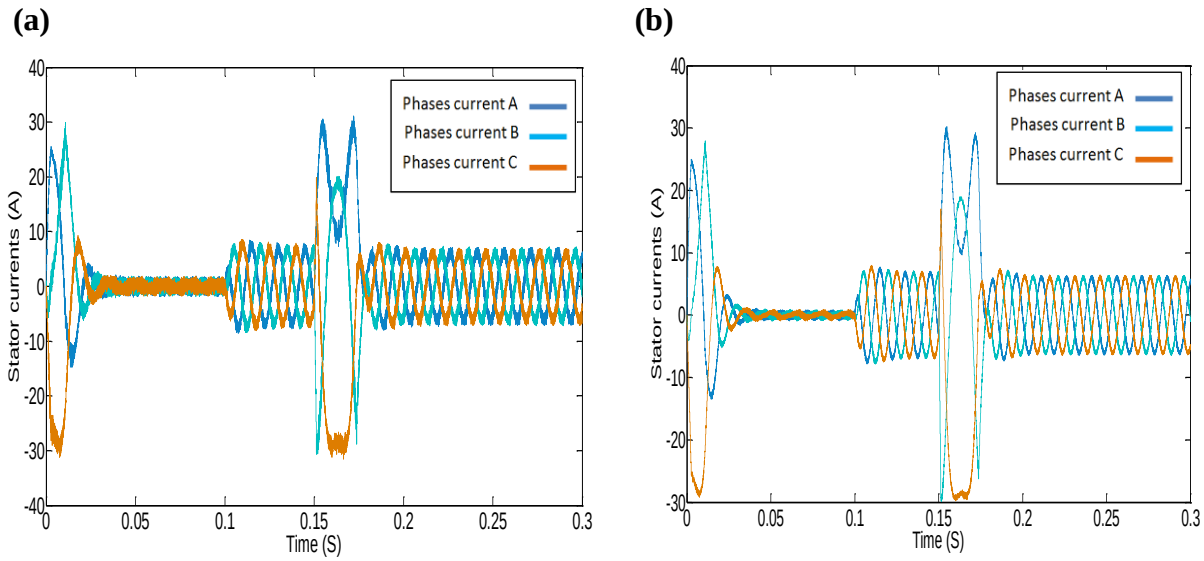

Figure II.12 Stator currents (A).

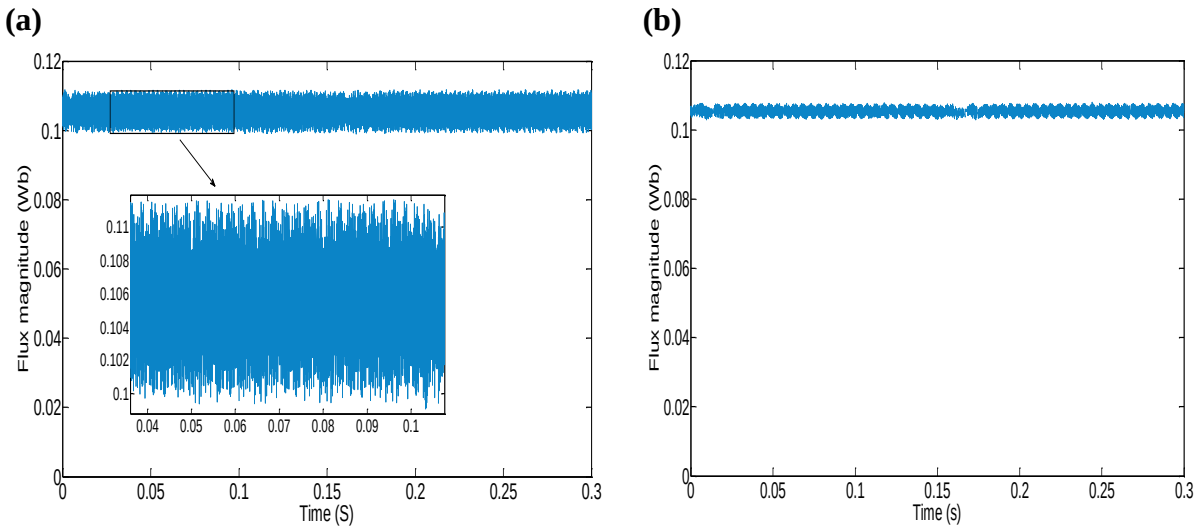

Figure II.13 Stator flux magnitude (Wb).

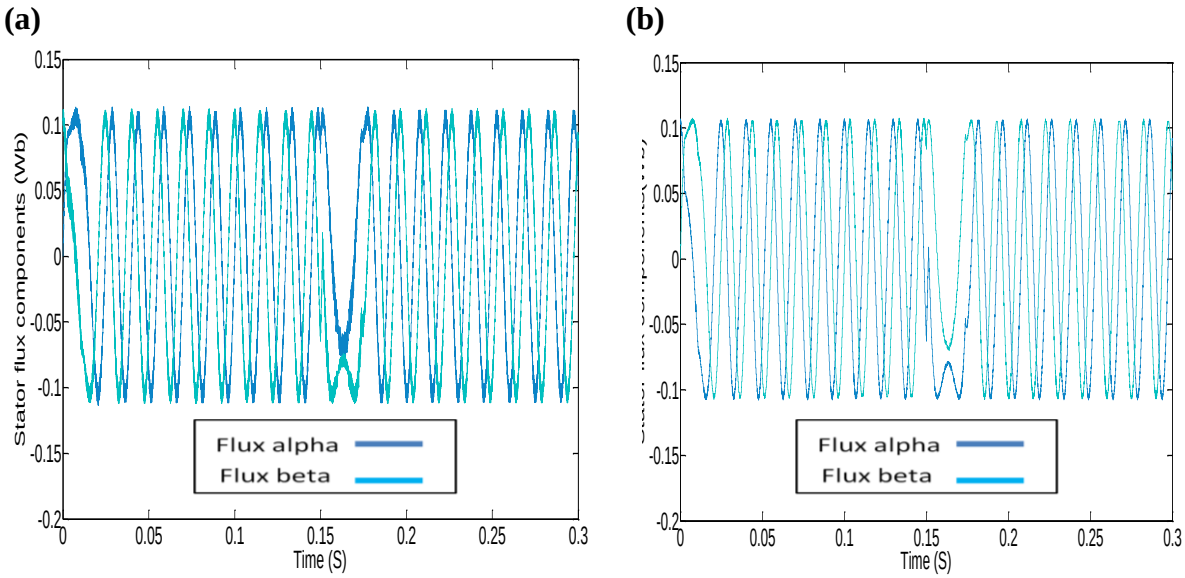

Figure II.14 Stator flux components (Wb).

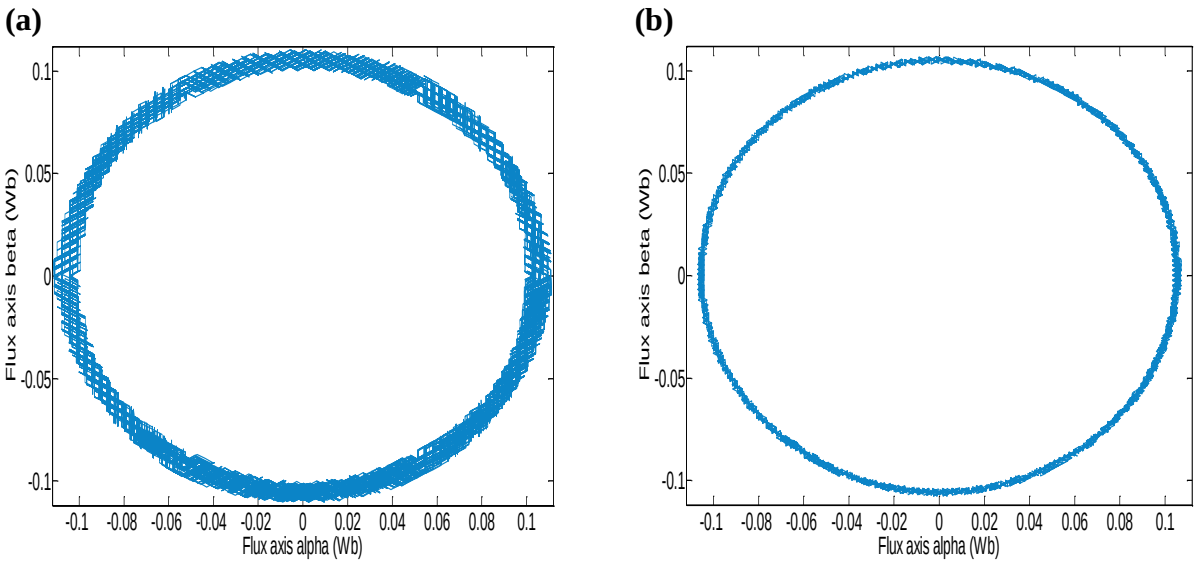

Figure II.15 Simulation results of stator flux trajectory (Wb).

Firstly, **Fig II.10a, b** illustrate the comparison between speed responses of conventional DTC and SVM-DTC depending to the rated speed target 1000 rpm, to the load disturbance introduction at (*t=0.1s*) and to the rated speed sense reversing -1000 rpm at (*t=0.15s*). So, it's clear to notice that both techniques show good dynamic behavior at starting up (dynamic state) and a stable behavior at steady state. It can also be noted that the external speed control loop rejects the disturbance of the applied load torque relatively quickly. Additionally, both control schemes kept the same fast speed response, which is confirmed by the identical PI speed controller used for both control strategies. So, there is no difference in the transient response for both control schemes.

Then, **Fig II.11a, b** illustrate the responses of the electromagnetic torque. From (**Fig II.11a, ZOOM**) it can be seen that it reaches its reference value with a large overshoot of the controller hysteresis band which is equal to ±0.05 N.m. **Fig II.11b** shows that the electromagnetic torque perfectly follows its reference and presents reduced ripples compared to C-DTC if we compare **Fig II.11a** and **Fig II.11b**.This is reside to the fact that the improved DTC utilize the modulated voltage vectors for actuates the inverter by using the SVM technique.

After that, **Fig II.12a, b** show respectively the stator phase's currents (i_{sa}, i_{sb}, i_{sc}) of conventional-DTC and improved DTC. It is clear that the proposed improved DTC presents smoother sinusoidal current waveform (better quality) than that of C-DTC. This can reflect the effectiveness of the integrated SVM technique. Moreover, this shows explicitly the importance of the proposed Closed Loop Torque Control-SVM (CLTC-SVM) strategie in terms of eliminating the harmonics of the stator current.

Next, **Figs II.13** to **II.15** show the waveforms of the magnetic stator flux, namely the flux amplitude, the flux components and the flux trajectory. From **Fig II.13a, b** it is clear to see that the amplitude of flux follows its reference perfectly in both cases, but it presents large ripples in the case of classical DTC as seen in **Fig II.13a** (**ZOOM**), which exceed the hysteresis band (±0.005 Wb) . In addition, from **Fig II.14b** the DTC-SVM presents better components sinusoid waveform than the conventional DTC. As to the trajectory of the stator flux, we can clearly see in **Fig II.15b** that it is purely circular and finer when compared to **Fig II.15a**. This indicates that the stator flux has fewer ripples.

II.7. Conclusion

We have seen in this chapter how to perform a decoupled control of electromagnetic torque and stator flux (conventional DTC) using a suitable choice of inverter voltage space vectors. One advantage of this type of control is that the fast dynamic responce. On the other hand, the main disadvantage is the presence of torque and flux ripples with a variable switching frequency. In the following, an elegant technique for improving the performance of the classical DTC have been studied. This techniques refered to the closed loop torque control based space vector modulation (CLTC-SVM). Numerical simulations results of each approach have been caried out . A comparison between the DTC and the improved DTC techniques, shows that the DTC based on closed loop torque control SVM gives better performances compared to the classical DTC (considerable reduction of torque and flux ripples). However the major drawbaks of the improved DTC technique is the high complexity of its implementation. The next chapter will focus on the development of advanced but simple control techniques to promote the torque control performance while keeping the complexity of implementation at a reasonable level.

ChapterIII

Finite State_Model Predictive based Control Methods for a Permanent Magnet Synchronous Motor Drive (PMSM)

This chapter is dedicated to the analysis and implementation of new emerging control strategies that based mainly on the model predictive control concept. First, the working principle of FCS-MPC is presented. Then, two well dominated predictive control methods (MPCC, MPDTC) are presented, analysed and discussed in order to control our PMSM drive. Finally, the technique that take our interest will be identified and selected to continue our effort to advance our improvements within the scope of this thesis.

III.1. Introduction

As the demand for the performance and efficiency of power converters and electrical drives increases, the development of new advanced control systems must take into account the true nature of these types of systems. Power converters and drives are non-linear systems, including time varying states, control variables and a finite number of switching states. Input signals for power converters are discrete signals that control the on/off transitions of each device. Several constraints and restrictions must be considered by the control, some of which are imposed for safety reasons, such as current limitations to protect the converter and its loads.

Appearing in 2004, through the impressive work of the Chilean J. Rodriguez and his team [80]. Finite Control Set-MPC (FCS-MPC) has received a lot of attention from industrialists and academics. Broadly stated, FCS-MPC is a very interesting alternative for the numerical control of power supply systems integrating converters [77].

Unlike the generalized predictive control GPC that involve a set of adjustment parameters, using expensive computation times and elaborate complex algorithms to perform a closed loop control. Finte–state or finite–set model predictive control (FS-MPC) uses a model of the system to predict its future behavior with only one or two prediction steps. This prediction is used by the control algorithm to obtain the optimal control according to a predefined optimization criterion. The main advantage of the FS-MPC method is its simplicity of implementation. The process does not need linear or non-linear controllers in the inner loops, no need for a modulator for actuates the inverter. In addition, the constraints are taken into account thanks to its flexibility which significantly reduces the overall cost of the drive system [80].

This chapter deals with the development of the FS-MPC control for piloting a synchronous variable speed drive with a permanent magnet (PMSM) . The PMSM is supplied by a three-phase two-level voltage source inverter 2L-VSI. Then, for actuates the VSI, two major control techniques namely, Model Predictive Current Control (MPCC) and Model Predictive Direct Torque Control (MPDTC) based on the FS-MPC philosofy are studyed and implemented. Only the technique that outperforms the other will be selected to continue our effort to advance our improvements within the scope of this thesis.

III.2. Concept of Model Predictive based Control (MPC)

A model predictive controller (MPC) can be imagined as a human driving a vehicle on the road (see **Fig III.1**). He observes the road and based on his experience of how the car behaves under certain conditions, predicts the future behavior of the vehicle. Then, he adjusts certain key factors (i.e. the accelerator pedal, brakes, wheel and gear ratio according to his experience) and applying a control action before a certain situation (shock, turn or a pedestrian crossing). This optimization problem can be easily solved (with varying degrees of accuracy) by ourselves, but for an embedded controller, it's an exceptional challenge. The small sampling intervals of the controlled system means that at each sampling time, the control loop has to execute and solve such an online problem optimization [20]. This explains why MPC was not widely used in motors and power converters in the early decades, as there was no available and reasonably inexpensive hardware to run these algorithms [19]. However, with the adoption and development of rapid microprocessors technology, these constranints are purely removed.

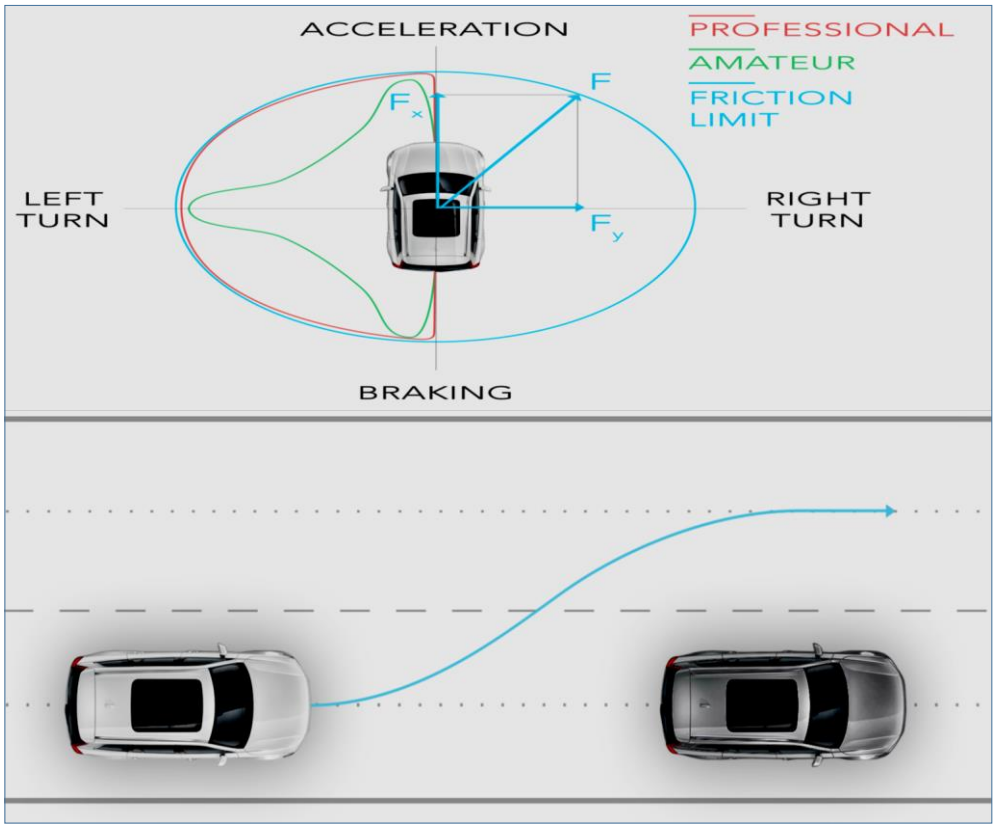

Figure III.1 A simplified analogy of MPC.

As mentioned earlier, the control theory for power electronics specifically MPC controller emerged in a rigorous manner, in parallel with the development of semiconductor devices and ahead of the evolution of control platforms. This section discusses the evolution in control platforms and how these platforms help power electronics implement control schemes in real time [108]. **Figure III.2** graphically presents the developments in semiconductor devices and integrated control platforms.

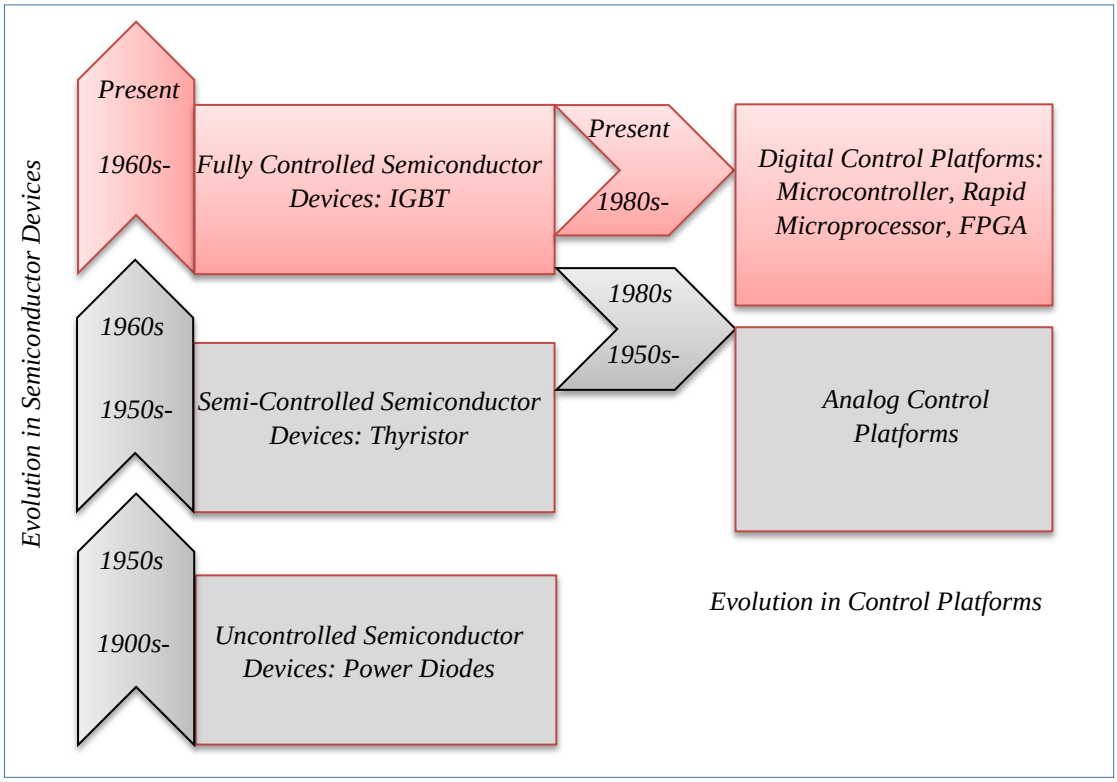

Figure III.2 Developments in semiconductor devices and integrated control platforms.

Conceptually, the basic idea of MPC is to predict the future state of the system on the basis of the measured (or estimated) variables and the applied control signals. The control action that will lead to a future state closest to the desired state of the system will be selected and applied to the system by the controller. This selection process is done through a so-called cost function (or objective function) that integrates the control strategies, constraints and objectives [23]. At the same time, the cost function can integrate any and multiple desired state variable for the control. Therefore, the MPC is inherently classified as a MIMO controller, unlike the FOC which uses SISO/PID controllers. **Figure III.3** shows the general MPC algorithm.

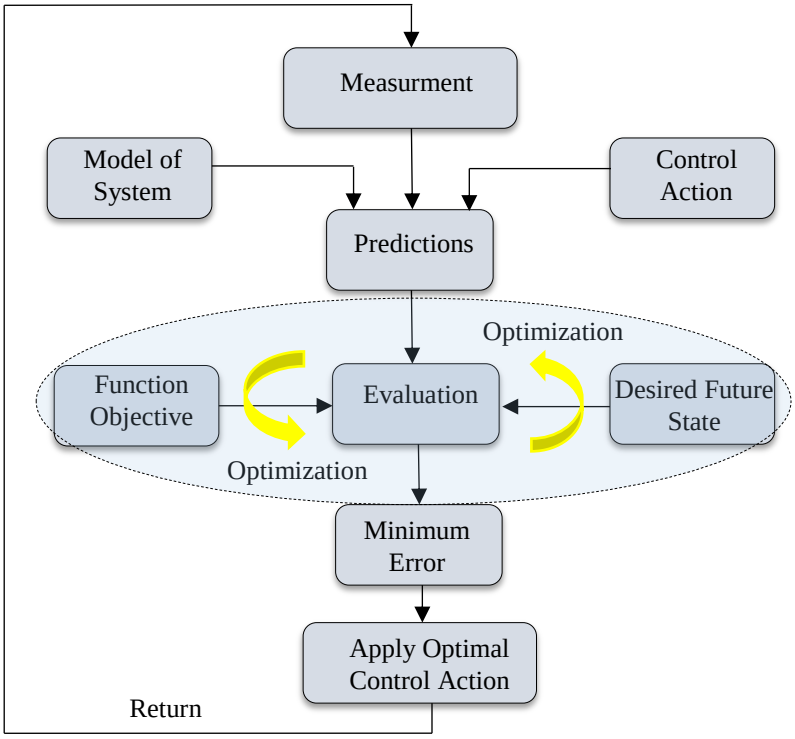

Figure III.3 General MPC algorithm.

III.3. The Philosophy of Finite State Model Predictive based Control (FS-MPC)

The finite state model predictive control (FS-MPC) is based on the discrete nature of power converters due to the limited number of their switching states (number of finite states) [20]. This has the effect of reducing the computational effort for both prediction and processing. As each converter has a limited number of switching states (for example, 8 states for a two-stage three-phase voltage inverter, 27 states for a three_level inverter), the prediction procedure is also limited to these states. Then an optimization procedure selects the optimal state (optimal voltage vector) to be applied to the load. The main elements of this control technique are therefore the mathematical model of the system and the predefined cost function (See **Figure III.4**) [23]. In this scheme (**Figure III.4**) the measured variables *x(k)* are used in the model to calculate the predictions *x(k+l)* of the controlled variables for each of the possible iterations (n), (i.e. all possible switching states). These predictions are evaluated using a cost function that takes into account the reference values $x^*(k)$ and also the restrictions imposed by the type of control applied. Thus, the optimal switching state *S(k+1)* is selected and applied to the power converter. **Figure III.4** illustarate the schematic diagram of the FS-MPC for PMSM.

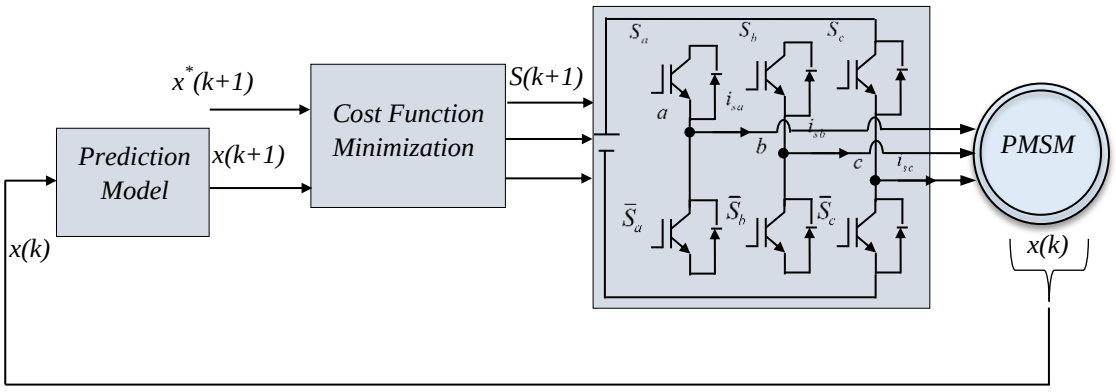

Figure III.4 Schematic diagram of the FS-MPC for PMSM.

For the design of the FS-MPC control, three essential steps must be carried out [20]:

- Determine the appropriate discrete model of the system to predict the future behavior of the controlled variables.
- Modeling of the power converter by identifying all possible switching states.
- Formulation of a cost function according to the desired objectives.

III.3.1.Prediction horizon

Since the FS-MPC for Motor Drives is a discrete controller, predictions are typically made in discrete time steps that are determined by the sampling time. At each sampling time, the predictive controller takes measurements of the control variables for prediction purposes to determine the optimal control action, then at the next sampling time, new measurements are taken into account for the next control prediction and so on, which is called the prediction horizon. [20], [108]. If the measured variables are taken at the *(k_th)* sampling time, predictions can be calculated for the *(k+1)th*, *(k+2)th* sampling time. The choice of the best ahead time for a given application depends on the available computing resources, sophisticated materiel and the desired performance [19]. Also, to a large extent, it depends on the sampling interval, the noise of the measurement signals and the accuracy of the model. Model noise and inaccuracy can both corrupt predictions especially over a long horizon, since each prediction is computed from the previous one, the effect of errors could be amplified. Increasing the prediction horizon quadratically increases the computational burden, which involve high cost and sophisticated system accordingly. **Figure III.5** illustarate the MPC working principle and prediction horizon.

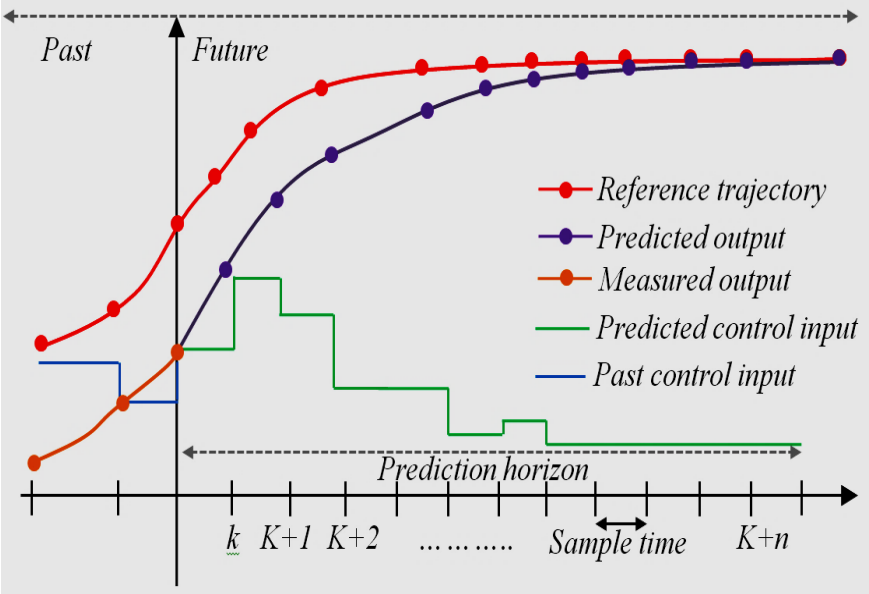

Figure III.5 MPC working principle and prediction horizon.

III.3.2.Cost Function Minimization

Basically, the cost function corresponds to a comparison between two controlled variables (for exemple: electromagnetic torque and stator flux) and their predictive values. This cost function will be evaluated for each prediction and the one that produces the lower value determines the (S_{abc}) switching state of the voltage inverter supplying the synchronous machine (in other words, the optimal voltage vector (u_s) applied to the machine stator). As a result, the generate pulses actuates the inverter [20].

An ideal cost function (g) value is equal to zero, which represents the perfect optimization of control variables. However, with unpredictable constraints, a zero (g) value is impossible. The cost evaluation in FS_MPC for two_level inverter leads to eight different cost function values (g_0_g_7). The idea behind using a cost function minimization lies mainly in identifying the minimum cost function value that correspond to the optimal switching state combination. As an example, assuming that the cost function (g_3) has a minimum value among all obtained optimization values, the corresponding indice of switching state is (S_3) with S_a = ‘0’, S_b = ‘1’, and S_c = ‘0’ is chosen as an optimal action and is directly applied to the inverter. The whole design procedure is performed during the *(k)th* sampling interval, and the optimal switching state is applied to the inverter at the next sampling instant. As a final note, the FS-MPC involves neither inner current PI controllers nor a modulation stage.

III.3.3.Merits of FS_MPC Over Conventional Counterparts' Strategies

A comparison between the classical linear control, classical non-linear control and FS-MPC strategy for a 2L_VSI is summarized in **Table III.1**. Unlike the FOC principle where the system model must be linearized, FS-MPC effectively handles non-linearities of the system. The discrete nature of the power converter and the lack of modulation stage greatly simplifies the FS_MPC optimization. The dynamic response obtained by FS_MPC impressively outperforms the linear control even during unpredictable situations. The Simplicity of concept and the efficient functioning are decisive aspects for the success of any new control technology. The analysis suggests that the FS_MPC strategy is an intuitive and powerful tool for controlling power converters compared with the classical linear control with proportional-integral (PI) regulator and nonlinercontrol with hysteresis comparator [20-26].

Table III.1 Comparison of linear (FOC), non_linear (DTC) and FS_MPC

Description	**Linear based PI Controller (FOC)**	**Non-linear based Hysteresis controller (DTC)**	**FS_MPC**
Model	Continous_Time Model for Complete System	Discrete_Time Model for Complete System	Discrete_Time Model for Complete System
Controller Design	PI Adjustment gains + Modulator Design	Hysteresis Adjustment Width + Switching Table Design	Cost Function Definition
Nature of Controller	Linear	Non_Linear	Non_Linear
Implementation Platform	Analog or Digital	Digital	Digital
Modulation	PWM/SVM	Not Required	Not Required
Switching Frequency	Fixed	Variable	Variable (but controllable)
Multivariable	Coupled	Decoupled	Decoupled
Constraints Inclusion	Not Possible	Not Possible	Easy to Include
Complexity of Concept	Medium with SPWM	Medium with conventional Switching Table	Simple and Intuitive
Steady-State Performance	Good in *dq* frame	Good in $\alpha\beta$ frame	Good in $\alpha\beta$, and *dq* frames
Transient Performance	Moderate	Excellent	Excellent
Computational Burden	Medium with SPWM	Medium with conventional Switching Table	Medium with 2L_VSI
Torque ripples	Low	Very_High	Relatively_High

III.3.3.1. Main caracterestic of the FS-MPC

- The concept is very intuitive, easy to understand and implement.
- It can be applied to a wide variety of systems.
- Multi-variable systems can be considered as well as constraints.
- Easy integration of non-linearity in the model.
- This method is suitable for incorporating modifications and extensions according to particular applications.
- A cost function that represents the desired system objective.
- Optimal control action is obtained by minimizing the cost function (see **Fig III.6**).

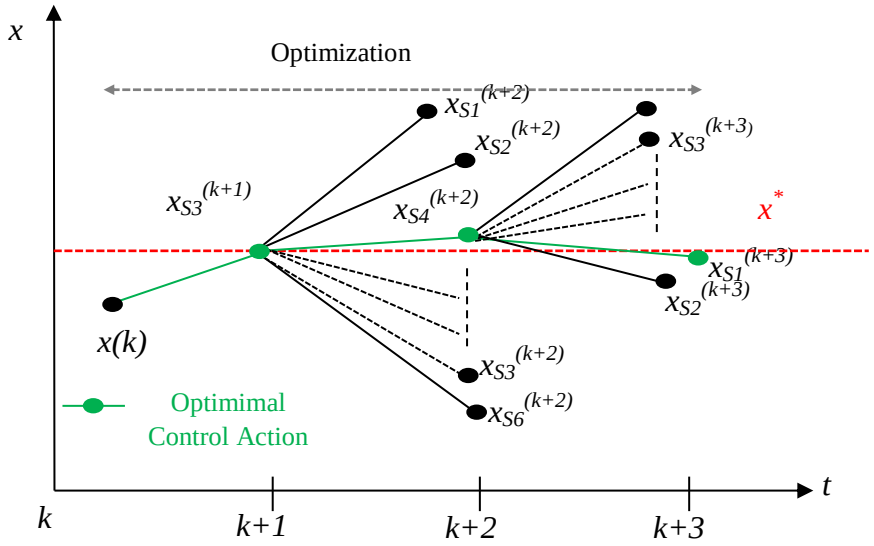

Figure III.6 FS-MPC working principle.

III.4. Finite State Predictive Current Control (FS-PCC) of PMSM

The PCC is a subclass of FCS-MPC where the FOC principle is adopted in this control strategy. It performs the control of the currents but with an optimization procedure, the oriented rotor flux in *(d-q)* coordinates is applied to the transformation of the fixed coordinates *(a,b,c)* of the stator in such a way that independent control of the current (i_d) producing the flux and the current (i_q) producing the torque [42].

III.4.1.Predictive Current Control Technique (PCC)

The proposed predictive current control algorithm includes three main phases: Firstly, discretized the appropriate system model and predict the future behavior of stator currents i_d *(k+1),* i_q *(k+1)* at next sampling instant, in second evaluated the proposed cost function (*g*) for all possible switching states *S(k).* Finally the output voltage vector (u_s) correspond to the minimum cost function (min (*g*)) is selected as the optimal control action. The global block diagram of PCC for PMSM drive is illustrated in **Figure III.7** .

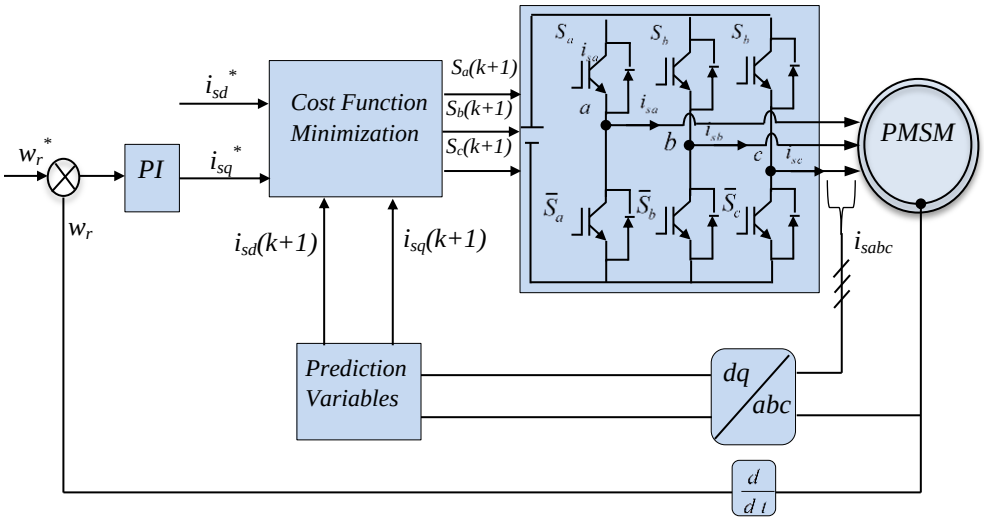

Figure III.7 Global block diagram of FS_PCC for PMSM.

III.4.1.1. Mathematical Model of PMSM Drive

The mathematical model of the PMSM drive in synchronous rotor reference frame (*dq*-frame) can be expressed as follows [42]:

$$\begin{cases} \dfrac{d_{id}}{dt} = \dfrac{1}{l_d}\left(u_d - R_s i_d + p w_r l_q i_q\right) \\ \dfrac{d_{iq}}{dt} = \dfrac{1}{l_q}\left(u_q - R_s i_q - p w_r \left(l_d i_d + \psi_{rm}\right)\right) \end{cases} \tag{3.1}$$

where i_d , i_q and u_d , u_q are, respectively, d-axis and q-axis stator currents and voltages. l_d, l_q are the d-axis and q-axis stator inductance, ψ_{rm} is the permanent magnet rotor flux. R_s is armature winding resistance, w_r denotes the mechanical rotor speed, and p is the number of pole pairs. The park model of the PMSM is detailed and demonstrated in **Appendix A**.

III.4.1.2. Discrete_Time System Model and Prediction of Stator Currents

The discrete model time is the first step of MPCC. For discretization, the first-order Euler's approximation method is considered and applied to the continuous time model Eq. (3.1) [20].

$$\text{Where, } \frac{dx}{dt} \approx \frac{x(k+1)-x(k)}{T_s} \tag{3.2}$$

Hence, the discrete and predicted model of the PMSM can be written as:

$$\begin{cases} i_d(k+1) = i_d(k) + \dfrac{1}{l_d}\left[-R_s i_d(k) + pw_r(k) l_q i_q(k) + u_d(k)\right] T_s \\ i_q(k+1) = i_q(k) + \dfrac{1}{l_q}\left[-R_s i_q(k) - pw_r(k) l_d i_d(k) - pw_r(k)\psi_{rm} + u_q(k)\right] T_s \end{cases} \tag{3.3}$$

As discused in Chapter.II for the all possible combination of switching functions (S_a, S_b, S_c) obtained from the inverter (seven distinct voltage vectors) (see **Table II.1**). Then it's clear that the inverter constitutes a finite set of voltage space vectors. However, the voltage vectors generated by the inverter in **Table II.1** are fixed in stationary frame, and of corse our predictive current control algorithme is implemented in (dq) rotating frame, and hence, a rotation operation of (u_α, u_β) components yield rotating vector in park frame as following:

$$\begin{bmatrix} u_d(k) \\ u_q(k) \end{bmatrix} = \begin{bmatrix} \cos(\theta) & \sin(\theta) \\ -\sin(\theta) & \cos(\theta) \end{bmatrix} \begin{bmatrix} u_\alpha(k) \\ u_\beta(k) \end{bmatrix} \tag{3.4}$$

The goal is to find the best space voltage vector, that yields to the minimum cost function.

III.4.1.3. The Performances Evaluation

The evaluation of performances is the last step of FS-PCC, the cost function evaluation here consists of the absolute values of currents errors. This classical formulation can be extended to handle other control objectives and constraints. So, the minimum value of cost function is defined as:

$$g = \left|i_d^* - i_d(k+1)\right| + \left|i_q^* - i_q(k+1)\right| + I_{max} \tag{3.5}$$

Where, (i_d^*) and (i_q^*) are reference values for d-axis and q-axis currents, respectively. $i_d\ (k+1)$ and $i_q\ (k+1)$ are predictions for d-axis and q-axis currents at the next sampling

instant. (i_q^*) is generated from a PI controller, and (i_d^*) is set zero according to the FOC principle to achieve a decoupled control and to achieve the maximum torque per ampere (MTPA) operation as [109].

I_{max} is added to the cost function (3.5) in order to prevent the over current through the stator winding.

$$\text{Where, } f\left(I_{\max}\right)=\begin{cases}\infty, if \sqrt{i_d\left(k+1\right)^2+i_q\left(k+1\right)^2} > I_{\max}\\ 0, if \sqrt{i_d\left(k+1\right)^2+i_q\left(k+1\right)^2} \le I_{\max}\end{cases} \tag{3.6}$$

III.4.1.4. Implementation of Control Scheme

The predictive control scheme is basically an optimization algorithm; thus it is digitally implemented in the microprocessor-based hardware. The flowchart for the digital implementation of PCC algorithm is illustarated in Figure 4.3.

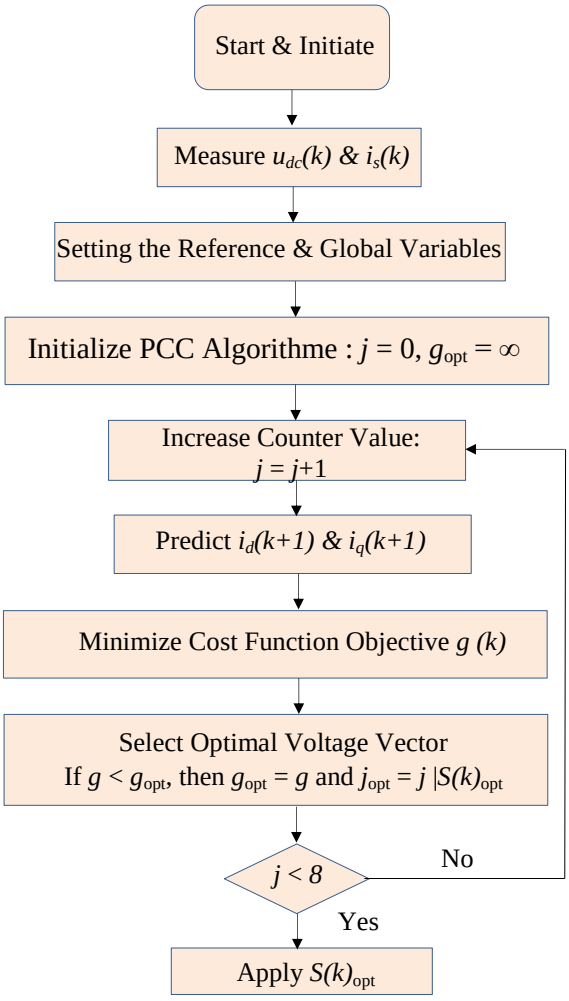

Figure III.8 Flowchart of PCC_PMSM supplied by 2L_VSI.

The PCC algorithm consists mainly of the following steps:

- The measured DC-link voltage and load currents must fed the predictive controller.
- The reference currents are defined either by the user and/or by a such adopted controller.
- The algorithm is initialized by setting the switching state combination *j* to 0 and the optimal cost function (gop) value to ∞.
- The algorithm then enters the compilation, where a counter increases *j* value in steps.
- The controlled variables are predicted based on the measured DC-link voltage and all possible switching states defined by the voltage source inverter.
- On the basis of the predicted load currents, a set of prediction valus are obtained.
- The predicted load currents are evaluated by a cost function *g*.
- The absolute error between the reference currents i_s^* and predicted currents i_s (k +1) is calculated.
- During each iteration, if $g < g_{opt}$, the minimum *g* value is stored as an optimal value g_{opt} and the corresponding switching state combination is stored as $j_{opt}|S\ (k)_{opt}$.
- The optimal switching combination is applied to the voltage source inverter and so on.

III.5. Finite State Model Predictive Direct Torque Control (FS-MPDTC) of PMSM

For a PMSM, it can be demonstrated that the magnetic stator flux and the electromagnetic torque can be controlled in a decoupled way by selecting one of the eight sequences possible or space voltage vectors that generated by the voltage source inverter; this can changes the amplitude of the stator flux vector and also the angle between the rotor and stator flux, as we explained earlier about the principle of DTC strategy in the second chapter. This principle corresponds to the conventionel methods of direct torque control of elctomechanical systems [26-33].

The same principle is used also for the Finite_State Model Predictive Direct Torque Control (FS_MPDCT) (i.e. decoupled control of stator flux and electromagnetic torque) and presented in this chapter, but with this emerging control strategy, predictions of future values of stator flux and electromagnetic torque are taken into account. Therefore, the switching table designe, hysteresis band adjusments and stator flux position information used in conventional DTC control are removed and replaced by a cost function minimization designe, that operates according to the future behavior of the controlled variables (flux and

torque). For a 2L_VSI, predictions are computed for the eight possible generated space voltage vectors Vs and the cost function selects the voltage vector that produces the best control of stator flux and electromagnetic torque. The Model predictive direct torque control of a three-phase PMSM can be schematized by the following figure :

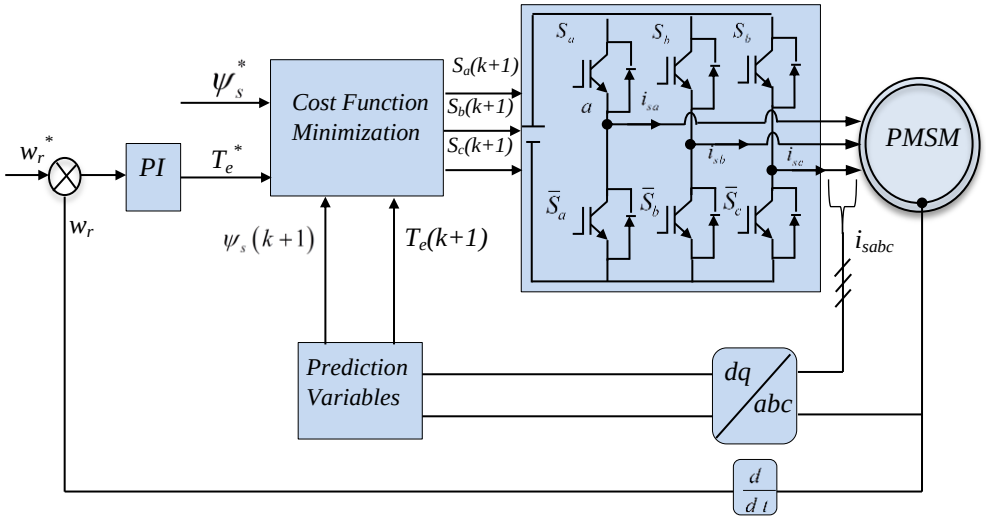

Figure III.9 Global block diagram of FS_PDTC for PMSM.

In this control scheme, the electromagnetic torque and stator flux should be optimized online to achieve the desired control performance of the PMSM drive. Thus, MPDTC can perform a fast torque control without utilizing hysteresis controllers and a lookup switching table as the case of the basic DTC method. Additionally, this control method uses all feasible voltage space vector (VSV)of the inverter and a performance criterion for evaluating the influence of each VV aiming forward to reduce the torque and flux ripples.

The Measurement and Estimation block is used to measure and calculate the current values at instant *(k)* of measurable and non-measurable variables, such as the stator current, electromagnetic torque and stator flux. Then, the prediction model calculates the future values of the controlled variables at instant *(k +1)*; in this case the controlled variables are: the stator currents, stator flux and electromagnetic torque. These predictions are calculated for all possible switching states depending on the topology of the voltage inverter powering the PMSM. For our application eight different switching states and seven voltage vectors can be considered; Finally, the minimization block chooses the optimal switching state that minimizes the corresponding cost function. This function contains the control law allowing an appropriate control of the electromagnetic torque and stator flux.

III.5.1.Predictions of the Control Variables (Torque & Flux)

Based on the predicted *d–q* stator current components Eq. (3.3), the predicted *d–q* stator flux components can be expressed as:

$$\begin{cases} \psi_d(k+1) = l_d i_d(k+1) + \psi_{rm} \\ \psi_q(k+1) = l_q i_q(k+1) \end{cases} \tag{3.7}$$

Hence, the magnitude of the predicted stator flux linkage is:

$$\left|\psi_s(k+1)\right| = \sqrt{\left(\psi_d(k+1)\right)^2 + \left(\psi_q(k+1)\right)^2} \tag{3.8}$$

Taking into account the prediction of Stator currents from Eq. (3.3), the predicted torque at instant *(k+1)* can be written as:

$$T_e(k+1) = \frac{3}{2} p\left(\psi_{rm} i_q(k+1) + \left(l_d - l_q\right) i_d(k+1) i_q(k+1)\right) \tag{3.9}$$

III.5.2.The Performances Evaluation

The cost function evaluation here consists of the absolute values of torque and flux errors. Since both controlled variables are different in units and magnitude a weighting factor *(λ)* should be added in the cost function [23]. This factor depends on the operating point and system parameters. In addition, it influences the performance of the controller because it determines the relative importance of torque and stator flux.

So, the minimum value of cost function is defined as:

$$g = \left|T_e^* - T_e(k+1)\right| + \lambda \left\|\psi_s^*\right| - \left|\psi_s(k+1)\right\| \tag{3.10}$$

where T_e^* and ψ_s^* are reference for torque and stator flux, respectively. $T_e(k+1)$ and $\psi_s(k+1)$ are predictions for torque and flux at the next sampling instant. λ is the weighting factor, The torque reference is generated from a PI controller, and the reference stator flux is set according to the maximum torque per ampere (MTPA) trajectory method as [109]:

$$\psi_s^* = \sqrt{\left(l_q T_e^*\right)^2 + \left(l_d i_d^* + \psi_{rm}\right)^2} \tag{3.11}$$

where i_d^* is the reference value of *d*-axis current which is set to zero to achieve (MTPA) operation.

III.6. Simulation Results

The performances of MPDTC and MPCC for a PMSM are verified by numerical simulation using MATLAB/SIMULINK software. The parameters used for the simulation are given in **Appendix B** [107].

At first, a unified monitoring scenario is employed for both control methods in order to perform a fair comparison. The monitoring scenario include: the starting up, the steady states at rated speed, rated load torque introduction and a maneuver of speed sense reversing. For the MPDTC, the chosen wheighting factor is equal to λ =3000.

III.6.1.Starting, steady state at rated speed, application of rated load torque and rated speed sense reversing operation

In this part, both control techniques (MPDTC and MPCC) was tested for a target rated speed of 1000 rpm with a rated load of torque insertion at t=0.1 s followed by a speed sense reversing operation at t=0.15. The Starting up situation and steady states with load torque application and the speed sense reversal are depicted. For that, **Figs III.10** to **III.15** show the rotor speed, electromagnetique torque, stator phases current and stator flux evolution.

Besides, as the wheighting factor (λ) has a strong effects on the performance of the controlled system such as the THD of stator currents, a detailled THD analysis of stator phase current with differents values of wheghting factors and under some specific conditions, are depicted in **Appendix C**. The figures are mentioned by **(a)** for the MPDTC, and **(b)** for the MPCC.

(a)

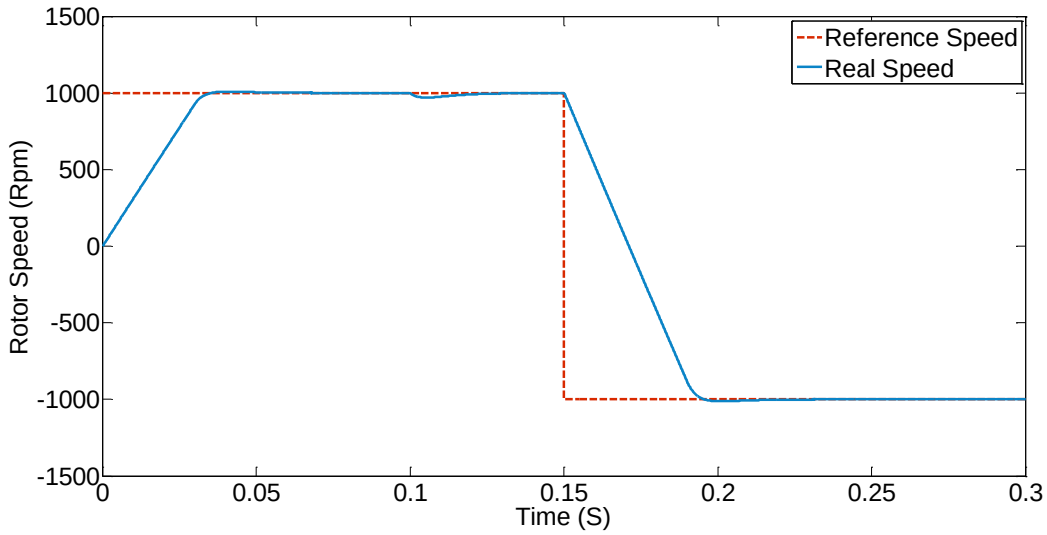

(b)

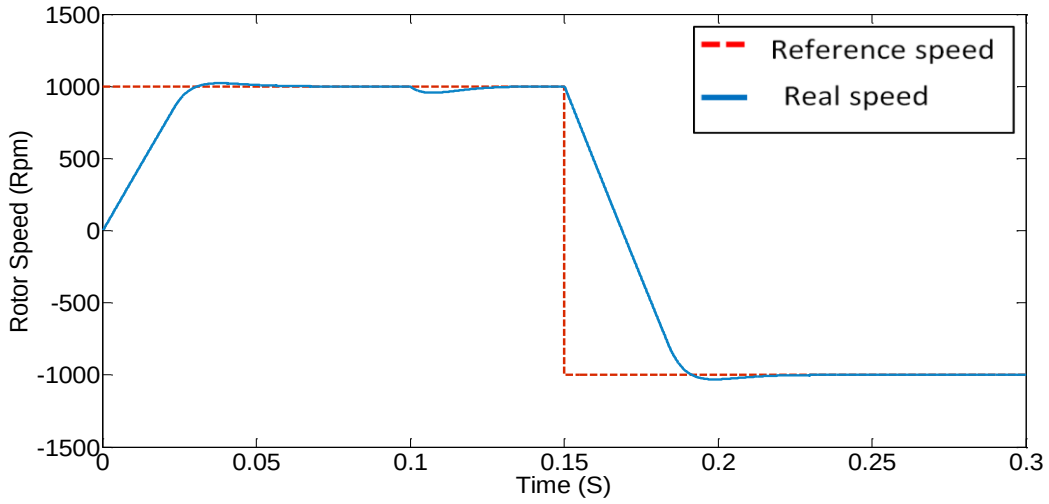

Figure III.10 Rotor speed (rpm).

(a)

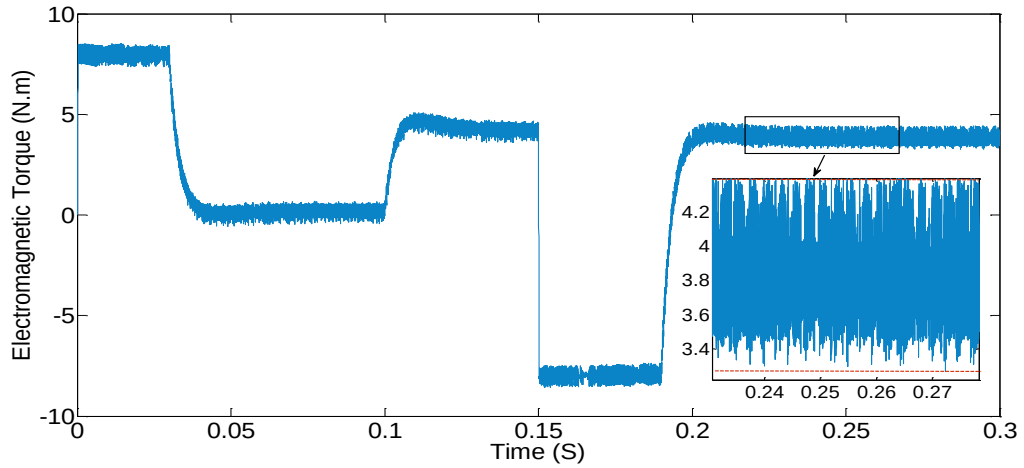

(b)

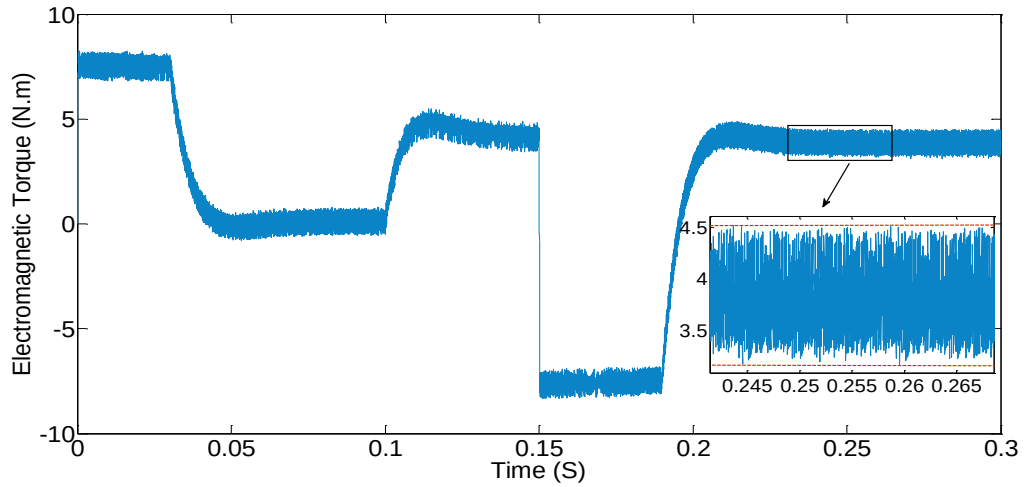

Figure III.11 Electromagnetic torque (N m).

(a)

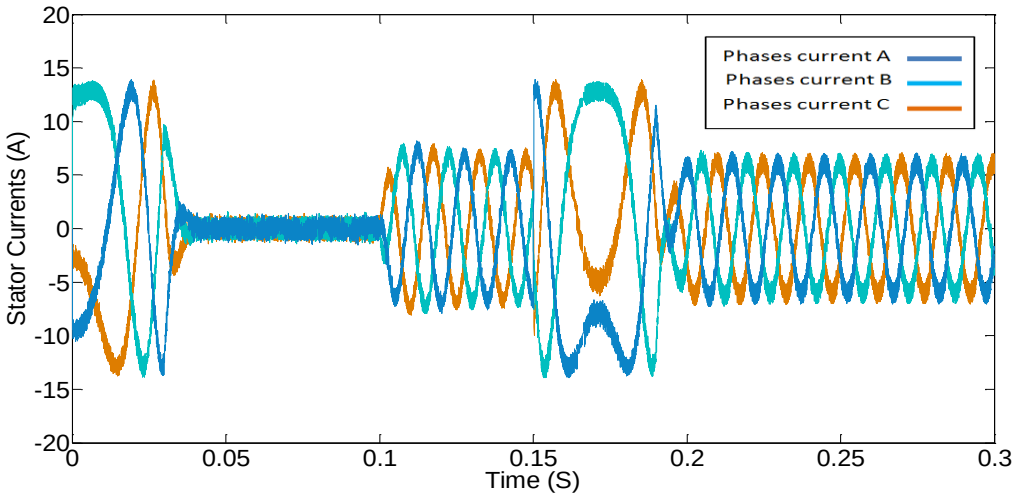

(b)

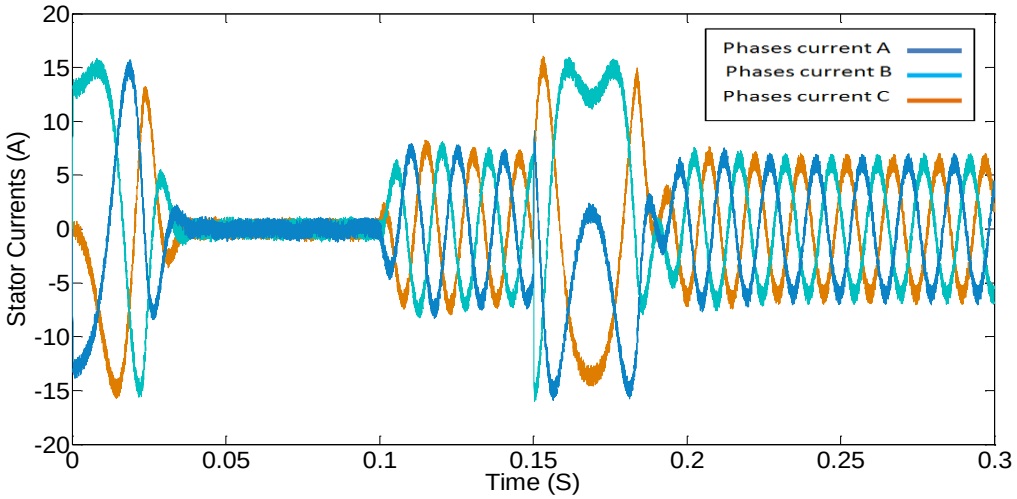

Figure III.12 Stator currents (A).

(a)

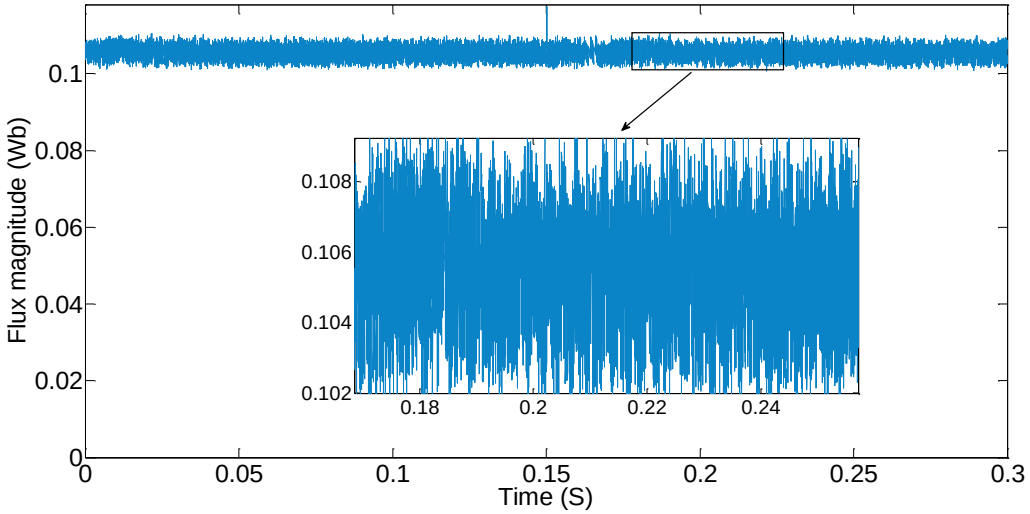

(b)

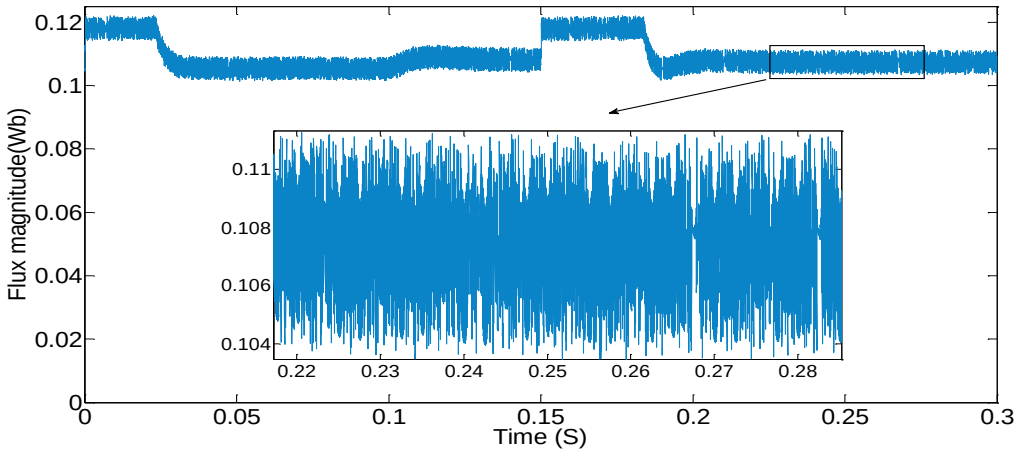

Figure III.13 Stator flux magnitude (Wb).

(a)

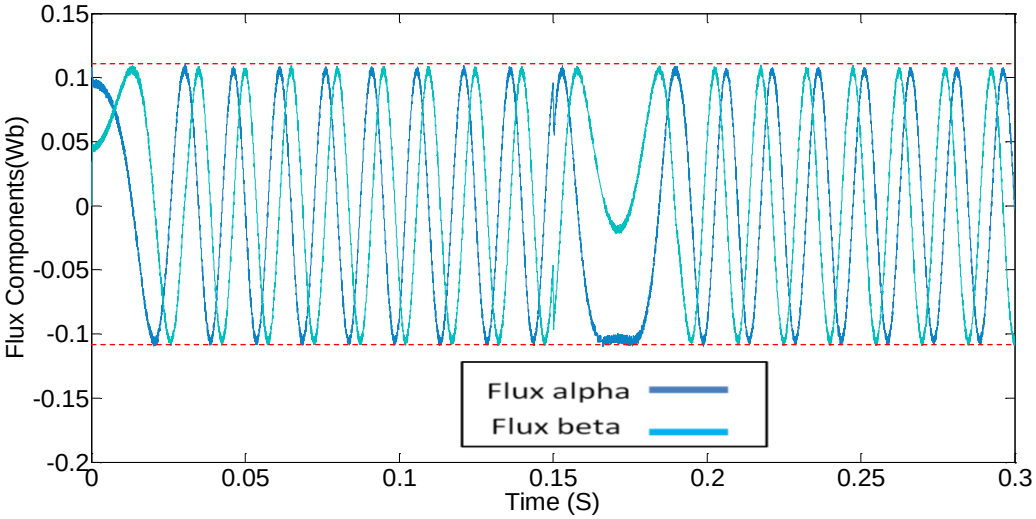

(b)

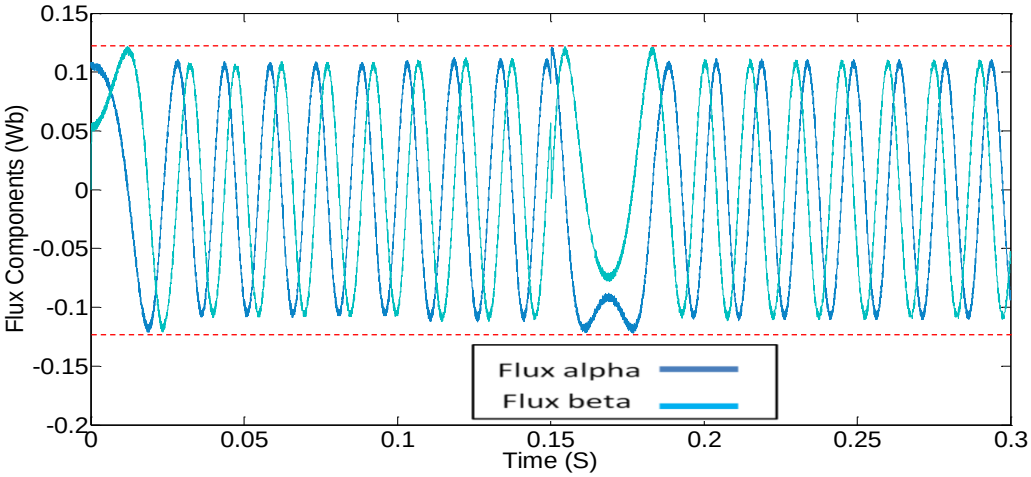

Figure III.14 Stator flux components (Wb).

(a) **(b)**

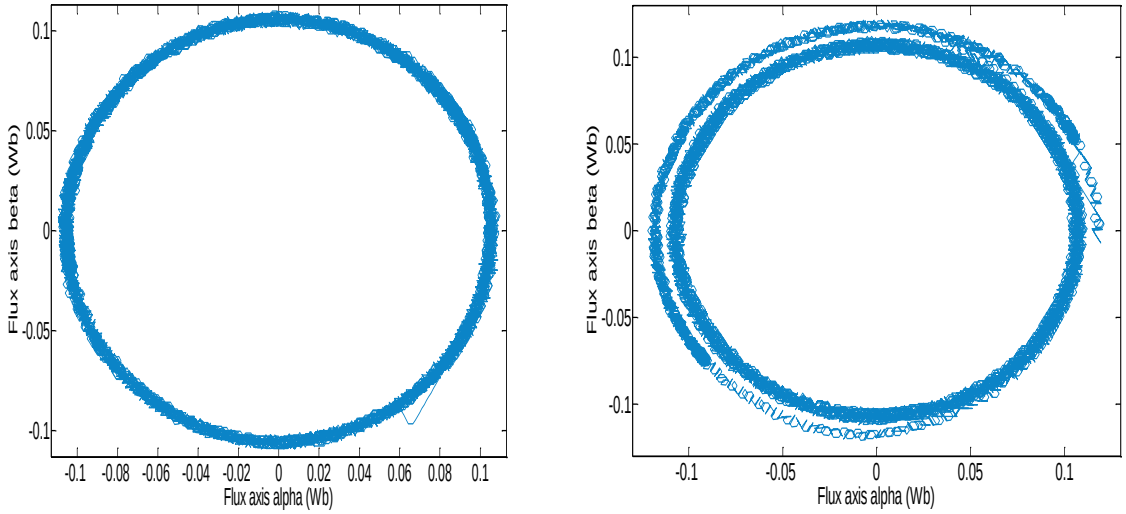

Figure III.15 Stator flux trajectory (Wb).

Firstly, **Fig III.10a, b** illustrate the comparison between speed responses of MPDTC and MPCC depending to the rated speed target 1000 rpm, to the load disturbance introduction at (*t=0.1s*) and to the rated speed sense reversing -1000 rpm at (*t=0.15s*). So, it's clear to notice that both techniques show good dynamic behavior at starting up (dynamic state) and a stable behavior at steady state. It can also be noted that the external speed control loop rejects the disturbance of the applied load torque relatively quickly. Additionally, both control schemes kept the same fast speed response; So there is no difference in the complete monitoring scenario. This is confirmed mainly by the identical PI speed controller used for both control strategies.

Then, **Fig III.11a, b** illustrate the responses of the electromagnetic torque. From (**Fig III.11a ZOOM, III.11b ZOOM**) it can be seen that the torque ripple range of the MPDTC method is about 0.9 Nm (from 3.4 Nm to 4.3 Nm); the value of the MPCC method is 1.3 Nm (from 3.2 Nm to 4.5Nm). Therefore, the MPDTC method has lower torque ripple than the MPCC method. This is reside to the used torque optimization stage included in the cost function.

After that, **Fig III.12a, b** show respectively the stator phase's currents (i_{sa}, i_{sb}, i_{sc}) of MPDTC and MPCC. It is clear to see that the MPCC has a slightly better current response than that of MPDTC. This can reflect to the effectiveness of the used cost function based currents minimization.

Next, **Figs III.13** to **III.15** show the waveforms of the magnetic stator flux, namely the flux amplitude, the flux components and the flux trajectory. From **Fig III.13a, b** it is

clear to see that the amplitude of flux in the case of MPDTC follows its reference perfectly with moderate level of ripples in comparison to the MPCC which presents a flux dropping and high flux ripples as seen in **Fig III.13b** (**ZOOM**) . In addition, from **Fig III.14a** the MPDTC presents better and uniforme components sinusoid waveform than that of MPCC. As to the trajectory of the stator flux, we can clearly see in **Fig III.15a** that it is purely circular and uniform when compared to **Fig III.15b**. This indicates that the stator flux has a relatively fewer ripple in one part and explains in the other part the efficiency of the used stator flux optimization step (the optimization procedure also includes the minimization of stator flux).

III.7. Summarize

The functioning of the two types of predictive control described in this chapter can be summarized by the following five steps:

- Measurements of stator currents and rotor speed (the stator voltages are reconstructed from the switching state of the inverter $S_{abc}(k)$ and the value of the DC voltage u_{dc}).
- These measurements are used for stator currents, electromagnetic torque and flux prediction for all the seven different voltage space vectors.
- The seven predictions are evaluated using the cost function minimization.
- The selection of the optimal voltage vector $u_s(k)$ that minimizes the cost function g.
- The application of the new selected voltage space vector to the machine terminals.

These steps are repeated at each sampling period T_s, of course taking into account for the new measurements of the controlled variables and their references.

Besides, a characteristic comparison of DTC, MPCC and MPDTC is developed in the following table.

Table III.2 Characterestic comparaison of DTC, MPCC and MPDTC

Characterestic	**DTC**	**MPCC**	**MPDTC**
External PI_ Speed Controller	Yes	Yes	Yes
Inner PI_Current Controller	NO	NO	NO
Controller Design	Hysteresis Adjustment Width + Switching Table Design	Cost Function Definition	Cost Function Definition

Control Variables	Torque /Flux	Current	Torque /Flux
Modulation	Not Required	Not Required	Not Required
Switching Frequency	Variable	Variable (but controllable)	Variable (but controllable)
Dynamic Responce	Excellent	Excellent	Excellent
Constraints Inclusion	Not Possible	Easy to Include	Easy to Include
Complexity of Concept	Medium with conventional Switching Table	Simple and Intuitive	Simple and Intuitive
THD of Stator Current	Very_High	Moderate	Relatively_High
Computational Burden	Medium	Medium with 2L_VSI	Relatively_High with 2L_VSI
Torque Ripples	Very_High	Very_High	Relatively_High
Flux Riplles	Very_High	Very_High	Relatively_High

III.8. Conclusion

In this chapter, the performance of both FS_PCC and FS_MPDTC strategies have been studied, investigated and compared, by means of performance verification using MATLAB/Simulink tool. Technically, the two controlled methods are direct control type without any PI current controllers or any modulation stage. The PCC method is characterized by a single predicted stage for stator current which make the computation time lower than the MPDTC that involve double predicted stage. This advantage makes the PCC method more suitable for applications with multi-level converters. Based on the obtained simulation results and the performances evaluation, it is very clear that the MPDTC practically outperforme the PCC method. Moreover, from the point of view of torque/flux control and undesirable ripples, the MPDTC method is characterized by the following features, such as the optimization procedure for both torque/ flux and the reduced level of ripples. However, conventional MPDTC selects only one voltage vector (VV) per control period by minimizing a standard cost function. Consequently, the torque and flux may not be controlled perfectly, and relative ripples inevitably take place in these controlled variables. To overcome this problem, the next chapter proposes the concept of the fuzzy logic-based duty cycle vector modulation, and two VVs instead of a single VV are applied during the whole control cycle to promote the torque control performance and reduce its undulations.

ChapterIV

Improved FS_MPDTC For PMSM_Drive using Fuzzy Logic System and EKF

This chapter is dedicated to the analysis and implementation of improved FS_MPDTC that based mainly on a fuzzy logic system and an extended kalman filter (EKF). First, The basic concepts of fuzzy logic and the basic operations pertinent to the study of fuzzy sets are proposed. Then, the relationship between torque ripple, switching frequency and switching losses is examined. Next, the concept of fuzzy logic-duty cycle control is presented, analysed and discussed. Finally, an extended kalman filter is introduced for the sugested improved FS_MPDTC in order to advance more our improvements within the scope of this thesis, which focuses mainly on minimizing the undesirable torque ripples.

IV.1. Introduction

The fourth chapter proposed an anhanced FS_MPDTC strategy to deal with the main drawbacks of the conventional_MPDTC. It is based on fuzzy logic modulator (FLM) to modulate (adjust) the appropriate reference voltages and therefore produces the inverter switching state combinations under a constant switching frequency. However, this modification moved a bit away from the basic principles of C_MPDTC. It integrates a modulaion block in the control structure which may reconfugured relatively differentl to the well established FS_MPC algorithm. In addition, the C_MPDTC selcts only one voltage vector for the entier switching period by minimzing a standard cost function. Consequently, undesirable ripples invetably take place in the selected control variables (i.e. torque and flux).

In order to cope with these limitations and achieve steady-state performance improvement, the concept of fuzzy logic is introduced. Besides, in comparaison to the existing multi-level converters, the used 2L-VSI slightly increases the computational load of the control algorithm. Consequently, in order to implement double-objective MPDTC (reduced ripples/computional burden), a two-level VSI with adjusted voltag vectors magnitude is designed to sequentially reduce the stator currents tracking error and the torque/flux fluctuations.

A convenient solution is proposed to adjust the magnitude of the selected voltage space vector (VSV) for each switching period according to certain criteria. For this reason, a fuzzy logic-based duty cycle vector modulation is utilized and two VSVs instead of single VSV are applied during the whole control cycle. In fact, the first VSV is selected by the FS_MPDTC algorithm and its actuation time is determined through a fuzzy inference mechanism by using a collection of linguistic if–then fuzzy rules. For the remaining of each switching period, a null VV is applied. In brief, the fuzzy logic-based duty cycle control method introduced in FCS-MPDTC not only helps to exploit both of the applied VSVs candidates during the overall control cycle, but also to simultaneously determine the optimum applied duration of the selected VSVs. As a result, the undesired ripples are significantly reduced in both controlled variables: torque and flux.

Moreover, this chapter also presents a design of a simplified EKF to promote the predictive behavior of the suggested improved strategy (FLM-MPDTC) by filtering out the undesired measurement noise, rejecting the external perturbations and avoiding the

excessive usage of mechanical sensors. Indeed, the use of multiple mechanical sensors leads to increase the complexity/cost of the system, which makes the system reliability adversely affected. So, the introduced EKF permits us to improve the prediction model and avoid the extra use of mechanical sensors. The global control strategy will be investigated by simulation performed by matlab simulink software.

IV.2. Concept of Fuzzy Logic (FL)

Fuzzy logic, or more generally the treatment of uncertainties, is one of the classes of artificial intelligence. Its main goal is to implement human knowledge (or heuristic rules), in the form of a computer program [110]. It was first known as a mathematical branch complementary to the theory of classical logic, then it found its place among the control techniques based on artificial intelligence. In 1965, Professor L. Zadeh proposed for the first time the theoretical bases of this approach in a famous article entitled (Fuzzy set) [111]. Since its introduction, the concept of fuzzy logic has been extended to many domains. One of the successful examples is the control, which has found many applications in industry.

Fuzzy logic does not necessarily substitute conventional control systems. It is complementary and it is used particularly when there is no precise mathematical model of the process to be controlled, or when the process has strong non-linearities or inaccuracies. Moreover, the interest of fuzzy logic lies in its ability to deal with imprecision, uncertainty and vagueness. Thus, the secret of fuzzy logic control is largely due to its ability to translate a control strategy of a skilled operator into a set of easily interpretable linguistic rules [110].

IV.3. Fuzzy Logic Characteristics

Humans can perceive, reason, imagine and decide on the basis of knowledge and expertise. their thinking is not binary (limited). The idea of fuzzy logic is to capture the imprecision of human thought and express it with appropriate mathematical tools. Solving a problem requires looking for a model that is as objective and certain as possible. Models of our brain can be quite complicated and also unclear, fuzzy and imprecise. Humans do not reason like computers: on all or nothing. Fuzzy logic inspires its characteristics from human reasoning. It is based on the observation that most phenomenon that cannot be represented using boolean variables which only take two values (0 or 1) [112].

As an exemple: can we consider a speed of sport car equal to 150 Klm/h fast or very fast ? Is it neither fast nor really very fast ? To answer these types of questions, fuzzy logic

considers the notion of an object belonging to a set, no longer as a boolean function, but as a function that can take any value from 0 to 1.

Fuzzy logic control combines a number of advantages and disadvantages. The most important advantages are [110], [114] :

- No need for rigorous mathematical modeling of the process ;
- The possibility to implement (linguistic) knowledge of the process operator;
- The control of the process with a complex behavior (highly non-linear and difficult for modeling);
- Simplicity of definition and design.

On the other hand, it has the following disadvantages [110], [112], [114]:

- The lack of precise procedure for the design of the fuzzy parameters (choice of the fuzzy set, determination of fuzzification, inferences and defuzzification);
- The approach is home-made and non-systematic (implementation of operators' knowledge is often difficult);
- The consistency of the priori fuzzy inferences is unguaranteed (appearance of contradictory inference rules possible).

IV.4. Fundamental Concepts of Fuzzy Logic

The fundamental concepts of the fuzzy logic system, are abbreviated as follow:

IV.4.1. Fuzzy Sets

In classical set theory, a simple proposition is either true or false. It means that an element either exists or does not exist as part of a set. So the degree of membership of an element to a set can only be equal to 0 or 1. On the other hand, a fuzzy set is defined by a membership function that can take all real values between 0 and 1. This is the basic element of fuzzy logic. It was first introduced by Zadeh in 1965. The concept of the latter aims to avoid the sudden passage from one class to another and to allow graduations in the belonging of an element to a class; that is to say, to allow an element to belong more or less to one class and strongly to another [114].

IV.4.2. Membership Function

A membership function is a curve that defines how each point of the input space (the universe of discourse) is matched to a membership value (or degree of membership) between 0 and 1. In all generality, a membership function of a fuzzy set is indicated by $\mu_A(x)$. The argument (x) refers to the characterized variable, while the index $'A'$ refers to the set concerned [115]. Membership functions can take different forms (see **Figure IV.1**).

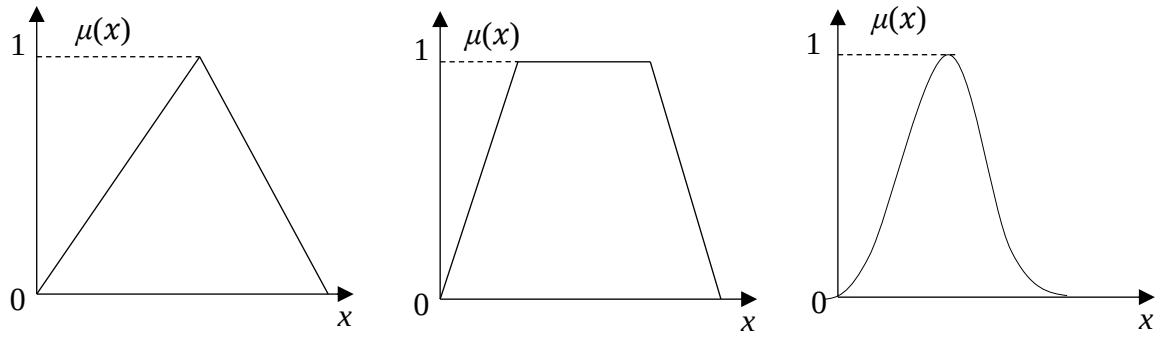

Figure IV.1 Different forms of membership functions (triangular, trapezoidal and sigmoid).

IV.4.3. Linguistic variables

The concept of linguistic variables also plays an important role in the context of fuzzy logic. A linguistic variable, as its name suggests, is a variable defined on the basis of words or sentences instead of numbers. Indeed, the description of a certain situation, phenomenon or process usually contains fuzzy expressions such as "some, many, often, large, small, slow, fast, ... etc.". Such expressions form the so-called linguistic variables of fuzzy logic.

IV.4.4. Fuzzy logic operators

Once the fuzzy sets are defined, mathematical operations have been developed and can be used for such sets. The mathematical operators developed are very similar to those related to the conventional set theory [114]. More precisely, the operators of intersection, union, complement and implication are translated by the operators AND, OR, NOT and THEN. Let A and B be two fuzzy sets, whose membership functions are $\mu_A(x)$, $\mu_B(x)$ respectively. The following table summarizes some of the functions used to perform the various basic fuzzy operations [113].

Table IV.1 Basic operators of fuzzy logic ($x= \mu A\ (x)$ and $y=\mu(y)$) [110].

Operator / Approach	AND	OR	NOT
Zadeh	$Min\ (x,y)$	$Max\ (x,y)$	$1-x$
Lukasievic	$Max(x+y-1,\ 0)$	$Min(x+y,1)$	$1-x$
Hanacher (β >0)	$\frac{xy}{(\beta+(1-\beta)(x+y-xy))}$	$\frac{x+y+xy(1-\beta)xy}{(\beta+(1-\beta)(x+y-xy))}$	$1-x$
Weber	$\begin{cases} x\ to\ y=1 \\ y\ to\ x=1 \\ 0\quad otherwise \end{cases}$	$\begin{cases} x\ to\ y=0 \\ y\ to\ x=0 \\ 1\quad otherwise \end{cases}$	$1-x$

On the other hand, fuzzy implication is built from such elementary fuzzy propositions. For this operation, there are still several methods. The most commonly used are given in the following table [113].

Table IV.2 Fuzzy Implication

Approach	Fuzzy Implication (THEN)
Zadeh	$Max\ \{Min(\mu_A(x),\ \mu_B(y)),\ 1-\mu_A(x)\}$
Mamdani	$Min\ (\mu_A(x),\ \mu_B(y))$
Reichenbach	$1-(x)+\mu_A(x)\mu_B(y)$
Willmott	$Max\{Min(\mu_A(x),\mu_B(y)),1-\mu_A(x)\}$
Deines	$Max\ \{1-\mu_A(x),\mu_B(y)\}$
Brown Godel	1 si $\mu_A(x)\leq \mu_B(y)$ $\mu_A(x)\mu_B(x)$ Otherwise
Lukasievic	$Max\ \{1,1-\mu_A(x)+\mu_B(y)\}$
Larsen	$\mu_A(x)\mu_B(y)$

IV.4.5. Fuzzy rule

The fuzzy rule is a relationship expressed by means of an implication between two fuzzy propositions [110], [113] Usually several fuzzy rules are necessary to make a decision in a given situation. We are interested in the case of several fuzzy rules in the field of control and regulation.

Fuzzy rules can be described in several forms:

- **Linguistically:** In this case, the rules are expressed explicitly as in the following example: ″ IF the torque error is small AND the flux error is small THEN use a small actuation time for the appropriate voltage vector ″.
- **Symbolically:** In this case, the linguistic description is replaced by symbols such as (VS, *M*,VB...etc) which indicate the designation of fuzzy sets (Very Small, Medium, Very Big...etc).
- **By inference matrix:** In this case, all the rules that are symbolically identified are summarized in a table called ″ Inference Matrix″. The inputs of the table represent the degrees of membership of the linguistic variables of the inputs to the different fuzzy sets, and the crossing of a column and a row gives the output fuzzy set defined by the rule.

IV.5. Fuzzy Logic Control

Fuzzy logic control can provide an efficient control law without the need for extensive modeling. In contrast to a standard controller or a controller with state feedback, the fuzzy logic controller does not handle a well-defined mathematical relationship, but uses inferences with several rules, based on linguistic variables. Through inferences with several rules, it is possible to take into account the experiences acquired by the operators of a technical process [114].

There are three steps involved in dealing with a problem using fuzzy logic [113] :

- Fuzzy quantification of inputs, also called fuzzification. It allows the conversion of input variables that are physical quantities into fuzzy quantities, or linguistic variables;
- The establishment of rules between outputs and inputs, called fuzzy inference ;

- Defuzzification which is the reverse operator of fuzzification. It consists in transforming the output linguistic variables into real or numerical variables.

The block diagram of a fuzzy controller is shown in the following figure [113], [115] :

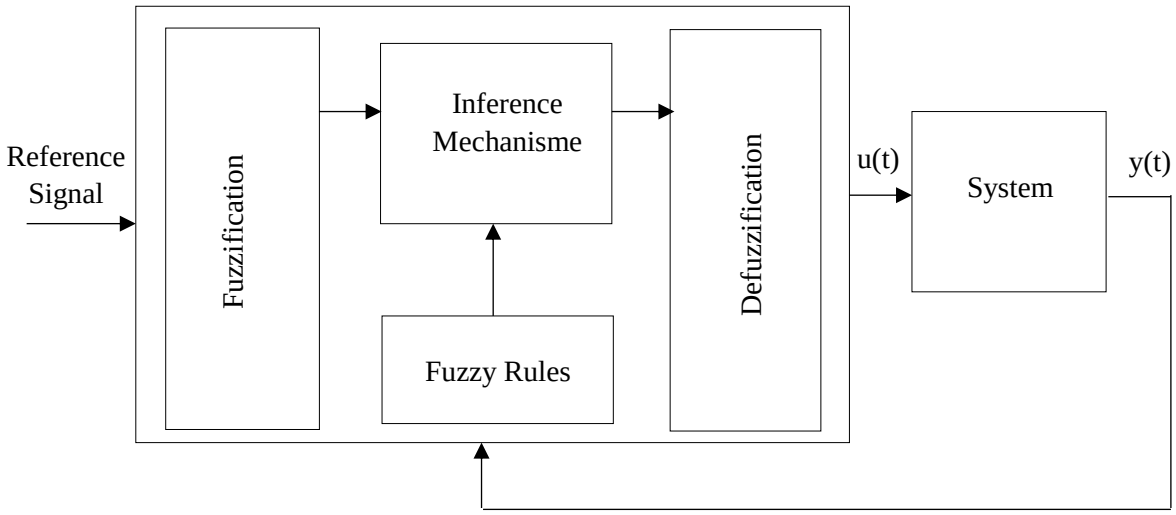

Figure IV.2 General block diagram of a fuzzy logic controller.

Where :

$u(t)$: is the control signal.

$y(t)$: is the output of the controlled system.

This fuzzy controller essentially consists of four parts: a fuzzification interface, a rule base, an inference mechanism and a defuzzification procedure or interface.

IV.5.1. Fuzzification interface

Fuzzification is the process of projecting real physical variables on fuzzy sets that describe the linguistic values taken by these variables. The fuzzification block performs the following functions:

- Definition of the membership functions of all input variables.
- Transformation of physical quantities (real or numerical) to linguistic or fuzzy quantities.
- Representation of scale that transfers the range of input variables to the corresponding range of discourse universes.

IV.5.2. Rules Basis

This block is based on certain knowledge that corresponds to the operator's expertise or skills on system behavior. It (rule base) is composed of all the information and knowledge in the field of application and the expected control result. It is used to determine the output signal of the fuzzy controller and the relationship between input variables transformed into linguistic variables and output variables converted also into linguistic variables [115]. Thus, it is constituted by a collection of data in the form "IF...THEN". In a general way, the *K_th* fuzzy rule can be expressed by the following relation :

IF x_1 is $F_{1(i)}$ and x_2 is $F_{2(i)}$, $\ldots x_n$ is $F_{n(i)}$ Then y_j is G_j

Where: $i = 1,\ldots,k$; k is the total number of rules; $F_{1(i)}$, $F_{2(i)}\ldots F_{n(i)}$ are the fuzzy sets of the inputs ($x_1, x_2 \ldots, x_n$) and $G_{j(i)}$ is the fuzzy set of the output y_j that corresponds to the *K_th* rule.

IV.5.3. Fuzzy Inference Mechanism

Fuzzy inference or decision logic is of course the core of the fuzzy controller, which has the ability to emulate human decisions and to determine fuzzy control actions using fuzzy implication and fuzzy logic inference rules [114]. It uses fuzzy variables transformed by fuzzification and inference rules to create and determine output variables, based on fuzzy operations applied to membership functions.

As we have mentioned, there are several possibilities for realizing the fuzzy operators that can be applied to the membership functions. We introduce the notion of inference echanism, allowing a numerical processing of the set of fuzzy rules. Generally, the most widely used methods are [110] :

- Max-Min inference method (Mamdani method).
- Max-Product Inference Method (Larsen's Method).
- Sum-Product inference method.

The following table summarizes the different inference methods used to realize the three fuzzy logic operators "AND, *O*R and THEN".

Table IV.3 Typical fuzzy inference methods [110].

Operator / Inference	AND	OR	THEN
Max-Min	Minimum	Maximum	Minimum
Max-Product	Minimum	Maximum	Product
Sum-Product	Product	Average	Product

IV.5.4. Defuzzification Interface

Inference methods generate a result that is a function of membership. However, the variable to be controlled is usually a continuous quantity, taking its value in an interval. It is therefore necessary to convert the fuzzy quantities into precise quantities. This can be done by using a defuzzification process. Defuzzification is thus the inverse phase of fuzzification [85, 116], allowing to maintain the link between the result of the inference and the output control quantity by switching from a representation in the form of linguistic variables to a representation in the form of physically applicable numerical variables. Then, these values are denormalized and applied to the process. There are several methods possible defuzzification. The most recognized and used are: the method of the maximum, the average of the maximum and the center-of-gravity method which remains the most frequently used [117].

- Maximum method: This method generates a control that represents the abscissa of the maximum value of the resulting membership function from the fuzzy inference rules.
- Maximum Average Method: This method generates a decision that represents the average value of all maximums, in the case where there are several values for which the resulting function is maximum.
- Center of Gravity Method (Centroid Method): This method generates an output equal to the abscissa of the center of gravity of the resulting membership function from fuzzy inference.

IV.6. Problem Statement

After introducing the concept of the fuzzy logic controller and its essential fundamentals, the problem that arises is how to integrate the fuzzy logic system (precisely the concept of the fuzzy logic duty cycle controller) in combination with MPDTC with the essential goal of reducing torque fluctuations.So, its important to present a brief review about the relationship betwwen torque ripples and some specific conditions.

IV.6.1. Relationship Between Torque Ripple, Switching Frequency and Switching Losess

Conventionally, FS_MPC is implemented without a modulator using high sampling frequency [42]. As a results, only the discrete voltage space phasor generated by the inverter can be applied. Depending on the operation conditions and the parameters of the control system, only the optimal voltage space vector remain applicable for the entiere switching period.

In that sense, the FS_MPC operates at a variable switching frequency, where the resulting voltage and current spectrum changes significantly, as a function of the sampling frequency and working environment. However, in most competitive applications, a constant switching frequency, referring to a control scheme based on the Pulse Width Modulation (PWM), is preferred for operational reasons. Another disadvantage of FS-MPC is that the quality of the controller depends on the accuracy of the model [42]. Alternatively, these inconveniences can be successfully managed by combining the strengths of both FS_MPC and PWM . The proposed control scheme follows the predictive scheme of FS_MPC and takes advantage of a constant switching frequency, but does so by generating the switching signals by means of pulse-width modulation.

A suggested solution is proposed to improve the steady-state behaviour through increasing the switching frequency (fs) (see **Fig IV.3**). Nevertheless, in some practical experiment, the increased switching frequency is proportional to the additional hardware and cost of the control system and in some cases the operation is invalid [118]. Consequently, the steady-state error introduced by conventional FS_MPC can be eliminated by integrating a modulator stage into the standard control scheme [42].

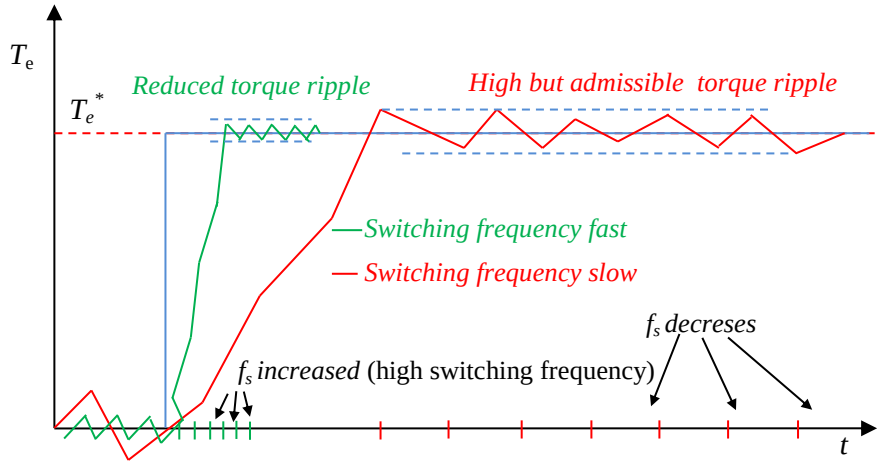

Figure IV.3 Torque ripple analysis according to the applied switching frequency.

As ilustrated in **Figure IV.3**, the fast dynamic response, and a small electromagnetic torque fluctuation are the main fetures when the switching frequency is selected to be high; nonetheless, the switching losses are proportionel to the selected switching frequency. Conversely, a slow dynamic response and a high level of ripple are obtained when the switching frequency is selected to be low; nonetheless, the switching losses are directly reduced [119]. Accordingly, the advantages of both approaches i.e. a high dynamic response, admissible torque ripples as well as a reduced switching frequency in the steady-state can be combined if the applied voltage vector during each switching period can be adjusted on-the-fly, i.e. during the operation of the electrical drive.

Note: Increasing the carrier signal frequency leads to enhanced dynamic behavior of the control, however, with the side effect of an augmented thermal stress of the power semiconductors due to the increased switching frequency.

IV.6.2. Reconfigurable Pulse-Width Modulation

In particular, DTC_SVM uses a vector modulation technique to generate the voltages applied to the machine under fixed switching frequency. Thus, once the switching frequency (fS) of the inverter is fixed according to a certain creterion the switching losses cannot be influenced anymore. Furthermore, the steady stetate performance of the control can exibiths an improved behavior. More specifically, the interest during steady state is mainly based on a measurement of a such control performance, which is selected in this study by the ripple of the electromagnetic torque (ΔT_e), which is also proportional to the switching frequency.

By convention, a compromise between the maximum admissible switching losses and the dynamic behaviour of the controller is found in order to select the switching frequency to be used.

For variable switching frequency control, the desired switching pattern should maximise the switching frequency during transient states to ensure that the desired reference value is reached as quickly as possible. Once the reference and actual value are close to each other, the switching frequency can be adjusted to a maximum permissible torque ripple, as shown in **Figure IV.4**. By reducing the switching frequency, the switching losses are also imediately reduced. This kind of control is refered as reconfigurable pulse-width modulation or by the variable switching time PWM i.e. the sampling time (T_S) can be varied without stopping the control platform to reconfigure the PWM units [119-120]. However, to achieve this type of dynamic behavior control, the bandwidth of the control platform must be very high, i.e. the computing power must be sufficient and the analog-to-digital conversion of the measured signals must be very fast.

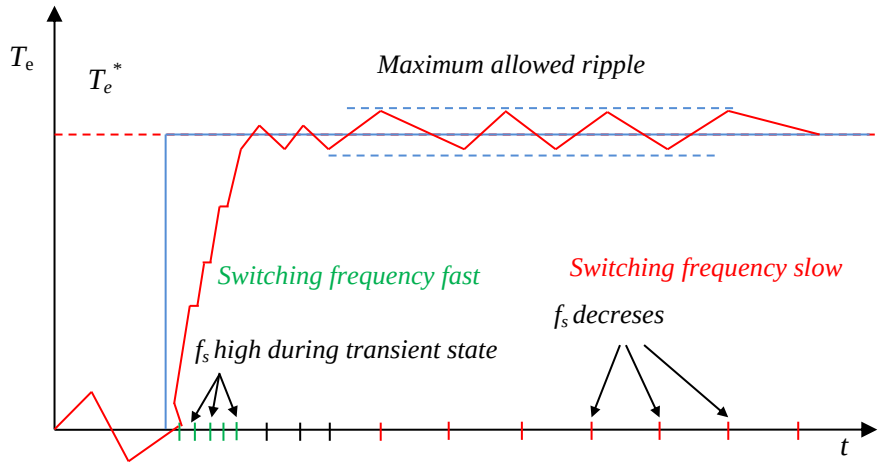

Figure IV.4 Torque control performance based-reconfigurable PWM.

In this sense and according to the specific conditions presented, particularly in relation to the chosen switching frequency, a convinient solution is proposed in this thesis to minimize the torque ripples without sacrificing the switching frequency, i.e. without increasing the switching frequency (i.e. without decreasing significantly the sampling time) which induces the improvement of the steady state and dynamic behavior.The proposed technique qualify to adjust the appropriate voltage vector on-the-fly for a portion of samling time which is reffered as duty cycle control. The latter is combined with the concept of fuzzy logic to realize a fuzzy logic duty cycle controller.

IV.7. Design of FLM-Based MPDTC PMSM Drive System with EKF

In standard FS-MPDTC-PMSM supplied by two-level inverter, there is a limited number of switching states and only one voltage space vector (VSV) is acted during each controlled period, and hence, the undesired ripples inevitably take place in the controlled variables (i.e., Torque and flux). In order to cope with these limitations and achieve steady-state performance improvement, a convenient solution is proposed to adjust the magnitude of the selected VSV for each switching period according to certain criteria. For this reason, a fuzzy logic-based duty cycle vector modulation is utilized and two VSVs instead of single VSV are applied during the whole control cycle. In fact, the first VV is selected by the FS-MPDTC algorithm and its actuation time is determined through a fuzzy inference mechanism by using a collection of linguistic if–then fuzzy rules. For the remaining of each switching period, a null VSV is applied. The flowchart of the proposed FLM-MPDTC with EKF is shown in **Fig IV.5**.

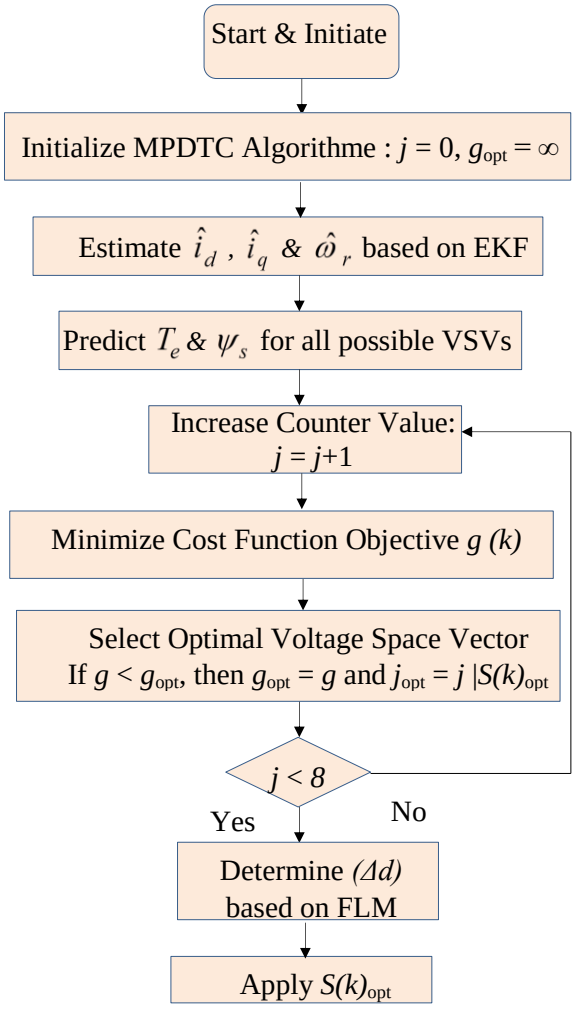

Figure IV.5 Flowchart of the proposed FLM-MPDTC with EKF for PMSM.

In brief, the fuzzy logic-based duty cycle control method introduced in FS-MPDTC not only helps to exploit both of the applied VSVs candidates during the overall control cycle, but also to simultaneously determine the optimum applied duration time of the selected VSVs. As a result, the undesired ripples are significantly reduced in both controlled variables: torque and flux. **Fig IV.6** shows the global schematic of our proposed FLM_based MPDTC-PMSM drive systems with EKF.

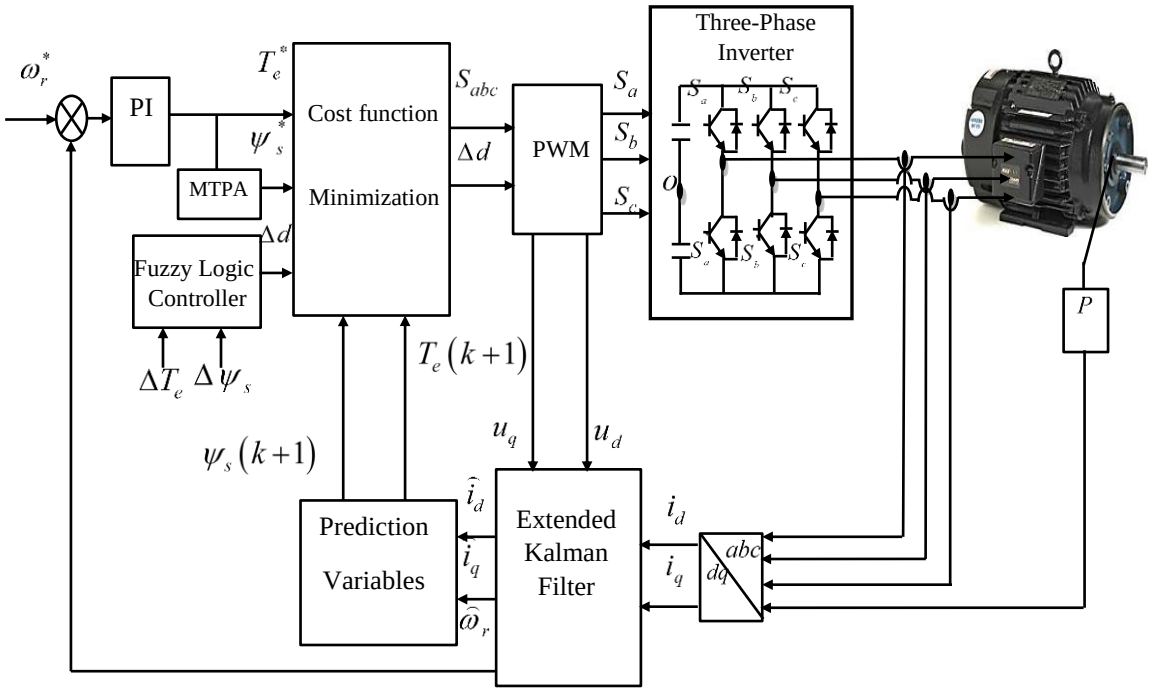

Figure IV.6 Schematic diagram of the proposed FLM-MPDTC with EKF for PMSM.

IV.7.1. Fuzzy Logic Modulator Design

In this subsection, a fuzzy logic modulator (FLM) is designed to determine the desired actuating time or reffered by duty cycle of the selected active voltage space vectors VSVs. Several Duty Cycle Vector Modulation (DCM) strategies have been suggested in the literature in order to improve the predictive torque control method; among them are: the torque ripple minimization [120], the root-mean-square ripple minimization [121], the mean torque control [29] and the torque deadbeat method [27]. Although better performance was achieved by reducing the torque and flux ripples and guaranteeing a constant switching frequency, the complexity of the system was increased, and more machine parameters were needed.

The proposed FLM is free of the system prameters, and therefore, it does not require any complex control algorithm or any additional calculation. In other words, regarding the uncertainties and/or nonlinearities of the controlled system, the proposed FLM is very simple, effective, and entails neither the states nor the parameters of the system.

Based on the fuzzy logic concept, the FLM includes four main parts: fuzzification, fuzzy rules, inference engine and defuzzification. The inputs of the FLM are the torque error (ΔT_e) and the flux error ($\Delta\psi_s$). The outputs are the desired duty ratios (Δd). The FLM provides either a large (increment) or small (decrement) duty cycle (ratio) for the selected active VSVs in order to optimize the electromagnetic torque ripples. As a result, a long duration is devoted for a large torque error and a little if the predicted torque reaches its reference. In this thesis, minimum, maximum and maximum operators are used as fuzzy operator, implication and aggregation, respectively, and centroid criteria are employed for defuzzification. **Figure IV.7** shows the sequence of switching state candidates in the proposed FLM. By adopting this procedure, the inverter is forced to apply an active and zero voltage vectors alternatively. As a result, the undesired ripples are significantly reduced in both control variables: torque and flux.

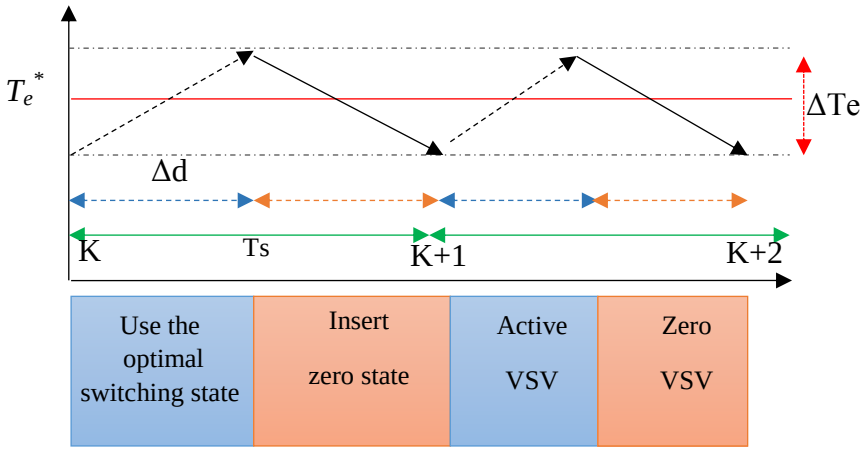

Figure IV.7 The sequence of switching state candidates in the proposed FLM.

Fuzzy logic inference inputs are defined as follows:

$$\begin{cases} input1: \Delta T_e = \sqrt{\left(T_e^* - T_e(k+1)\right)^2} \\ input2: \Delta\psi_s = \sqrt{\left(\psi_s^* - \psi_s(k+1)\right)^2} \end{cases} \quad (4.1)$$

The inputs and outputs of the FLM are scaled and normalized as follows:

$$\begin{cases} e_{nT} = k_T \Delta T_e \\ e_{n\psi} = k_\psi \Delta \psi_s \\ \Delta kd_{en} = k_{\Delta d} \Delta d \end{cases} \quad (4.2)$$

Where k_e, k_ψ, $k_{\Delta d}$ are the normalization factors. For the fuzzification, the inputs and outputs set (i.e. $\Delta\psi_s$, ΔT_e and Δd) are normalized to the interval [0.01, 0.1], [0.1, 0.8] and [0, 1] respectively. **Figures IV.8, 9** and **10** show the corresponding membership functions. The used variables for the fuzzy sets are : E (Error), D (duration), Z (zero), S (Small), M (Medium), L (Large) and VL (Very-Large). Hence, the fuzzy rules are summarized in **Table IV.4**.

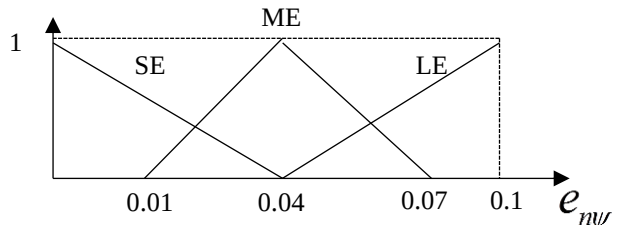

Figure IV.8 Normalized fuzzy sets of flux error

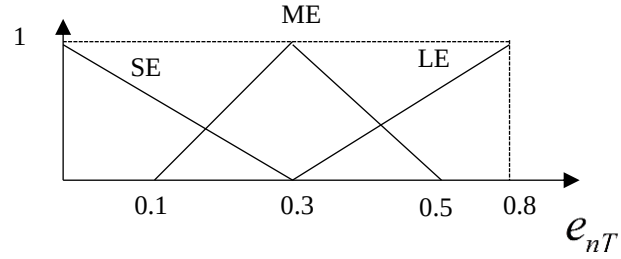

Figure IV.9 Normalized fuzzy sets of torque error

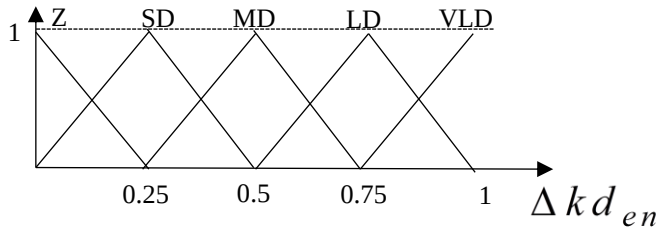

Figure IV.10 Normalized fuzzy sets of duty-cycle

Table IV.4 Fuzzy rules for duty-cycle (Δd)

(Δd)		e_{nT}		
		SE	ME	LE
$e_{n\psi}$	SE	Z	MD	LD
	ME	SD	MD	LD
	LE	LD	LD	VLD

Then, the fuzzy inference consists to mimic the strategy of human thinking in order to deduce fuzzy control actions using fuzzy implication and collection of linguistic if-then fuzzy rules. Consequently, the implication (Mamdani's Min–Max) applied in the rules has the form:

R_{11}: If ΔT_e is A_{SE} and $\Delta\psi_s$ is B_{SE} then $U_{\Delta d}$ is U_Z

R_{12}: If ΔT_e is A_{ME} and $\Delta\psi_s$ is B_{SE} then $U_{\Delta d}$ is U_{MD}

R_{ij}: If ΔT_e is A_i and $\Delta\psi_s$ is B_j then $U_{\Delta d}$ is U_{ij}

Where A_i, B_i are the membership functions (MFs) of (ΔTe) and (Δψs) respectively, and $U_{\Delta d}$, is the MF of the output variable of the fuzzy modulator.

Finally, the defuzzification consists of transforming the fuzzy information established by the inference engine to crisp values. In this study, a defuzzification method based on gravity center is used to calculate the desired duty ratio (Δd) as given in eq.(4.3).

$$\Delta d = \frac{\sum_{k=1}^{N_r} \Delta d\, \mu_{(k)}(\Delta d)}{\sum_{k=1}^{N_r} \mu_{(k)}(\Delta d)} \tag{4.3}$$

Where N_r is the total number of rules, (Δd)is the outputs value of the FLM and $\mu_{(k)}(\Delta d)$ denotes the output membership degree for (k-th) rule .

The fuzzy controller generates a number between 0 and 1, it is a filling of signal in one period (0 to 100%). What's more, the duty ratio controller prepares an optimal voltage vector for optimizing torque and flux ripples. **Figure IV.11** show a simplified diagrame of duty-ratio controller switching state [122].

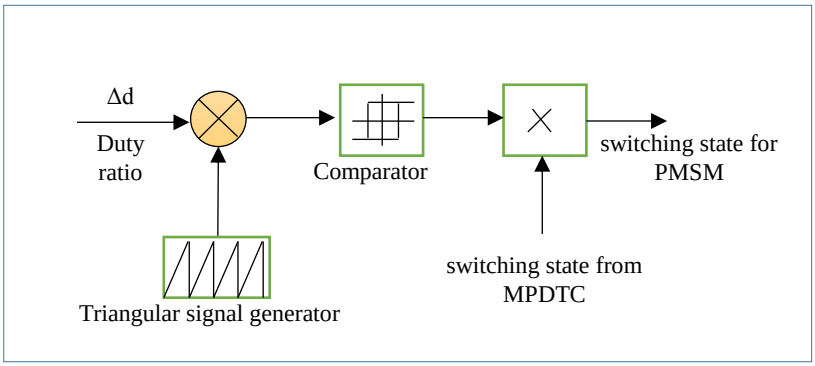

Figure IV.11 Duty ratio Controller switching state.

From the obtained duty ratio after the defuzzification, the predicted currents can be rewritten as:

$$\begin{cases} i_d^{k+1} = i_d^k + \dfrac{1}{L_d}\left[-R_s i_d^k + p\omega_r^k L_q i_q^k + u_d^k \Delta_d\right] T_s \\ i_q^{k+1} = i_q^k + \dfrac{1}{L_q}\left[-R_s i_q^k - p\omega_r^k L_d i_d^k - p\omega_r^k \psi_{rm} + u_q^k \Delta_d\right] T_s \end{cases} \tag{4.4}$$

From this eq. (4.4), both torque and flux predictions can be obtained also. However, something important must be highlighted which is the null VSV should be applied for $(1-\Delta d)$ T_s period.

IV.7.2. Extended Kalman Filter Design

The EKF is an optimal recursive state observer based on the knowledge of the statistical model of system noises and measurements errors [123]. In this work, a simplified EKF observer is used to estimate the current components (dq-axis) and the rotor speed.

IV.7.2.1. Notation

The notation $x \in \Re^n$ is the system state vector, $f(.,.,.)$ defines the system's dynamics, $u \in \Re^m$ is the deterministic control input, $y \in \Re^p$ is the observation vector, and $c(.,.,.)$ is the measurement function. $x_{(0/0)}$ is the system initial condition considered as random Gaussian vector. The notations $\hat{x}(k+1/k)$ and $\hat{x}(k/k)$ denote the prediction of the state vector at instant $(k+1)$ and the state vector at the previous instant (k), respectively. $'K'$ and $'I'$ are the filter gain and the identity matrix, respectively. $F(k)$ and $C(k)$ define the Jacobian matrix of partial derivatives of the system *f* with respect to x and the Jacobian matrix of partial derivatives of c with respect to x, respectively. $y(k+1)$ is the new observation vector. For the innovation process, the notations $\hat{x}(k+1/k+1)$ and $P(k+1/k+1)$ are the estimated state vector and the covariance matrix, respectively. The notations A_d, B_d and C_d are the system, input and measurement matrices, respectively. $\{w(k)\}, \{v(k)\}$ are zero-mean white Gaussian noises with covariance *Q(k)* and *R(k)*, respectively.

Taking into account the estimations of the system covariance and measurement noise, the PMSM is represented by the following nonlinear stochastic model:

$$\begin{cases} \dot{x}(t) = f\left(x(t),u(t)\right) + w(t) \\ y(t) = c\left(x(t)\right) + v(t) \end{cases} \tag{4.5}$$

Where *w(t)* is the process noise, and *v(t)* is the measurement noise. The covariance matrices of *w(t)* and *v(t)* are *Q* and *R*, respectively.

And

$$x(t) = \begin{bmatrix} i_d & i_q & \omega_r \end{bmatrix}^T,\ u(t) = \begin{bmatrix} v_d & v_q \end{bmatrix}^T,\ \ y(t) = \begin{bmatrix} i_d & i_q \end{bmatrix}^T. \tag{4.6}$$

The implementation of EKF algorithm is as follows [123]:

• Initialize the state vectors and covariance matrices:

$$x_{(0/0)}, p_{(0/0)}, Q, \mathrm{R} \tag{4.7}$$

• State prediction:

$$\hat{x}\left(k+1/k\right) = f\left(\hat{x}(k/k), u(k), x_{k/k}\right) \tag{4.8}$$

• Calculation of covariance matrix of prediction:

$$P\left(k+1/k\right) = F\left(k\right)P\left(k/k\right)F^T\left(k\right) + Q\left(k\right) \tag{4.9}$$

Where

$$F\left(k\right) = \frac{\partial f}{\partial x}\left(x\left(k/k\right), u\left(k/k\right), w\left(k/k\right)\right)\Big|_{x(x)=\hat{x}(k/k)} \tag{4.10}$$

• Calculation of optimal filter gain matrix:

$$K\left(k+1\right) = P\left(k+1/k\right)C^T\left(k\right)\left(C\left(k\right)P\left(k+1/k\right)C^T\left(k\right) + R\left(k\right)\right)^{-1} \tag{4.11}$$

With

$$C\left(k\right) = \frac{\partial c\left(x\left(k\right)\right)}{\partial x\left(x\left(k\right)\right)}\Big|_{x(x)=\hat{x}(k)} \tag{4.12}$$

• Innovation process**:**

$$\hat{x}\left(k+1/k+1\right) = \hat{x}\left(k+1/k\right) + K(k+1)\left(y\left(k+1\right) - C\left(k\right)\hat{x}\left(k+1/k\right)\right) \tag{4.13}$$

$$P\left(k+1/k+1\right) = \left(I - K\left(k+1\right)C\left(k\right)\right)P\left(k+1/k\right) \tag{4.14}$$

Where $\hat{x}$ is the estimated state, P is the covariance matrix of the filter error. Considering *w(t)* and *v(t),* assume the sampling time Ts, the linearized and discrete model of the PMSM can be obtained by using Eq.(4.15):

$$\begin{cases} x(k+1) = A_d x(k) + B_d u(k) + w(k) \\ y(k) = C_d x(k) + v(k) \end{cases} \tag{4.15}$$

Thus, in accordance to Eq. (4.15) we can deduce the following matrices:

$$A_d = \begin{bmatrix} 1 - \frac{R_s}{L_{d\,s}} & P\omega_r & 0 \\ -P\omega_r & 1 - \frac{R_s}{L_{q\,s}} & \frac{-P\psi_{rm}}{L_q} \\ 0 & 0 & 1 \end{bmatrix}, B_d = \begin{bmatrix} \frac{1}{L_d} & 0 & 0 \\ 0 & \frac{1}{L_q} & 0 \end{bmatrix}, C_d = \begin{bmatrix} 1 & 0 & 0 \\ 0 & 1 & 0 \end{bmatrix} \tag{4.16}$$

The initial values of covariance matrices (according to the general guide provided in [124]) have been chosen to:

$$P_{(0/0)} = diag\begin{bmatrix} 0.1 & 0.1 & 0.01 \end{bmatrix}, Q = diag\begin{bmatrix} 0.0005 & 0.0005 & 1 \end{bmatrix}, R = diag\begin{bmatrix} 10 & 10 \end{bmatrix}.$$

The covariance matrix *R* is increased due to the fact that the measurements of the currents are subjected to external noise, and should be weighted less by the filter.

IV.8. Simulation Results

To study the performance of the improved MPDTC based on a FLM and EKF, the MATLAB/ Simulink model of the proposed composed control strategy is developed. Meanwhile, simulation model of conventional-MPDTC is also conducted in order to demonstrate the feasibility of the proposed FLM-MPDTC-EKF. The proposed improved system is composed of a PMSM drive, predictive torque/flux controller, fuzzy logic modulator, and an extended kalman filter estimator. Compared to the C-MPDTC, the proposed improved MPDTC operates at a constant switching frequency, as the proposed FLM-MPDTC incorporates a modulator for the overall control scheme. The parameters used for the simulation are given in **Appendix B** [107].

At first, a unified monitoring scenario is employed for both control methods (MPDTC, FLM-MPDTC-EKF) in order to perform a fair comparison. The monitoring scenario include: the starting up, the steady states at rated speed, rated load torque introduction and a maneuver of speed sense reversing. For both control methods, the chosen wheighting factor is equal to λ =3000.

IV.8.1. Starting, steady state at rated speed, application of rated load torque and rated speed sense reversing operation

In this part, both control techniques (MPDTC and FLM-MPDTC-EKF) was tested for a target rated speed of 1000 rpm with a rated load of torque insertion at t=0.1 s followed by a speed sense reversing operation at t=0.15. The Starting up situation and steady states with load torque application and the speed sense reversal are depicted. For that, **Figs IV.12** to **IV.16** show the stator phases current , electromagnetique torque and stator flux evolution.

Besides, as the wheighting factor (λ) has a strong effects on the performance of the controlled system such as the THD of stator currents, a detailled THD analysis of stator phase current with differents values of wheghting factors and under some specific conditions, are depicted in **Appendix C**. Also, to show the filtering capability of the used EKF against noisy currents an external random noise is injected to the measured currents. The figures are mentioned by **(a)** for C-MPDTC, and **(b)** for FLM-MPDTC-EKF.

(a)

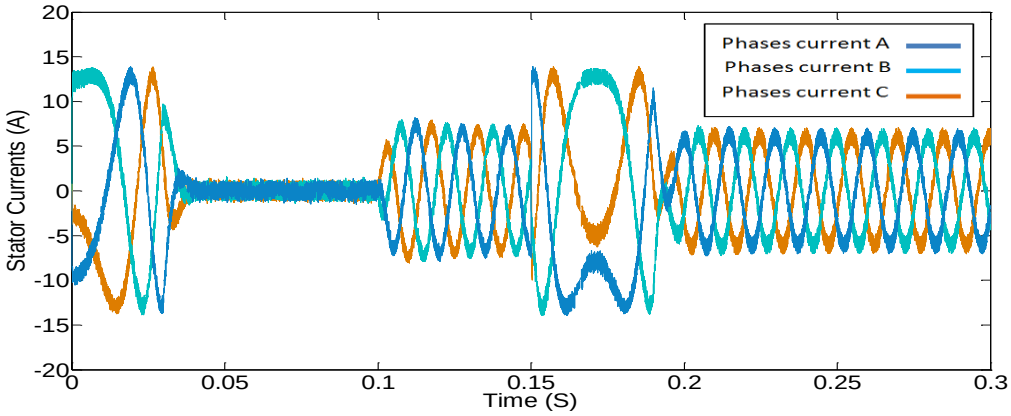

(b)

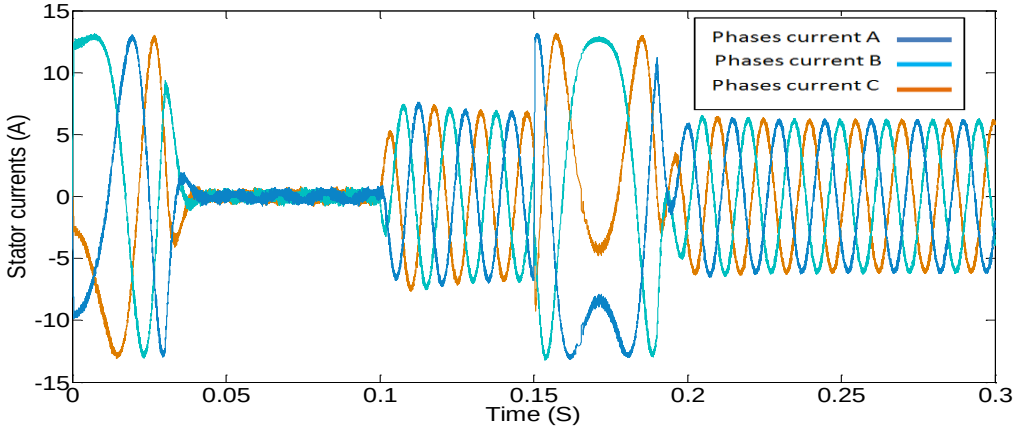

Figure IV.12 Stator currents (A).

(a)

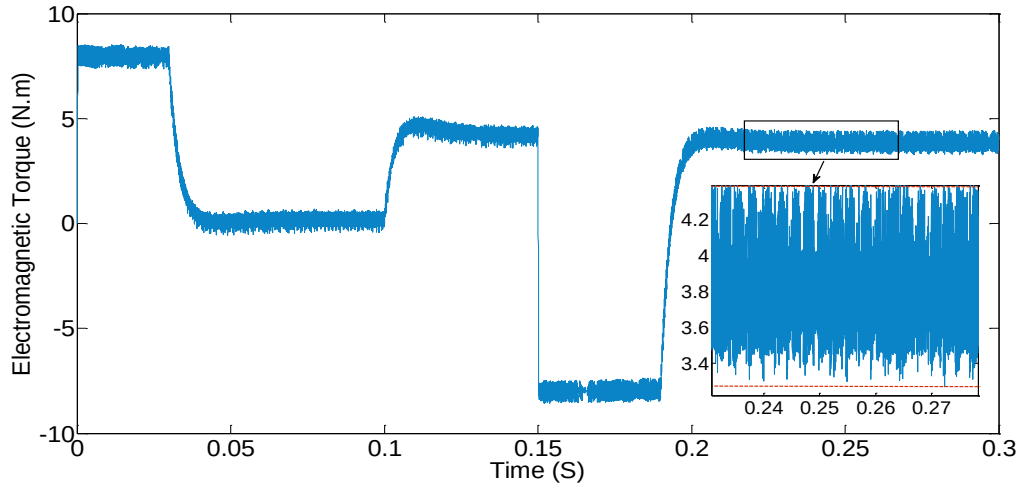

(b)

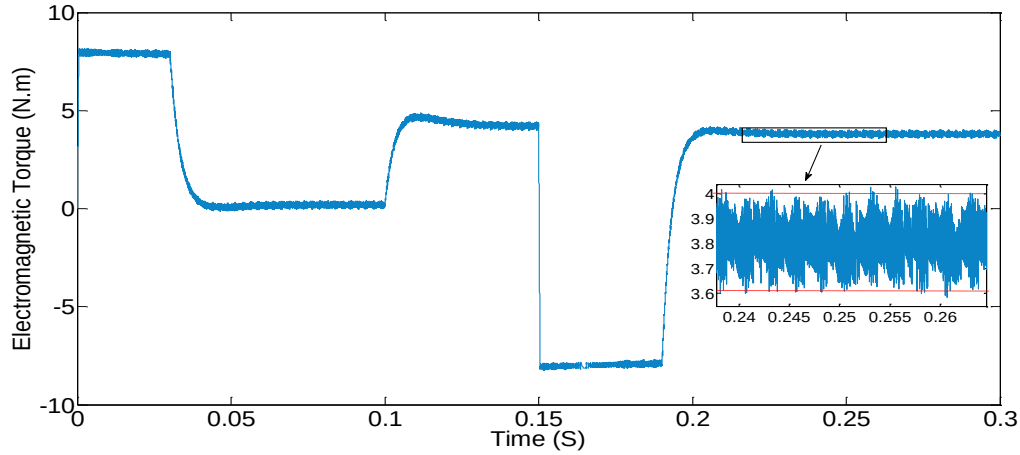

Figure IV.13 Electromagnetic torque (N m).

(a)

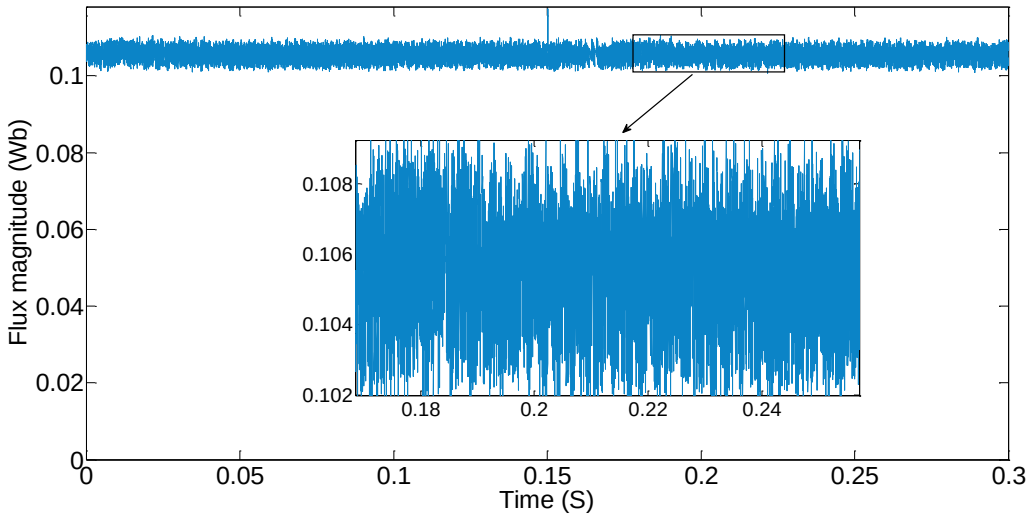

(b)

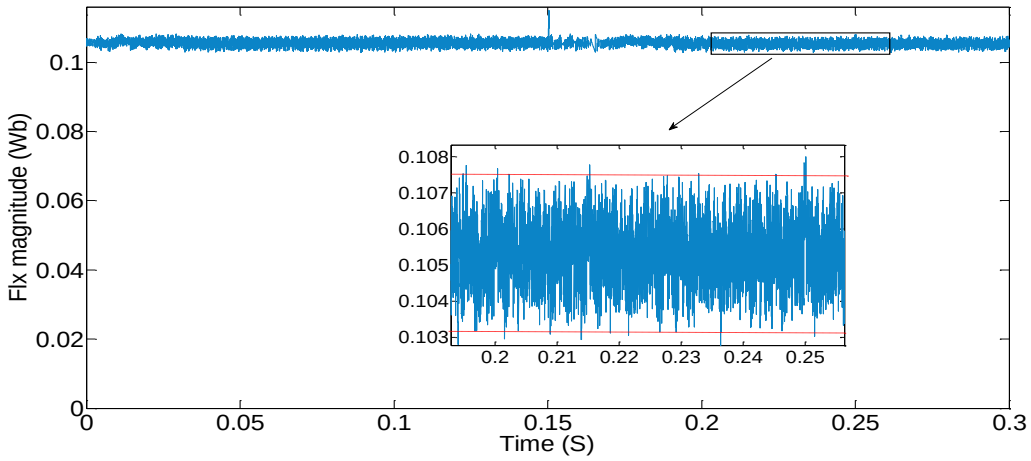

Figure IV.14 Stator flux magnitude (Wb).

(a)

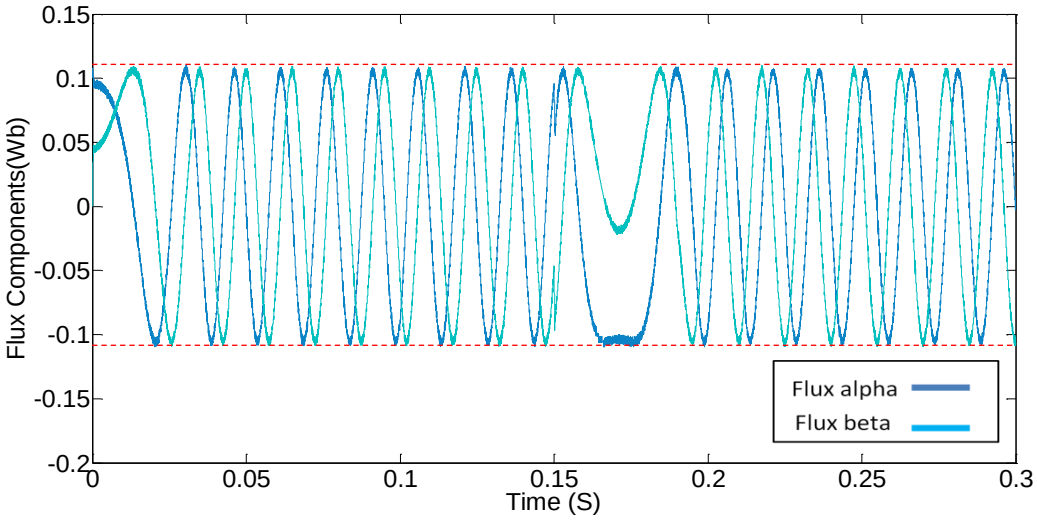

(b)

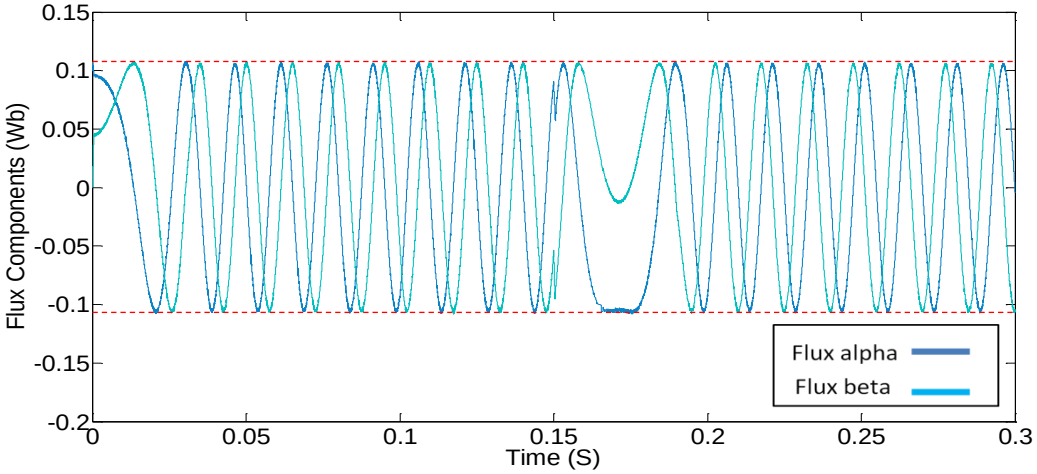

Figure IV.15 Stator flux components (Wb).

(a) **(b)**

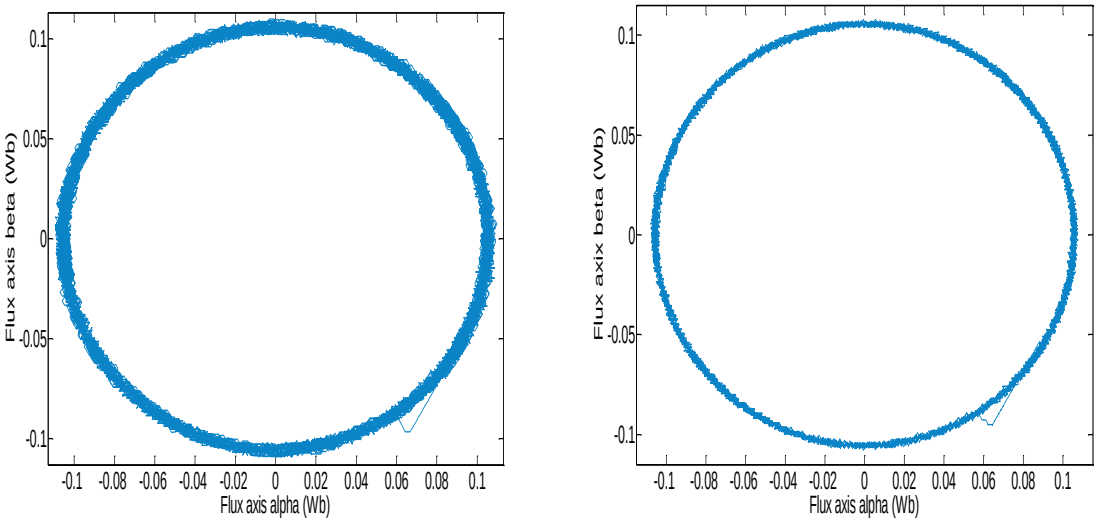

Figure IV.16 Stator flux trajectory (Wb).

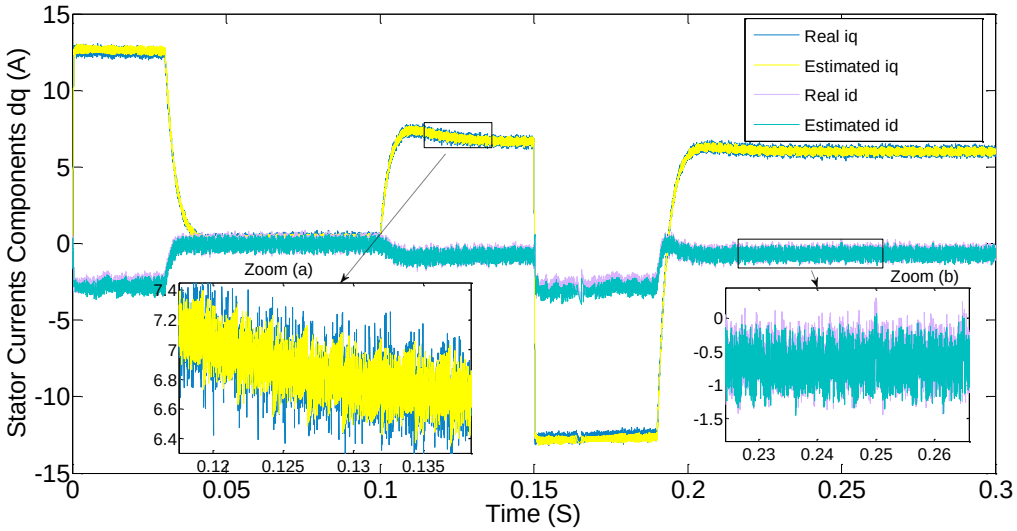

Figure IV.17 Estimated currents.

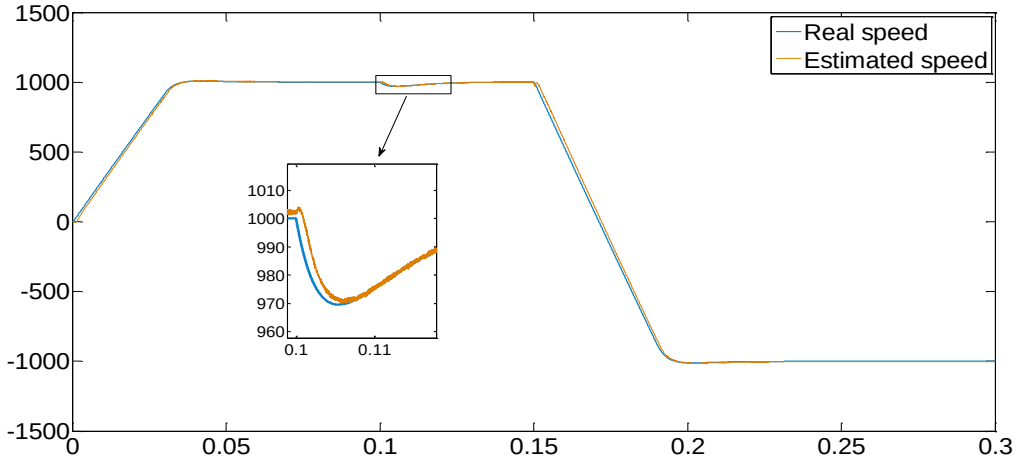

Figure IV.18 Estimated speed.

Firstly, **Fig IV.12a, b** show respectively the stator phase's current (isa, isb, isc) of C-MPDTC and improved MPDTC during all the mentioned operating points. It is clear that the proposed improved MPDTC presents smoother sinusoidal current waveform than the C-MPDTC. This refers to the effectiveness of our proposed FLM based duty cycle determination and to the filtering capability of the used EKF. Moreover, this explicitly shows the importance of the proposed combined control strategies in enhancing the stator current waveform by eliminating the harmonics, which also leads to improve the prediction model.

Then, **Fig IV.13a, b** illustrate the responses of the electromagnetic torque. From (**Fig IV.13a ZOOM, IV.13b ZOOM**) it is worth mentioning that the proposed improved MPDTC offers better steady state and dynamic performances of torque with remarkable reduction of ripples than the conventional-MPDTC; it can be seen that the torque ripple range of the improved strategy is about 0.35 Nm (from 3.65 Nm to 4 Nm); the value of the C-MPDTC strategy is 1 Nm (from 3.4 Nm to 4.4 Nm). This is mainly due to the proposed improved MPDTC that uses two voltage vectors during the whole control cycle, which leads to regulate the torque more accurately, and thanks to the predictive controller that uses the filtered (estimated) currents for the prediction of the controlled variables instead of the noisiest currents (measured).

Next, **Figs IV.14** to **IV.16** show the waveforms of the magnetic stator flux, namely the flux amplitude, the flux components and the flux trajectory. From **Fig IV.14a, b** it is clear to see that the amplitude of flux in both cases follows their references perfectly but with reduced level of ripples in the case of the improved MPDTC. In addition, from **Fig IV.15a, b** the improved MPDTC presents better sinusoid waveform than that of C-MPDTC.

As to the trajectory of the stator flux, we can clearly see in **Fig IV.16a,b** that the stator flux trajectory of the proposed improved MPDTC has a finer circular form than the one obtained by the C-MPDTC.

Thus, it can be judged that the composed control strategy permits to mitigate considerably the undesired ripples. More precisely, applying an active voltage vector followed by a zero voltage vector is the reason of the minimized torque and flux ripples. So, it is important to highlight that the composed FLM-MPDTC with EKF preserves the decoupled control of torque and flux of the basic DTC and ensures improvement in the steady state and dynamic performances. Moreover, it is worth mentioning that the fuzzy rules are defined to reduce the torque ripples. However, it is possible to modify these rules in order to reduce certain concerned objectives (e.g. reducing current or stator flux ripples).

The fuzzy rules were constructed after different simulation tests under different working conditions of the motor. Furthermore, this fuzzy logic modulator is possible to be applied with either synchronous machines or induction ones by using any power converter topology as interface between the machine and the predictive controller.

On the other hand, in order to check the estimation performances and the unique properties of the EKF, simulation tests were conducted in the same operating conditions. **Figs IV.17** and **IV.18** illustrate, respectively, the tracking capability of d-q current components and speed in the enhanced control strategies FLM-MPDTC with EKF and without EKF. As presented in (**Fig IV. 17 ZOOM a, b**), the estimated currents (id, iq) of the proposed MPTDC with EKF are smoother than the real currents of the FLM-MPTDC without EKF because the improved MPDTC-EKF uses the filtered currents, for the prediction of the controlled variables (current, torque and flux) instead of the noisy currents and this specialty enhances the prediction model. Furthermore, as shown in **Fig IV.18**, the estimated speed is free from noise and has good tracking performance even if the speed is reversed which confirms the filtering capability and the estimation accuracy of the simplified EKF. Also, it can be seen from (**Fig IV.18 ZOOM**) that the under-shoot due to the load torque application in the case of FLM-MPDTC without EKF is relatively considerable than the case of EKF-based FLM-MPDTC. This is mainly attributed to the external disturbance rejection capability of the EKF. Thus, the designed EKF qualifies not only in tracking the states (d-q current components and speed) of the PMSM with high accuracy, but also for improving the prediction model of the studied system by avoiding the measurements noise and perturbation.

From the obtained results, distinctive improvements were achieved by our proposed control strategy (FLM-MPDTC-EKF). These improvements include mainly the fixed switching frequency and the significant reduction of both torque ripples and THD compared to the C-MPDTC method.

IV.9. Conclusion

This chapter develops an improved Model Predictive Direct Torque Control (MPDTC) strategy based on a fuzzy logic modulator (FLM) and an extended Kalman filter (EKF), which can solve the main drawbacks associated with the conventionel-MPDTC method. First, we have discussed the fundamentals and concepts of fuzzy logic and fuzzy logic control. Second, in order to cover the problem of undesired torque ripples, the relationship between torque ripple, switching frequency and switching losses is examined. Third, in

order to promote the torque control performance, a fuzzy logic modulator is designed and integrated in the global control scheme. Unlike the usual voltage space vectors (VSVs) selection in the C-MPDTC, the proposed FLM-MPDTC is actuating with two VSVs (i.e. one active voltage vector followed by a zero voltage vector) in each control cycle. This technique significantly reduces both torque and flux ripples. Therefore, it aims to control the torque more precisely by forcing the inverter to apply an active and zero VSVs alternatively. Also, the proposed FLM system has the ability to judiciously determine the optimal application duration time of the appropriate VSVs independently to the system states and its parameters. So, the effectiveness of the fuzzy logic is proven when the modeling of a system is difficult, which is the case of our system (duty cycle based-vector modulation). Finally, this paper also presents a design of a simplified EKF to promote the predictive behavior of the suggested improved strategy (FLM-MPDTC) by filtering out the undesired measurement noise, rejecting the external perturbations and avoiding the excessive usage of mechanical sensors. The effectiveness of the proposed combined FLM-MPDTC-EKF strategies is well tested and compared with C-MPDTC and FLM-MPDTC methods via simulations performed by MATLAB/Simulink software. The obtained results show an important reduction in ripples for both torque and flux, and a considerable reduction in THD.

Over and above, such an approach is expected to avoid the drawbacks associated with fuzzy logic systems, does not require the knowledge and/or information of human expertise of the controlled system and does not needs the tedious calculation of scaling factors. For this reason, the next chapter focuses on the learning ability, and on the control of a PMSM driven by three-phase inverter using a feed-forward ANN-based MPDTC, which has not been reported in the literature, where the benefits of MPDTC are combined with those of the neural network.

ChapterV

Supervised Imitation Learning of a Fuzzy Logic Duty Cycle Controller Based on the FS_MPDTC of PMSM Drive.

In this chapter, neural networks are chosen in order to take advantage of their capabilities for data acquisition and essentially for learning. A detailed study of this particular learning machine will be presented and the results of the simulations will also be discussed.

V.1. Introduction

In the last few years finite control set or finite control state model predictive control (FCS-MPC) has received a great deals of interest for both electronic and machinery fields.The main reason behind using this emerged control thechnique reside purely in these owen destinctive facts as reported in chapter 3. However, conventional finite state model predirctive direct torque control FS-MPDTC apply only one voltage vector for the entier control cycle and the consequences are technically studied and discussed in chapter 4.In the same perspective, the concept of duty cycle is introduced to improve the predictive behavior and the control performences. Among sevral propositions and sofisticated applied ideas, the most effective control thechnique used for duty cycle determination purpose is the fuzzy logic system. However, as we know the fuzzy controller involve a set of parameters should be optimized and carefully tuned. So, a time consuming often imposes limitation and the globale time exucution of the applied controller is also extended. To remove these limitations, we propose to imitate the predictive controller based on fuzzy logic duty cycle structure that achieves remarquable performance as the original improved conterpart controller. Our proposed imitator is an artificial neural network (ANN) trained offline using data labelled by the improved FS-MPDTC algorithm using fuzzy logic duty cycle controller. The proposed method has been tested and evaluated using digital simulation and the results have confirmed a good match between the imitator and the predictive-fuzzy duty cycle controller performance.

V.2. Neural Networks:

One of the challenges facing human beings today is to copy the nature and reproduce its own modes of reasoning and behaviour. Neural networks were born out of this desire. The inspiration for neural networks comes from the effort to model the human brain mathematically with the first work in 1943 by Mac Culloch and Pitts. They suppose that the nervous impulse is the result of a simple calculation carried out by each neuron. They had a promising start in the late 1950s, but the lack of depth in the theory put their work on hold until the 1980s [5].

Artificial neural network is a technique that is very popular in many areas of technology application and scientific research. This technique can be used in cases of difficult problems that cannot be described by precise mathematical approaches where they are very complicated to manipulate [125]. The fields of application of these neural networks are very

wide: classification, image and speech processing, process estimation and identification [125-127] control of electrical systems [128-131]. Artificial neural networks offer a completely different approach to problem solving and they are sometimes called the sixth generation of computing.

What is more, artificial neural networks represent the mathematical models of distributed processing, composed of several non-linear computational elements (neurons), operating in parallel and connected to each other by weights [5].What's more, the neural networks form a family of non-linear functions, allowing to build, by learning, a very large class of models and controllers. In a network model, neurons can be interconnected by using their output as inputs to other neurons. The interconnection of neurons forms the layers of a neural network.

A neural network is a system of interconnected non-linear operators, receiving signals from the external environment through its inputs, and delivering output signals, which are in fact the activities of certain neurons [5], [85]. The control by the artificial neural network of induction or synchronous motors is carried out only when such a given control paradigm is used as a teacher to simplify the learning procedure of the targets goals.

V.2.1. Biological Nervous System

The nervous system has more than 1,000 billion interconnected neurons. Although not all neurons are the same, their shapes and certain characteristics make it possible to classify them into different classes. Indeed, it is also important to know that not all neurons behave similarly depending on their position in the brain. **Figure V.1** show the main parts of biological nervous system.

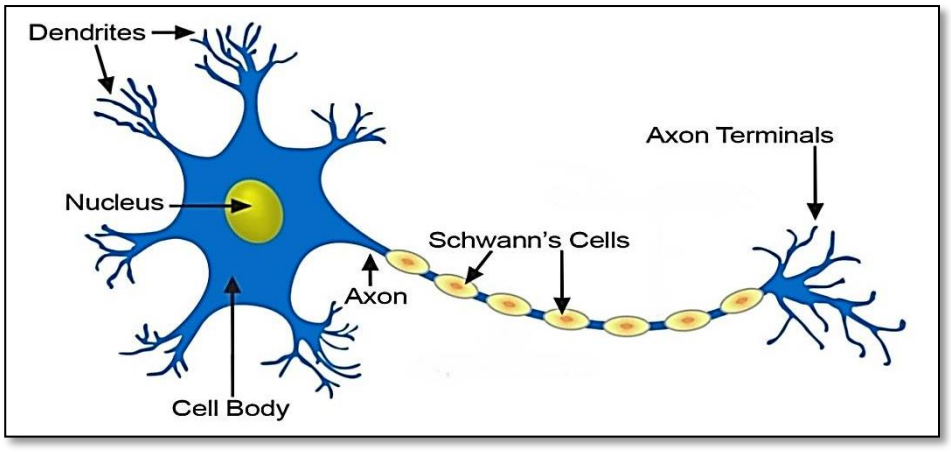

Figure V.1 Main parts of biological nervous system.

Neurons are nerve cells that can be decomposed into three main parts (**Figure V.1**) [125], [134]:

- **Dendrites:** their role is to capture information from other neurons. This information takes the form of chemical intermediates called neurotransmitters released in the synapses. The capture of these substances by the dendrites gives rise to an electrical signal called an action potential that is carried to the cell body.
- **The cell body:** which makes the sum of all the impulses that it receives; if this sum exceeds a certain threshold, it sends an impulse itself through the axon.
- **Axon:** The part that transmits the signals emitted by the cell body to other neurons.

V.2.2. Artificial Neural Networks:

Artificial neural networks are highly connected networks of elementary cores (neurons) operating in parallel. Each elementary core calculates a unique output based on the information that it receives. Any layered structure of networks is obviously a network.

A fully connected, multilayer, forward-propagating neural network with only one hidden layer is most often used in nonlinear system control applications because of its reliability and the ability to determine its equations for control purposes [5], [85], [134], [135]. We distinguish three types of layers:

- **Input layer:** the neurons of this layer receive the input values of the network and transmit them to the hidden neurons. Each neuron receives a value, so there is no summation.
- **Hidden layers:** each neuron in this layer receives information from several previous layers, performs the summation weighted by weights, and then transforms it according to its activation function. Then, it sends this response to the neurons of the next layer.
- **Output layer:** it plays the identical role as the hidden layers, the only difference between these two types of layers is that the output of the neurons of the output layer is not linked to any other neuron.

The table below shows an analogical comparison between a biological neuron and an artificial neuron:

Table V.1: Analogical comparison between biological and artificial neuron.

Artificial neuron	**Biological neuron**
Wheight of connexions	Synaptic terminals
Outputs	Axones terminals
Inputs	Dendrites
Activation Function	Nucleus

V.3. The Basic Topologies of Neural Networks

The neural network is composed of several neurons that are usually organized in different levels called network layers. Neurons belonging to the same layer have the same characteristics and use the same type of activation function. The mode of connection between neurons in a network defines its architecture and influences its operation. Indeed, the two major topologies of neural networks are :

- **Feedforward networks:**

Also called unidirectional networks (unlooped networks), a feedforward neural network performs one or more algebraic functions of its inputs by combining the functions performed by each of its neurons [132]. It can be single-layer or multi-layer, partially or completely connected (all neurons of the same layer are connected to each node of the next adjacent layer) [133]. This network is represented graphically by a set of neurons connected to each other (**Figure V.2**), in such a network, the information data circulates from the inputs to the outputs without "going back", if one moves in the network, from any neuron, following the connections, one cannot go back to the starting neuron. The neurons that perform the last calculation of the function composition are the output neurons, while those that perform intermediate calculations are the hidden neurons [5], [85], [132].

- **Recurrent networks**

These are neural networks with a feedback or recurrent network (**Figure V.3**). Their connection graph is recurrent: when moving through the network according to the direction of connections, it is possible to find at least one path that returns to its starting point (such a way is referred to as a " recurrent cycle ". Recurrent neural network (RNN) models are mostly used for speech recognition and digital aplications of smart system (pc , smart phone, smart tab) such as youtube and google researche application [5], [85], [132].

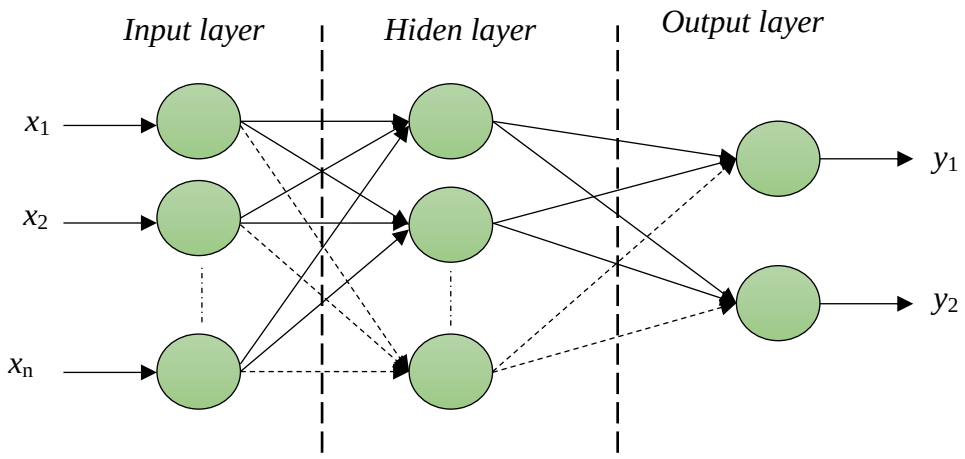

Figure V.2 Feedforward neural network topology.

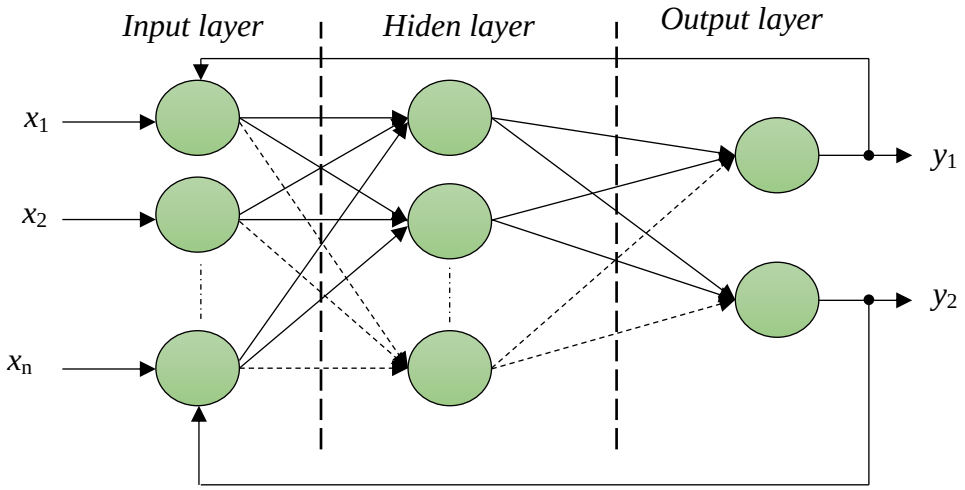

Figure V.3 Recurrent neural network (RNN) model.

V.4. Types of Neural Networks

There are different types of neural networks that use different mechanisms to determine their own rules. Each type of artificial neural network has its own unique tasks and among these types we can highlight the following:

V.4.1. Neuron Formel

In the form of a simplified mathematical model of the biological neuron, the formal neuron has a number of inputs, the dendrites, a structure that processes the inputs in an all-or-nothing fashion, and an axon that carries the neuron's response. Formal neuron is elementary units in an artificial neural network .The first modelling of a neuron came from the important work of Mac Culloch and Pitts (1943). **Figure V.4** illustrates a basic

model of a formal neuron [136], [137], [138].The mathematical model of a neuron is given by the relation (5.1) [5].

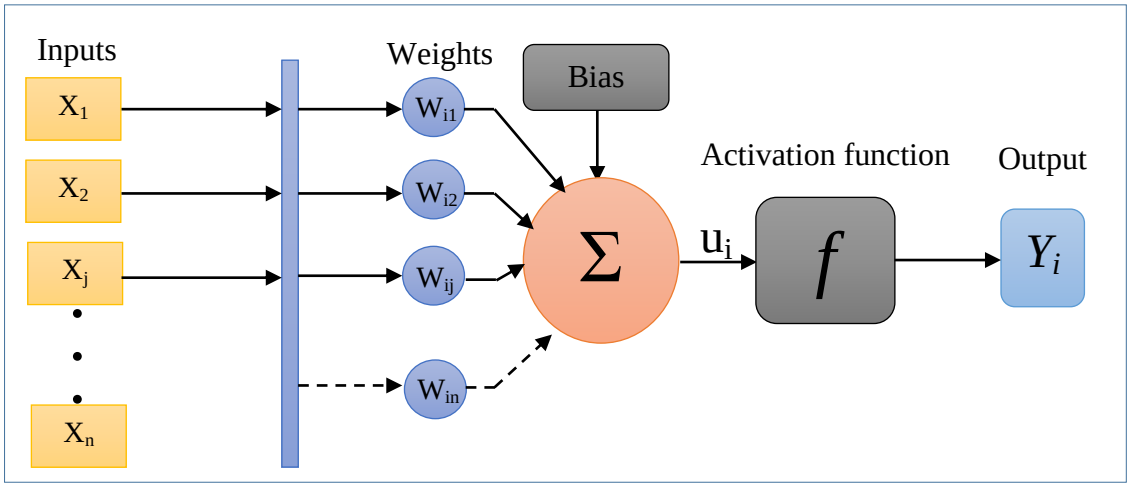

Figure V.4 Mathematical basic model of the formal neuron.

$$y_i = f(u_i) = f\left(\sum_{j=0}^{n} w_{ij} x_j \pm b\right) \tag{5.1}$$

With (x_j) and (y_i) representing the inputs and outputs of the neuron, (b) is the bias of the neuron; input often takes the values -1 or +1 which offers the possibility to add flexibility to the network by allowing to vary the neuron's trigger threshold by adjusting weights and bias during learning, (w_{ji}) are the synaptic weights of the connections between the inputs and the output. They measure the importance of each connection which are of course not all equal. The formal neuron will realize the weighted sum of the weights of different inputs. Then, the activation function (f) will calculate the output according to this sum. The choice of this activation function is an important part of neural networks. Among these functions, we can name: the threshold function, hyperbolic tangent, linear,... .

To calculate the output of a certain neuron in such a layer li, the outputs of all neurons in the next layer are multiplied by associated weights and summed with the bias term (b). The result is processed through an activation function, to generate output (y_i). This output then becomes one of the inputs for the layer above, (l_i + 1) and so on.

V.4.2. Multi-Layer Perceptron

The multilayer perceptron (MLP) (**Figure V.5**) is a class of feedforward artificial neural network that has at least three layers of nodes. The first one is the input layer, the second one is called the hidden layer and constitutes the core of the neural network. The third is often called the output layer. The MLP is most often used in non-linear system control applications [139], [140], [141]. It is specially trained using a supervised learning technique called the backpropagation (BP) algorithm [142], which aims at minimizing the overall error measured at the output layer by the formula defined below:

$$e(t) = y_d(t) - y_m(t) \tag{5.2}$$

Where $y_d(t)$ denotes the desired output, and $y_m(t)$ the measured output of the neuron. There are certainly other variants of neural networks [143-145], but they are rarely used in control systems. Let us mention the Kohonen networks which are mainly used in the classification and also hopfield network which require more computing time.

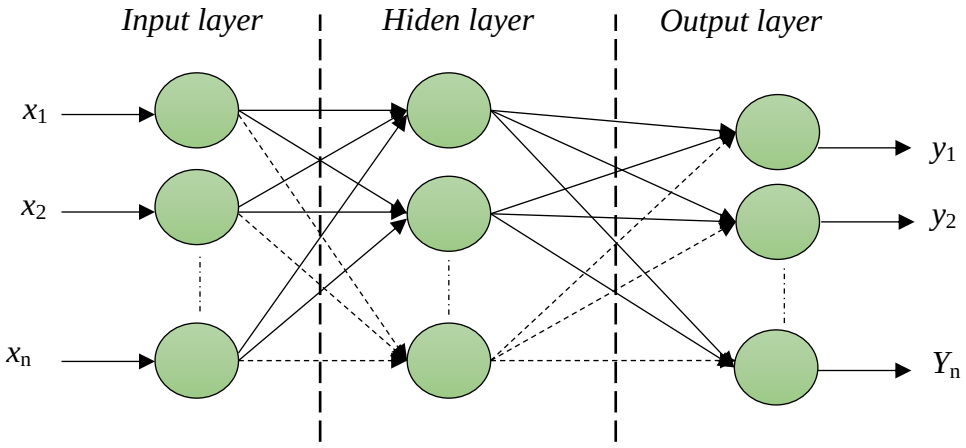

Figure V.5 Multi layer perceptron (MLP).

The BP algorithm uses a supervised iterative learning procedure, where the MLP is trained with a collection of predefined inputs and outputs. The overall error $e(t)$ is evaluated by equation (5.3), this error can be smoothed out by such minimization algorithm [144].

$$E_g(t) = \frac{1}{2}\sum_{i=1}^{n}\left(y_{d,i}(t) - y_{m,i}(t)\right)^2 \tag{5.3}$$

V.5. Activation Functions

Activation functions are mathematical equations that determine the output of a neural network. The function is attached to each neuron in the network and determines whether it should be activated ("fired up") or not, based on whether each neuron's input is relevant for the model's prediction.

V.5.1. Different Types of Activation Functions

There are many different forms of the activation functions, the most commonly used are shown as follow [5], [138]:

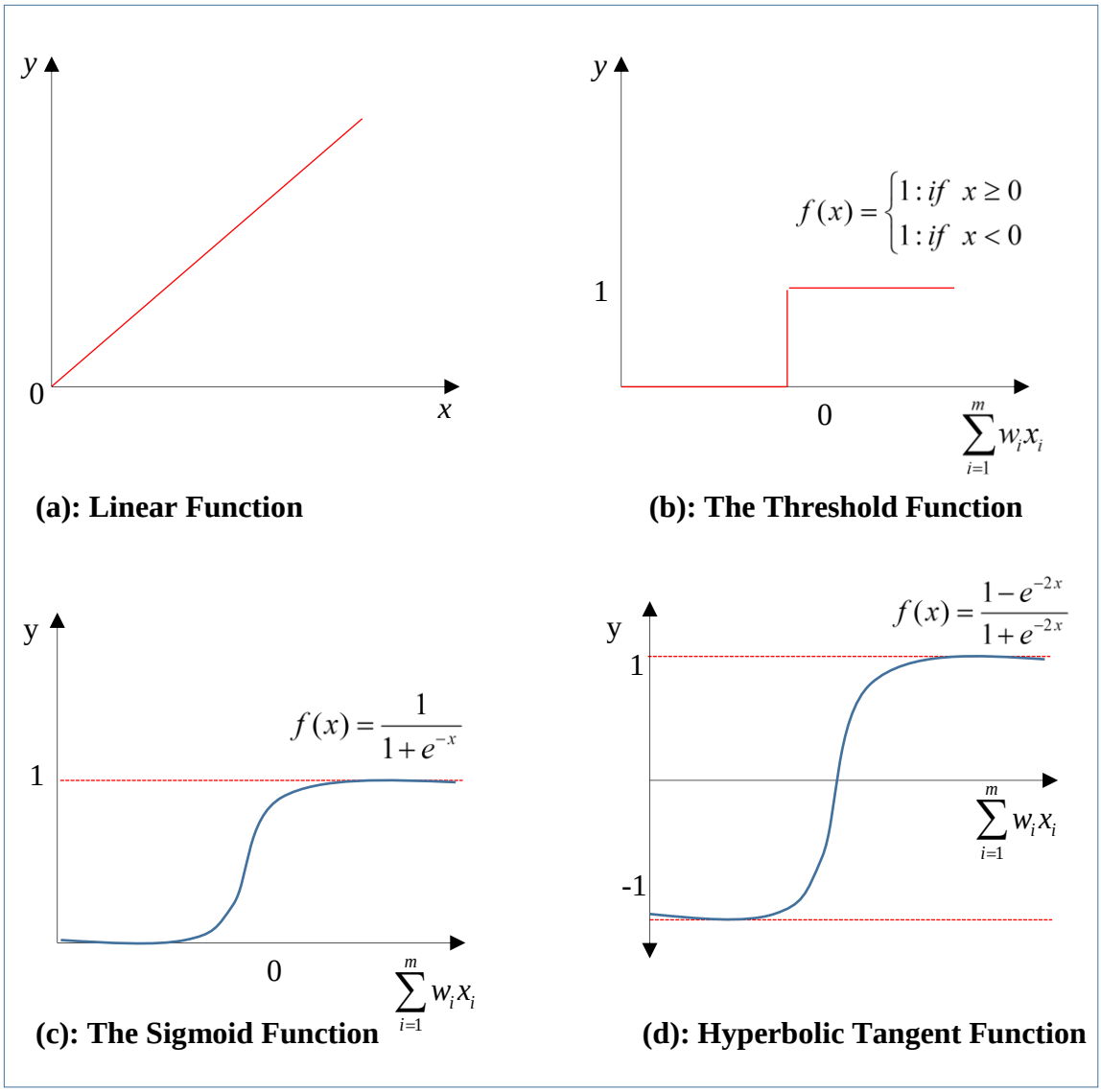

Figure V.6 Different forms of the activation functions.

V.6. The Concept of Learning

One of the fundamental properties of a neural network is certainly the ability to adapt its environment in order to improve its performance during the control of a process. This is the phase during which neural network performance is modified to reach the desired behaviour. It can be considered as a problem of updating coefficients (weight and bias) of the connections within the network, in order to accomplish the required task [146]. Learning is the main characteristic of ANNs and it can be done in different ways and according to different rules. There are two main classes of learning algorithms: Online and offline "batch".

V.6.1. Offline Learning "Batch" and Online Learning

Learning (also called training) is a flexible and efficient way to extract a stochastic structure from an environment. To start this process the initial weights are chosen randomly. Then, the training, or learning, begins. Two different types of learning are used, namely offline or data-based learning and online learning [5].

- In the case of data-based learning (**Figure V.7**), a supervisor (i.e. external desired data or teacher) is involved in order to provide to the network input-output data pairs; the procedure uses all the samples over and over again using a certain training algorithm, so that its performance approximates the expected goals as closely as possible.

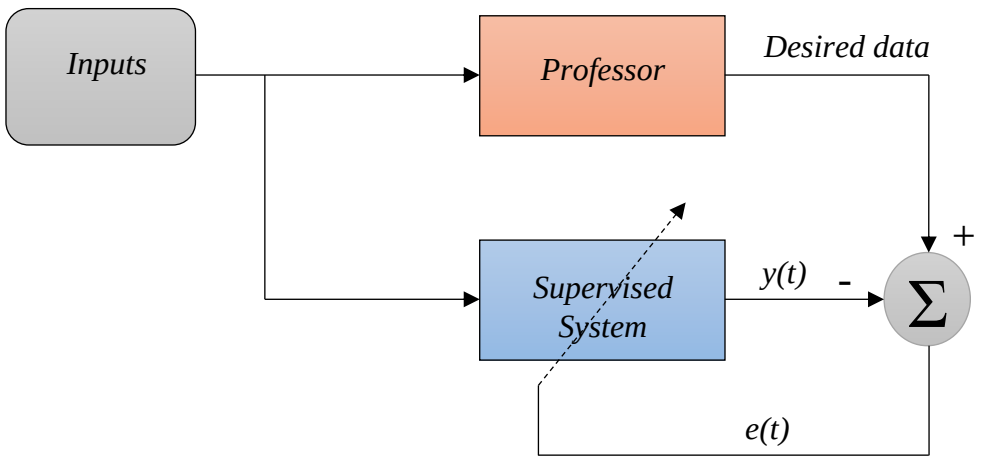

Figure V.7 Data-based learning.

- In the case of online learning, which is essentially unsupervised learning, the network is equipped with inputs but without the desired outputs (i.e. without external help). Therefore, the system must decide for itself which characteristics are to be used to accommodate the input data. This is often referred to as self-organization or adaptation. At the present time, however, the vast majority of neural network work is done in supervised learning systems. Supervised learning delivers results [147].

So in simple terms, offline learning is a bit like preparing for an exam, where you get a batch of content (data) to review (learning) and then move into the examination for the test. On the other hand, online learning is like taking a course, in which you develop your skills step by step and learning a little each time. Anyway, you can just treat them simply as:

- Offline learning is where the data is prepared in advance.
- Online learning is where the data comes to you sequentially from where you need to learn from it in a sequential fashion.

V.7. Learning Algorithms

In expert systems, the expert's knowledge has an enumerated form; it is expressed in the form of rules. In the case of neural networks, the knowledge has a distributed form; it is coded in the weights of the connections, the topology of the network, the transfer functions of each neuron, the threshold of these functions and the learning method used. The two most widely used learning algorithms are :

V.7.1. Back-Propagation Algorithm

This algorithm is used in feedforward-type networks, which are layered neural networks, having an input layer, an output layer, and at least one hidden layer. There is no recursivity in the connections, and no connections between neurons of the same layer.

The principle of back-propagation consists in presenting the network with a vector of inputs, and computing the output through the layers [139-143]. The back-propagation algorithm allows to calculate the gradient of this error efficiently: the number of operations (multiplications and additions) to be performed is indeed proportional to the number of network connections, as in the case of the calculation of the network output. This algorithm thus makes it possible to learn a MLP [143]. Let the vector ‘‘ W ’’ contain the synaptic weights, y_d (t) denotes the desired output, and y_m (t) the measured output of the neuron.

The quadrature error is therefore :

$$E_w(t) = \frac{1}{2}\sum_{i=1}^{n}\left(y_{d,i}(t) - y_{m,i}(t)\right)^2 \quad (5.4)$$

The back-propagation is a gradient descent, which therefore changes the weights (i.e. allow the adjustment of the weights w_{ij} (t) of the hidden layers.

$$\Delta W_{ij} = -\eta \frac{\partial E}{\partial w_{(i,j)}} \quad (5.5)$$

Where η : is the step of learning.

The algorithm consists in calculating an error term ‘‘ε’’, specific to each neuron and to make the weight modifications from the upper layers to the lower layers. This learning method is the most used in neural network training because of its simplicity. However, it has the disadvantage of having a very slow convergence [5].

V.7.2. Levenberg-Marquardt Algorithm

The Levenberg-Marquardt algorithm is an effective, simple and robust method for approximating a function. Basically, it consists in solving the equation:

$$\left(J^t J + \lambda I\right)\delta = J^t E \quad (5.6)$$

Where (J) is the Jacobian matrix for the system, (λ) is the Levenberg’s damping factor, (δ) is the weight update vector that we want to find and (E) is the error vector containing the output errors for each input vector used on training the network. The (δ) tell us by how much we should change our network weights to achieve as much as possible better solution. The (J^tJ) matrix can also be known as the approximated ‘‘Hessian’’.

The (λ) damping factor is adjusted at each iteration, and guides the optimization process. If reduction of (E) is rapid, a smaller value can be used, whereas if an iteration gives insufficient reduction in the residual, (λ) can be increased, giving a step closer to the gradient descent direction [148].

V.7.2.1. Computing the Jacobian

The Jacobian is a matrix of all first-order partial derivatives of a vector-valued function. In the neural network case, it is a N-by-W matrix, where N is the number of entries in our training set and W is the total number of parameters (weights + biases) of our network. It

can be created by taking the partial derivatives of each output in respect to each weight, and has the form [148]:

$$J = \begin{bmatrix} \frac{\partial F(x_1, w)}{\partial w_1} & \cdots & \frac{\partial F(x_1, w)}{\partial w_W} \\ \vdots & \ddots & \vdots \\ \frac{\partial F(x_N, w)}{\partial w_1} & \cdots & \frac{\partial F(x_N, w)}{\partial w_W} \end{bmatrix} \tag{5.7}$$

Where $F(x_i, w)$ is the network function evaluated for the i-th input vector of the training set using the weight vector ‘‘w’’ and (w_j) is the j-th element of the weight vector ‘‘w’’ of the network. In traditional Levenberg-Marquardt implementations, the Jacobian is approximated by using finite differences. However, for neural networks, it can be computed very efficiently by using the chain rule of calculus and the first derivatives of the activation functions.

V.7.2.2. Approximating the Hessian

For the least-squares problem, the Hessian generally doesn’t needs to be calculated. As stated earlier, it can be approximated by using the Jacobian matrix with the formula:

$$H \approx J^t J \tag{5.8}$$

V.7.2.3. Solving the Levenberg-Marquardt Equation

Levenberg's main contribution towards this method, is the introduction of the damping factor (λ) . This value is added to each member of the approximate hessian diagonal before the system is solved for the gradient. In principle, (λ) starts with a small value. Then the Levenberg-Marquardt equation is solved, usually using an (LU) decomposition. However, the system can only be solved if the approximate hessian has not become singular (having no inverse). Once the equation is solved, the weights (w) are updated using (δ) and the network errors for each input in the training set are recalculated. If the new sum of the quadratic errors has decreased, (λ) is decreased and the iteration ends. Otherwise, the new weights are rejected and the method is repeated with a higher value for (λ). This adjustment for (λ) is made using an additional adjustment factor (v), usually defined as 10. Thus, if (λ) is expected to increase, it is essential to multiply it by v. On the other hand, if it is expected to decrease, it is divided by (v). The process is repeated until the error decreases. When this is done, the current iteration is terminated [148].

V.7.2.4. Main Steps of Levenberg-Marquardt Algorithm

- Compute the Jacobian (by using finite differences or the chain rule)
- Compute the error gradient:
  $g = J^t E$
- Approximate the Hessian using the cross product Jacobian (eq. (5.8)):
  $H = J^t J$
- Solve $(H + \lambda I)\ \delta = g$ to find δ
- Update the network weights (w) using (δ)
- Recalculate the sum of squared errors using the updated weights
- If the sum of squared errors has not decreased :
  Reject the new weights, increase(λ)using (v) and go to step 4.
- Else decrease (λ) using (v) and stop.

V.8. Design of Neural Network

The steps towards the design of a neural network can be organized in four essential stages:

V.8.1. Analyisis and Collection of Samples

The design of a neural network always starts with the analysis of data samples. This step is crucial and will help the designer to choose the most adequate type of neural network to solve his problem. These samples will help to define the type of neural network, the learning algorithm and the way to conduct the testing and validation phase.

V.8.2. Type and Structure

The type and structure of a neural network depends on the type of samples. First of all, a type of network must be chosen: a typical perceptron, a multilayer perceptron, a Hopfield network, a Kohonen network, the number of neurons, etc. You should test several possibilities and choose the topology that offers the best results.

V.8.3. Learning

Once the architecture of a neural network has been chosen, it is essential to carry out a learning process in order to calculate the weights allowing the neural network to be as close

as possible to the desired objective. During this phase, two main aspects are taken into account :

- **Forward Propagation:**

Forward propagation is to supply the neural network with input values and to obtain an output that we call predicted value. Direct propagation is also referred as inference. When we feed the input values to the first layer of the neural network, it happens without any mathematical operation. The second layer takes the values from the first layer and applies multiplication, addition and activation operations and passes this value to the next layer. The same operation is being repeated for the following layers and we finally get an output value of the last layer.

- **Back-Propagation:**

After forward propagation, we get an output value which is the predicted value. For calculating the error, we compare the predicted value with the desired output value. So, a minimization function is used to calculate the error value. Then we calculate the derivative of the error value with respect to each neural network weight. In that sense, Back-Propagation uses chain rule which is a form of partial derivative. More precisely, in the chain rule we first calculate the derivatives of the error value with respect to the values of the weights of the last layer. We call these derivatives the gradients and use these gradient values to calculate the gradients of all hiden layers but we moving in the opposite direction (i.e. from the output to the input). We repeat this process until we get minimal error with respect to the desired target.

V.8.4. Testing and Validation

Once the network has been trained, tests should be carried out to check that the resulting network reacts correctly.

V.9. Artificial Neural Network Based Duty Cycle Controller for MPDTC-PMSM Drive

A high-performance PMSM drive system is characterized by a reduced level of ripple, which causes the drive to functioning in stable situations over a wide range of varying operating conditions. As shown in the previous chapter, the duty cycle based on fuzzy logic controller is a key option for allevating the undesired torque ripples. It’s yet that the fuzzy

controller performed efficiently and accurately, even if under some harsh environments and unexpected load disturbances. However, the fuzzy controller suffer from the fact that an accurate tuning of its own parameters (i.e scaling factors, membership functions and fuzzy rules) are required for their design. These parameters generally only work well under a certain range of conditions for which they were designed. For further understanding, in the case of a fuzzy logic controller, the inputs and outputs must be scaled (normalized) to adapt the designed memberships function seeking to delivre the requsiste duty ratios. On the contrary, in the case of ANN controller, our designed neuronal immitator take directely the same inputs with respect to the targets (duty ratios) without additional normalized gains for the learning process. So, the errors between the outputs produced by the neural networks and the desired results (targets) are calculated and propagated backward to update online the weights and biases of the neural networks using certain minimization algorithme.

In applying the above imitator to this research thesis, ANN is used only to mimic the fuzzy logic duty cycle controller, which means suitable weights are determined to precisely follow the desired performances (targets). **Figure V.8** shows a schematic diagram of the MPDTC using Neural Network Duty Cycle Determination (NNDCD). The architecture includes a multilayer neural network to replace the fuzzy logic duty cycle controller.

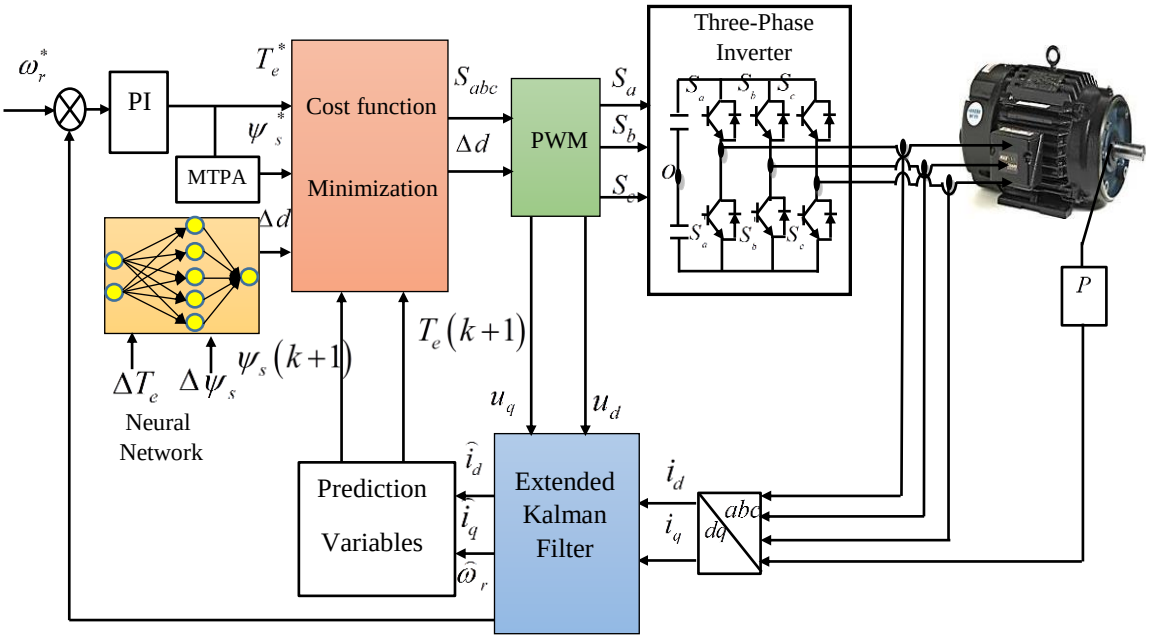

Figure V.8 Schematic diagram of the proposed neural network based duty cycle controller for MPDTC-PMSM drive.

This neural network is composed of an input layer, one hidden layer and an output layer. The input layer is composed of two neurons, designated respectively by the torque error and the flux error . The hidden layer consist of five neurons. The output layer consists of single neuron that produce the requisiste duty cycles to be applied for the optimum voltage vectors across the synchronous machine through the voltage inverter. A linear type activation function on the input and output layers and another non-linear activation function of hyperbolic tangent type is used for the hidden layer. The structure of the neural network used in our case is given in **Figure V.9**.

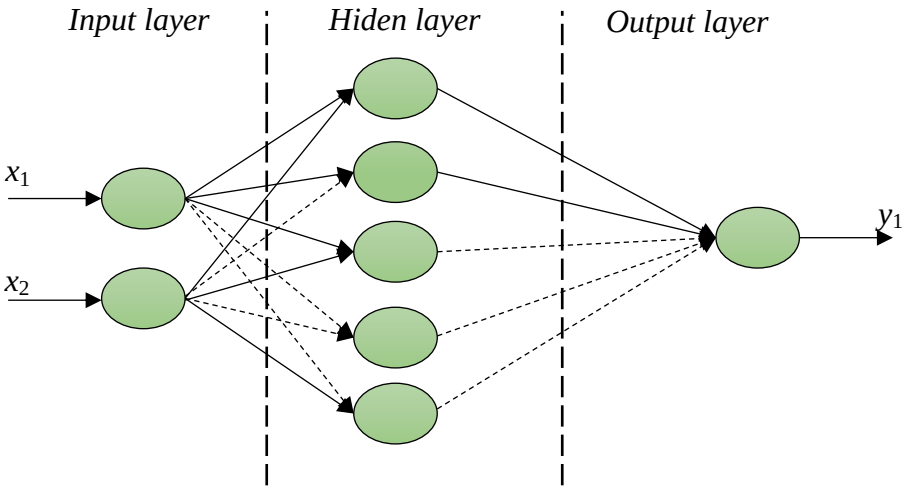

Figure V.9 Structure of the neural network used for duty cycle determination.

Once the structure is defined, training of the neural network is a mandatory step during which the synaptic weights of different links between neurons in the network will be initialized in a random way and will be corrected using the gradient backpropagation algorithm. Thus two matrices of weights (w1, w2) and two bias vectors (b1, b2) with initial values are available. The supervised learning phase of the network will be carried out using the fuzzy inference table (chapter 4) as a teacher. The training set comprises an input data matrix (X) containing vectors representing the different possible combinations of the inputs data (ΔTe, $\Delta \psi s$) forming the selection table and the matrix (Y) of the desired outputs (Δd) that correspond respectively to the outputs associated with the inputs vector that the network must deliver. The weights are adjusted in such a way as to minimize the sum of the quadratic errors between the mains output voltage duty cycles and the desired ones representing the basis for learning using backpropagation. After learning all the examples of the learning base, the adapted network must be able to specify the suitable voltage vectors application cycles (ratios).

V.10. Simulation Results

To study the performances of the improved MPDTC based on a FLM-EKF and the improved MPDTC based on ANN-EKF , the proposed composed control strategies are developed under the MATLAB / Simulink platform. In this section, the control startegy that take our interest is composed of a PMSM drive, predictive torque/flux controller, artificial neural network, and an extended kalman filter estimator. The parameters used for the simulation are given in **Appendix B** [107].

At first, a unified monitoring scenario is employed for both control methods (MPDTC-FLM-EKF, (MPDTC-ANN-EKF) in order to perform a fair comparison. The monitoring scenario include: the starting up, the steady states at rated speed, rated load torque introduction and a maneuver of speed sense reversing. For both control methods, the chosen wheighting factor is equal to λ =3000.

V.10.1. Starting, steady state at rated speed, application of rated load torque and rated speed sense reversing operation

In this part, both improved control techniques was tested for a target rated speed of 1000 rpm with a rated load of torque insertion at t=0.1 s followed by a speed sense reversing operation at t=0.15. In this sub-section, we are only interested in the analysis and discussion of the generated stator current and torque/flux ripples. For that, **Figs V.10** to **V.14** show the stator phases current, electromagnetique torque, and stator flux evolution.

A detailled THD analysis of stator phase current of the developed control techniques, are depicted in **Appendix C**. The figures are mentioned by **(a)** for the MPDTC-FLM-EKF, and **(b)** for the MPDTC-ANN-EKF.

(a)

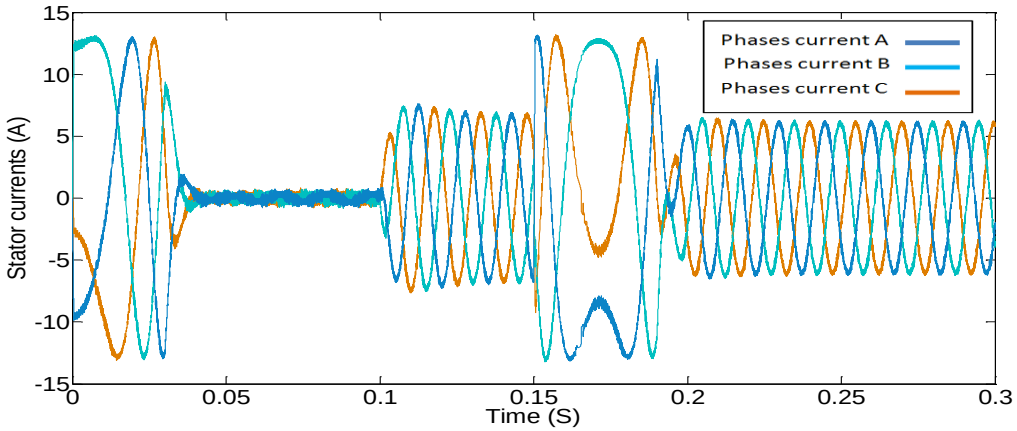

(b)

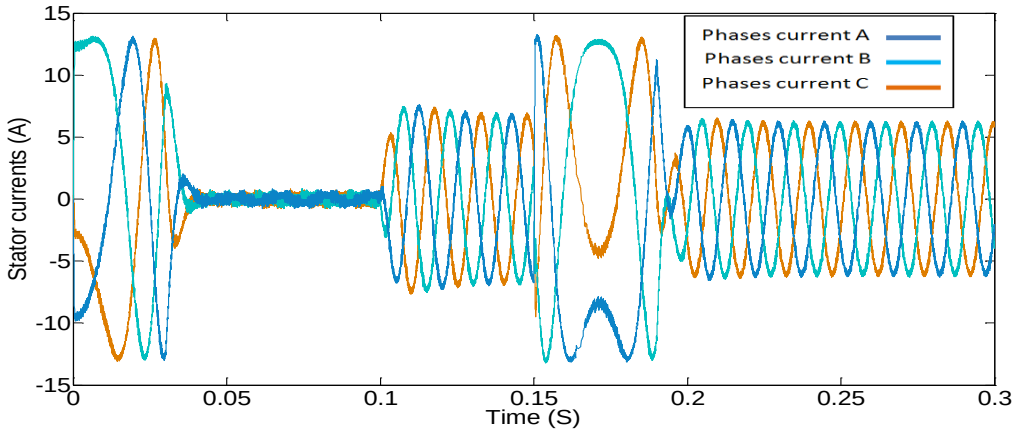

Figure V.10 Stator currents (A).

(a)

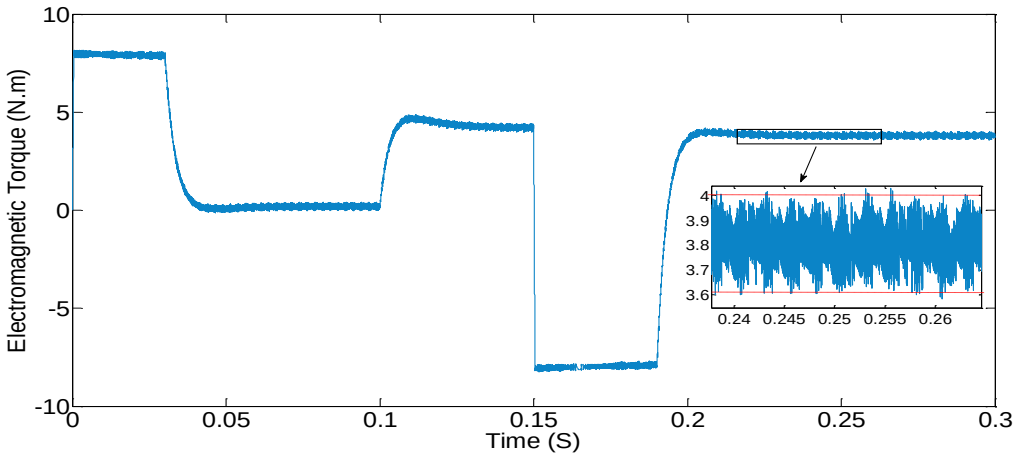

(b)

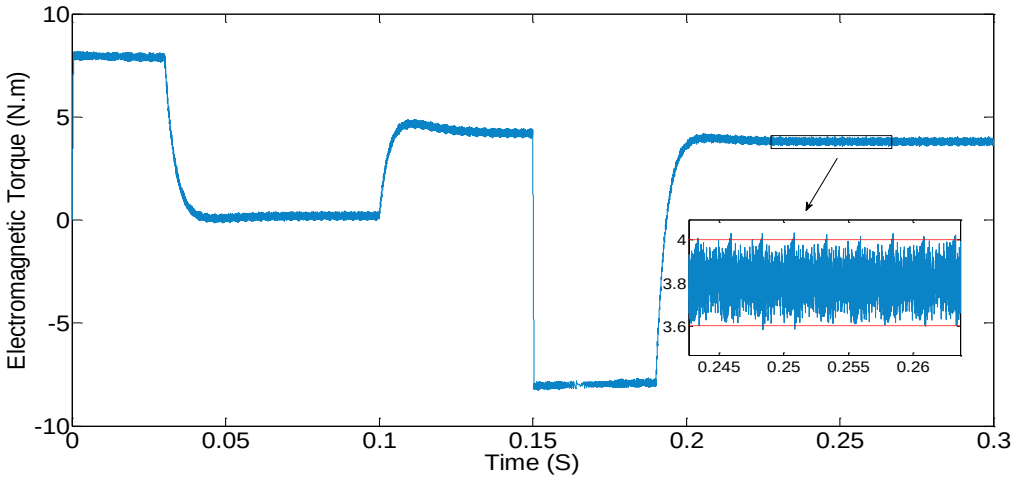

Figure V.11 Electromagnetic torque (N m).

(a)

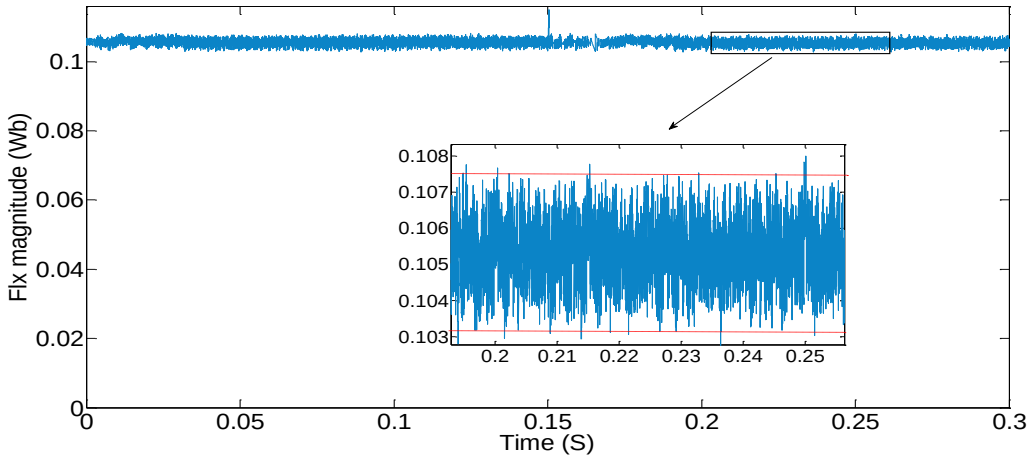

(b)

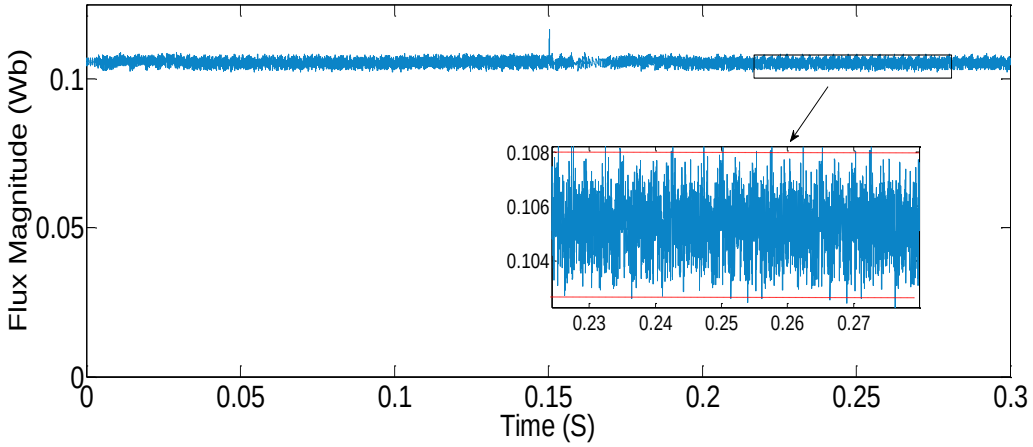

Figure V.12 Stator flux magnitude (Wb).

(a)

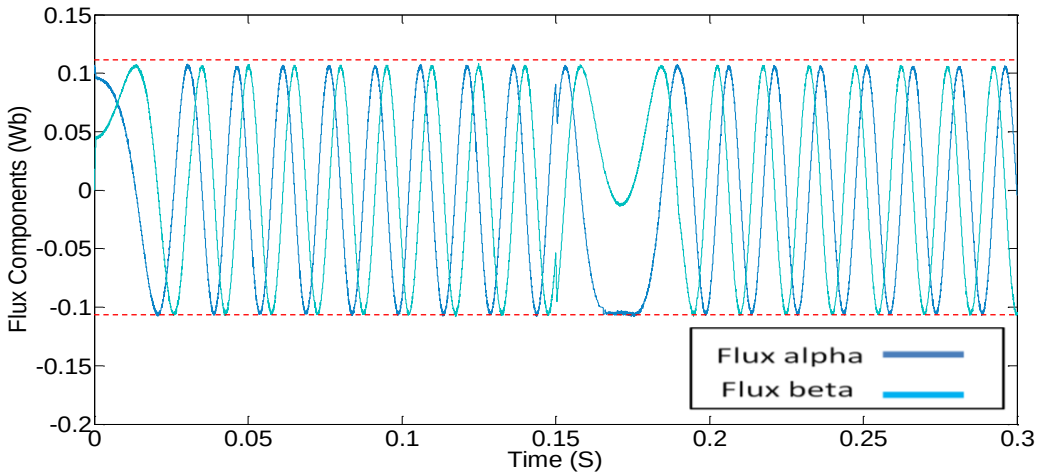

(b)

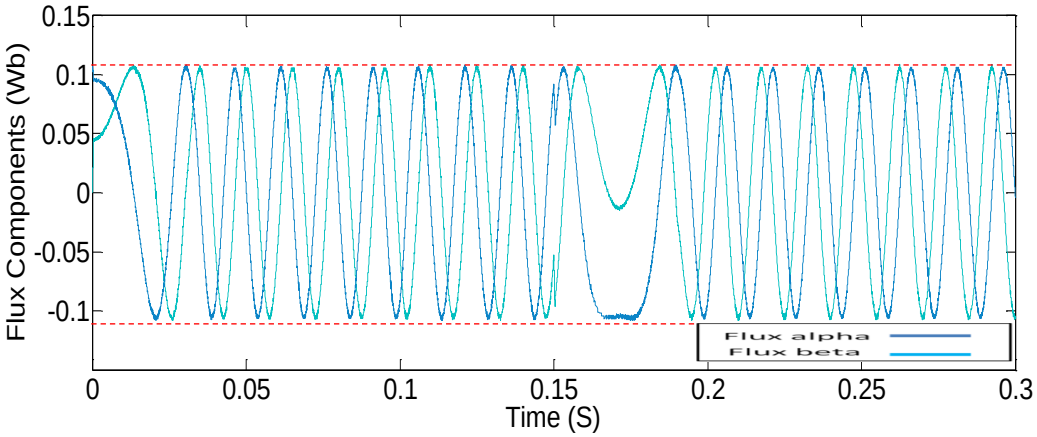

Figure V.13 Stator flux components (Wb).

(a) **(b)**

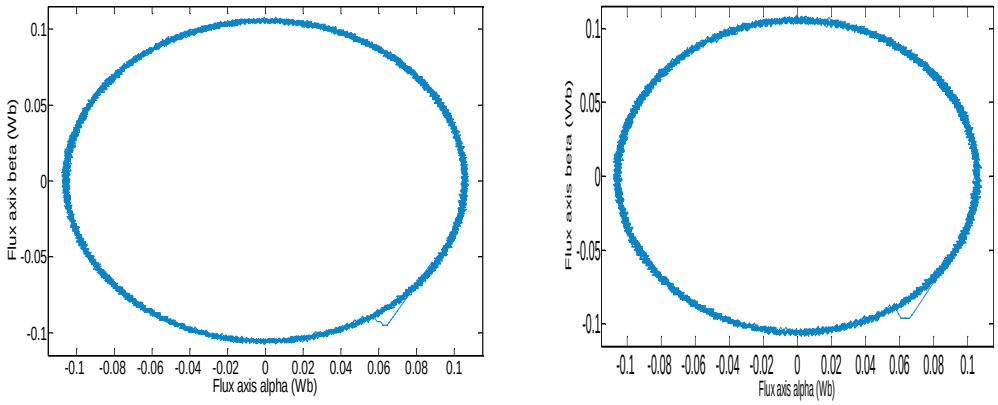

Figure V.14 Stator flux trajectory (Wb).

Firstly, **Fig V.10a, b** show respectively the stator phase's currents (i_{sa}, i_{sb}, i_{sc}) of MPDTC-FLM-EKF and MPDTC-ANN-EKF. It is clear to see that the technique that based on FLM has a slightly better current response than that of MPDTC-ANN-EKF. This can reflect to the effectiveness of the used FLM based on fuzzy logic system.

Then, **Fig V.11a, b** illustrate the responses of the electromagnetic torque. From (**Fig V.11a ZOOM, V.11b ZOOM**) it can be seen that the torque ripple range of the MPDTC-FLM-EKF method is about 0.35 Nm (from 3.65 Nm to 4 Nm); the value of the MPDTC-ANN-EKF method is 0.4 Nm (from 3.6 Nm to 4Nm). Therefore, the MPDTC-FLM-EKF method has a slightly lower torque ripple than that based on ANN.

Next, **FigsV.12** to **V.14** show the waveforms of the magnetic stator flux, namely the flux amplitude, the flux components and the flux trajectory. From **Fig V.12a, b** it is clear to see that the amplitude of flux in both cases follows their references perfectly but with slightly lower level of ripples in the case of MPDTC-FLM-EKF in comparison to the

MPDTC-ANN-EKF as seen in **Fig V.12b** (**ZOOM**). In addition, **Fig V.13a,b** exhibit almost the same quality and also the same uniform sinusoidal flux wave components. As to the trajectory of the stator flux, we can clearly see in **Fig V.14a,b** that both control techniques present almost the same circular and the same uniform trajectory. This indicates that the stator flux has a relatively fewer ripple in one part and explains in the other part the efficiency of the used intelligent/stochastique combined control techniques.

V.11. Summarize

Judging from the obtained results and technical discussions, it is clear to notice that the technique based on the fuzzy control system ensures a better performance compared to the ANN-based MPDTC-EKF technique. Furthermore, it is interesting to note that the fuzzy control is characterized by a significant attenuation of torque, current and flux ripples. This is confirmed by the results obtained from the comparison of torque/flux ripple deviations. Also from these results, we can see that the performance of the synchronous machine, controlled by a duty cycle-neural controller is generally acceptable despite the fact that fuzzy logic duty cycle-controller outperforms this neural controller. This is due to the fact that there is no general rule for choosing neural network parameters. It is generally difficult to determine these choices from the tests alone. However, the data acquired from the neural network system remains a key option that can be used in another controlled system using a duty cycle controller but without involving scaling factors and therefore being time-consuming as is the case with the fuzzy logic system.

V.12. Conclusion

In this chapter, the performance of both improved control pradigms (MPDTC-ANN-EKF, MPDTC-FLM-EKF) have investigated and compared, by means of performance verification using MATLAB/Simulink tool. It is worth noting that although the simulated results of the proposed neural imitator can accomplish perfectely the outlined objectives to some degree, they provide a stronger foundation for researches and applications, where the methodology of the suggested approach presented in this thesis can be further enhanced and developed. Therefore we can say that neural networks are good at recognizing structures and objectives, but they are not good at explaining how they make decisions.On the other hand, fuzzy logic systems, which can reason with imprecise information, are good at explaining their decisions, but they cannot automatically acquire the rules they use to make those decisions.

General Conclusion

General Conclusion

The work carried out within the context of this thesis deals with the Model Predictive Direct Torque Control (MPDTC) of a synchronous machine as a solution to the problems encountered in the Direct Torque Control (DTC) pradigme. In fact, DTC is robust against machine parametric variations and does not require any current regulators. In addition, it offers a number of significant advantages over the oriented flux vector control. However, the DTC pradigme also has a significant drawbacks. On the one hand, the switching frequency is highly variable, which can lead to acoustic noise problems, and therefore, degrades the performance of the overall control systems. On the other hand, the amplitude of flux and torque ripple still a major and cibled problems associated with the use of hysteresis controllers. In this context, the present research work essentially covers these main points:

- The reduction of the high level of ripples and harmonics caused by the variable switching frequency due to the use of hysteresis comparators.
- The design of an improved direct torque control (DTC) using space vector modulation (SVM).
- The design of innovative predictive control paradigms to improve the conventionele DTC scheme.
- The reduction of the high level of ripples harmonics of MPC caused by selecting only one voltage vector per sampling period.
- The design of improved predictive torque control strategy using fuzzy logic modulator and extended kalman filter
- Reducing the computational load of MPC by selecting two voltage space vectors using duty cycle controller .
- The design of improved predictive torque control strategy using artificial neural network imitator in combined with extended kalman filter.

.

Considering all the work carried out in this present thesis, several interesting perspectives have been considered:

- Experimental validation of the results obtained by the different control strategies proposed in this thesis.
- Establishment of a PMSM model taking into account the parametric variations.
- Development of robust controls law in combined with MPC such as backstepping control, passivity based control and synergetic control.
- Optimization of the proposed fuzzy controllers gains by an innovative optimization methods.
- Development of a type 2 fuzzy controller offering tendency and additional benefits for the whole control system.

Appendix

A.1 Appendix A: Park model of the permanent magnet synchronous machine

This transformation, applied to the real variables (voltages, currents and flux), makes it possible to obtain fictive variables called the *d-q* or Park components. This can be interpreted as a transforming the three phase variables (voltages, currents, and flux) from fixed reference frame (*a,b,c*) to a rotating frame (*d-q*), see (Figure A.1). This change of reference frame makes the dynamic equations of the machine simpler, which simplifies their study and analysis [149].

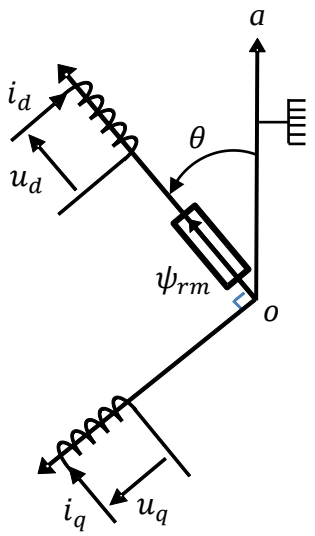

Figure A.1 Equivalent representation of PMSM in the (d,q) frame.

The shift from the real axis quantities (a,b,c) to the axis quantities (d,q,o) is done by the following transformation:

$$[x_{dqo}] = [p(\theta)][x_{abc}] \qquad (A.1)$$

Where *x* can be a current, voltage or flux and θ represents the position of the rotor polar axis with respect to the axis (a) of the stator phase. The indices (*d,q*) indicate that the stator quantities are projected on the longitudinal and transverse axes.

Park's transformation matrix is given by :

$$[p(\theta)] = \frac{2}{3}\begin{bmatrix} \cos(\theta) & cos\left(\theta - \frac{2\pi}{3}\right) & cos\left(\theta - \frac{4\pi}{3}\right) \\ -sin(\theta) & -sin\left(\theta - \frac{2\pi}{3}\right) & -sin\left(\theta - \frac{4\pi}{3}\right) \\ \frac{1}{2} & \frac{1}{2} & \frac{1}{2} \end{bmatrix} \qquad (A.2)$$

The feedback of the axis quantities (*d,q,o*) to the real axis quantities (*a,b,c*) is done by the inverse Park matrix $[p(\theta)]^{-1}$ expressed by :

$$[p(\theta)]^{-1} = \begin{bmatrix} \cos(\theta) & -\sin(\theta) & 1 \\ cos\left(\theta - \frac{2\pi}{3}\right) & -sin\left(\theta - \frac{2\pi}{3}\right) & 1 \\ cos\left(\theta - \frac{4\pi}{3}\right) & -sin\left(\theta - \frac{4\pi}{3}\right) & 1 \end{bmatrix} \quad (A.3)$$

Stator power supply are assumed to be symmetrical (i.e. the currents form an equilibrated system ($i_a(t) + i_b(t) + i_c(t) = 0$)). Besides, the homopolar component of the third line of the system $[x_{dqo}] = [p(\theta)][x_{abc}]$ is systematically null.

A.1.1. Electrical equations of the PMSM in Park's frame

The three-phase system of electrical equation is expressed as:

$$[u_s(t)] = R_s\,[i_s(t)] + \frac{d}{dt}[\psi_s(t)] \quad (A.4)$$

In a Park frame linked to the rotating field, by applying the transformation to the three-phase system of electrical equation (A. 4), we can write :

$$\begin{aligned} [u_{dqo}(t)] &= [p(\theta)][u_{abc}(t)] \\ &= [p(\theta)](R_s[i_{abc}(t)] + \frac{d}{dt}[\psi_{abc}(t)]) \\ &= R_s([i_{dqo}(t)] + [p(\theta)]\ \frac{d}{dt}[\psi_{abc}(t)]) \end{aligned} \quad (A.5)$$

Also :

$$[\psi_{abc}(t)] = [p(\theta)]^{-1}[\psi_{dqo}(t)] \quad (A.6)$$

Thus :

$$[u_{dqo}(t)] = R_s\,[i_{dqo}(t)] + [p(\theta)]\ \frac{d}{dt}([p(\theta)]^{-1}[\psi_{dqo}(t)]) \quad (A.7)$$

Besides, we can write:

$$[p(\theta)]\,\frac{d}{dt}([p(\theta)]^{-1}[\psi_{dqo}(t)]) = [p(\theta)]\ \frac{d}{dt}([p(\theta)]^{-1})[\psi_{dqo}(t)] + \frac{d}{dt}([\psi_{dqo}(t)]) \quad (A.8)$$

The derivative of the matrix $[p(\theta)]^{-1}$:

$$\frac{d}{dt}([p(\theta)]^{-1}) = \omega \begin{bmatrix} -sin(\theta) & -cos(\theta) & 0 \\ -sin\left(\theta - \frac{2\pi}{3}\right) & -cos\left(\theta - \frac{2\pi}{3}\right) & 0 \\ -sin\left(\theta - \frac{4\pi}{3}\right) & -cos\left(\theta - \frac{4\pi}{3}\right) & 0 \end{bmatrix} \quad (A.9)$$

After simplification, on the basis of the usual trigonometric relations, we obtain:

$$[p(\theta)]\frac{d}{dt}([p(\theta)]^{-1}) = \omega\begin{bmatrix}0 & -1 & 0\\ 1 & 0 & 0\\ 0 & 0 & 0\end{bmatrix} \quad \text{(A. 10)}$$

By substituting (A. 8) in (A. 7), we obtain :

$$[p(\theta)]\frac{d}{dt}([p(\theta)]^{-1}[\psi_{dqo}(t)]) = \omega\begin{bmatrix}0 & -1 & 0\\ 1 & 0 & 0\\ 0 & 0 & 0\end{bmatrix}[\psi_{dqo}(t)] + \frac{d}{dt}([\psi_{dqo}(t)]) \quad \text{(A. 11)}$$

From which we derive the expression of the stator voltages of the PMSM in the reference (d,q):

$$\left[u_{dqo}(t)\right] = R_s\,[i_{dqo}\,(t)] + \omega\begin{bmatrix}0 & -1 & 0\\ 1 & 0 & 0\\ 0 & 0 & 0\end{bmatrix}[\psi_{dqo(t)}] + \frac{d}{dt}([\psi_{dqo}(t)]) \quad \text{(A. 12)}$$

We have noted that the homopolar component is zero (the power supply is assumed to be symmetrical and the machine is symmetrical), so :

$$\begin{bmatrix}u_d(t)\\ u_q(t)\end{bmatrix} = R_s\begin{bmatrix}i_d(t)\\ i_q(t)\end{bmatrix} + \omega\begin{bmatrix}-\psi_{q(t)}\\ \psi_{d(t)}\end{bmatrix} + \frac{d}{dt}\begin{bmatrix}\psi_{d(t)}\\ \psi_{q(t)}\end{bmatrix} \quad \text{(A. 13)}$$

A.1.2. Flux equations of the PMSM in Park's frame

The expression of stator flux in (d,q) frame is given by :

$$\begin{bmatrix}\psi_d(t)\\ \psi_q(t)\end{bmatrix} = \begin{bmatrix}l_d & 0\\ 0 & l_q\end{bmatrix}\begin{bmatrix}i_{d(t)}\\ i_{q(t)}\end{bmatrix} + \begin{bmatrix}\psi_{rm}\\ 0\end{bmatrix} \quad \text{(A. 14)}$$

Where :

$\psi_d(t)$: The stator flux component on the longitudinal axis (d),

$\psi_q(t)$: The stator flux component on the transverse axis (q),

l_d : The stator inductance according to the d-axis,

l_q : The stator inductance according to the q-axis,

ψ_{rm} : The maximum value of the flux created by the magnets.

A.1.3. Mechanical Equations

The dynamic equation of the PMSM is given by the following:

$$\frac{d\omega_r}{dt} = \frac{1}{J}(T_e - T_L - f_r\omega_r) \quad (A.15)$$

The electromagnetic torque is expressed by:

$$T_e = \frac{3}{2}\, p\left[\left(l_d - l_q\right) i_d\, i_q + \psi_{rm} i_q\right] \quad (A.16)$$

For a surface mount PMSM ($l_d = l_q$) :

$$T_e = \frac{3}{2}\, p\, \psi_{rm} i_q\ . \quad (A.17)$$

A.1.4. State space representation of PMSM in Park's frame

The state model of a linear system is usually written in the following matrix form :

$[\dot{X}] = [A][X] + [B][U]$

$[Y] = [C][X]$

Where :

$[X]$: Vector of state variables;

$[U]$: Control vector ;

$[Y]$: Output vector ;

$[A]$: State matrix ;

$[B]$: Control matrix ;

$[C]$: Observation matrix.

For a PMSM powered by a voltage inverter, we selected the following choices :

- The vector of state variables: $[X] = [i_{d(t)}\ \ i_{q(t)}\ \omega_{r(t)}\ ]^t$
- The vector of control and disturbances: $[U] = [u_{d(t)}\ \ u_{q(t)}\ \ T_L\ ]^t$
- Outputs vector : $[Y] = [i_{d(t)}\ \ i_{q(t)}\ \omega_{r(t)}]^t$

With :

$$[A] = \begin{bmatrix} \frac{-Rs}{l_d} & \frac{p\omega_r l_q}{l_d} \\ \frac{-p\omega_r l_d}{l_q} & \frac{-\mathrm{Rs}}{l_q} \end{bmatrix} ; [B] = \begin{bmatrix} \frac{1}{l_d} & 0 & 0 \\ 0 & \frac{1}{l_q} & \frac{-p\omega_r l_d}{l_q} \end{bmatrix} ; [C] = \begin{bmatrix} 1 & 0 \\ 0 & 1 \end{bmatrix} \quad \text{(A.18)}$$

By substituting (A. 14) in (A. 13), We obtain :

$$\begin{cases} \frac{d}{dt} i_{d(t)} = \frac{-R_s}{l_d} i_{d(t)} + \frac{p\omega_r l_q}{l_d} i_{q(t)} + \frac{1}{l_d} u_{d(t)} \\ \frac{d}{dt} i_{q(t)} = \frac{-p\Omega_r l_d}{l_q} i_{d(t)} + \frac{-R_s}{l_q} i_{q(t)} + \frac{-p\omega_r l_d}{l_q} \psi_{rm} + \frac{1}{l_q} u_{q(t)} \end{cases} \quad \text{(A. 19)}$$

The complete PMSM model, which presents strict coupling and non-linearities, can be expressed in the following vector form:

$$\begin{bmatrix} \frac{di_d}{dt} \\ \frac{di_q}{dt} \\ \frac{d\omega_r}{dt} \end{bmatrix} = \begin{bmatrix} \frac{1}{l_d} \left(R_s i_d + l_q p\omega_r i_q\right) \\ \frac{1}{l_q} \left(-R_s i_q - l_d p\omega_r i_d - p\omega_r \psi_{rm}\right) \\ \frac{1}{J} \left(\frac{3}{2} p\left(l_d - l_q\right) i_d i_q + \frac{3}{2} p\psi_{rm} i_q - f_r \omega_r\right) \end{bmatrix} + \begin{bmatrix} \frac{1}{l_d} & 0 & 0 \\ 0 & \frac{1}{l_q} & 0 \\ 0 & 0 & -\frac{1}{J} \end{bmatrix} \begin{bmatrix} u_d \\ u_q \\ T_L \end{bmatrix} \quad \text{(A. 20)}$$

B.1 Appendix B: The parameters used for the simulation

Table B.1 Control and PMSM parameters

Main parameters	Value and Units
PMSM parameters	
Rated power (P_n)	**1.5 KW**
Rated speed (w_n)	**1000 rpm**
Rated torque (T_n)	**4 Nm**
DC-bus voltage (V_{dc})	**350 V**
Stator resistance (R_s)	**0.129 Ω**
dq-axis Inductance ($L_d = L_q$)	**0.00355H**
PM flux linkage (ψ_{rm})	**0. 1054Wb**
Number of pairs of poles (P)	**4**
Moment of inertia (J)	**0.00243 Kg m^2**
Viscous coefficient (f)	**0.001871Nms/rad**
Control scheme parameters	
Proportional gain (K_p)	**0.1**
Integral gain (K_i)	**8.1**
Optimal Weighting factor (λ)	**3000**

C.1 Appendix C: Analysis THD of the stator current of the overall control techniques

C.2 Investigated Control Techniques

C.2.1 Conventional DTC

THD of the stator current

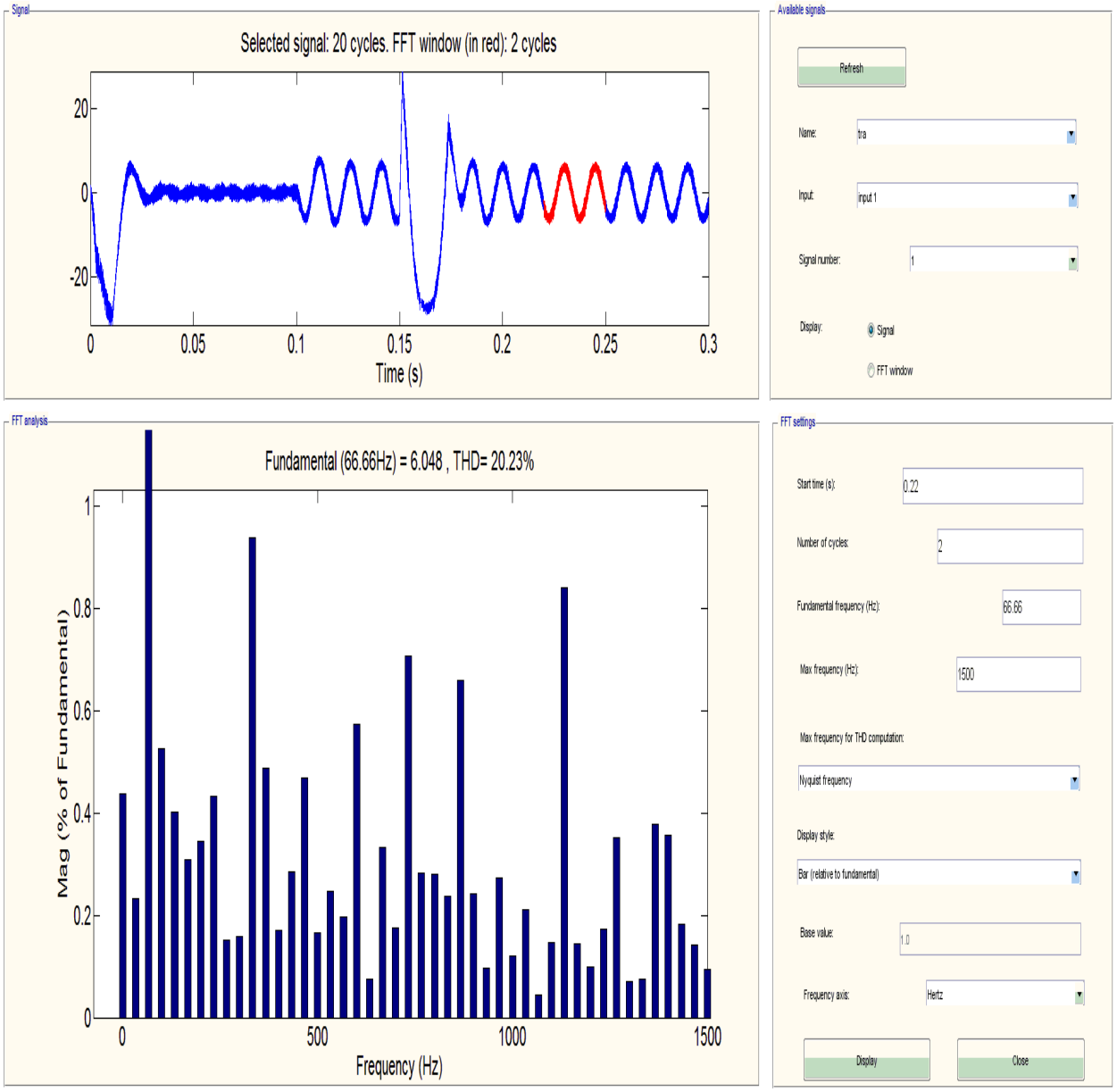

Figure C.1. Analysis of the spectral harmonic behavior of the stator current isa (DTC).

C.2.2 Improved DTC by using SVM technique

THD of the stator current

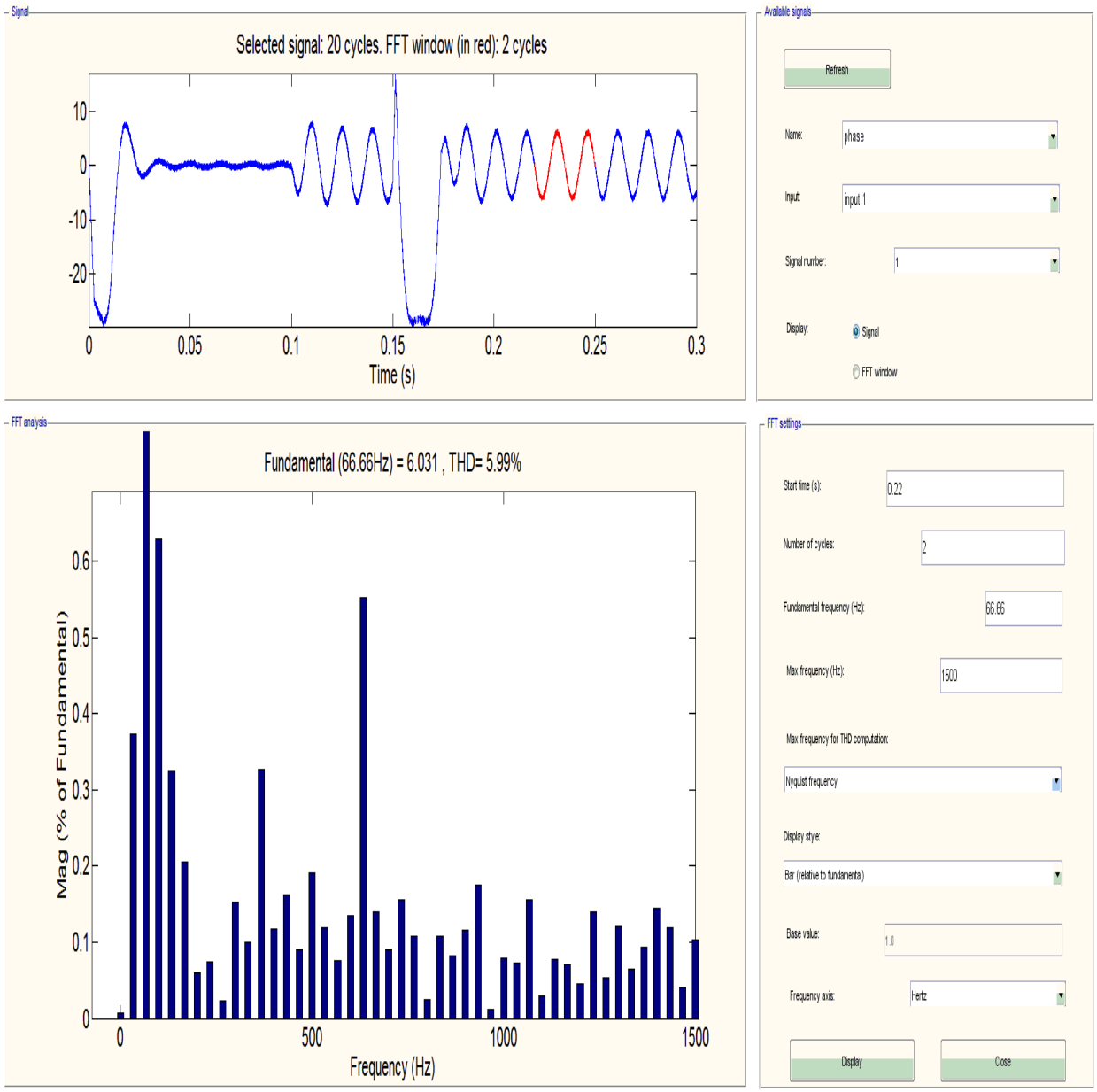

Figure C.2. Analysis of the spectral harmonic behavior of the stator current isa (DTC-SVM).

C.2.3 Conventional Predictive Current Control (PCC)

THD of the stator current

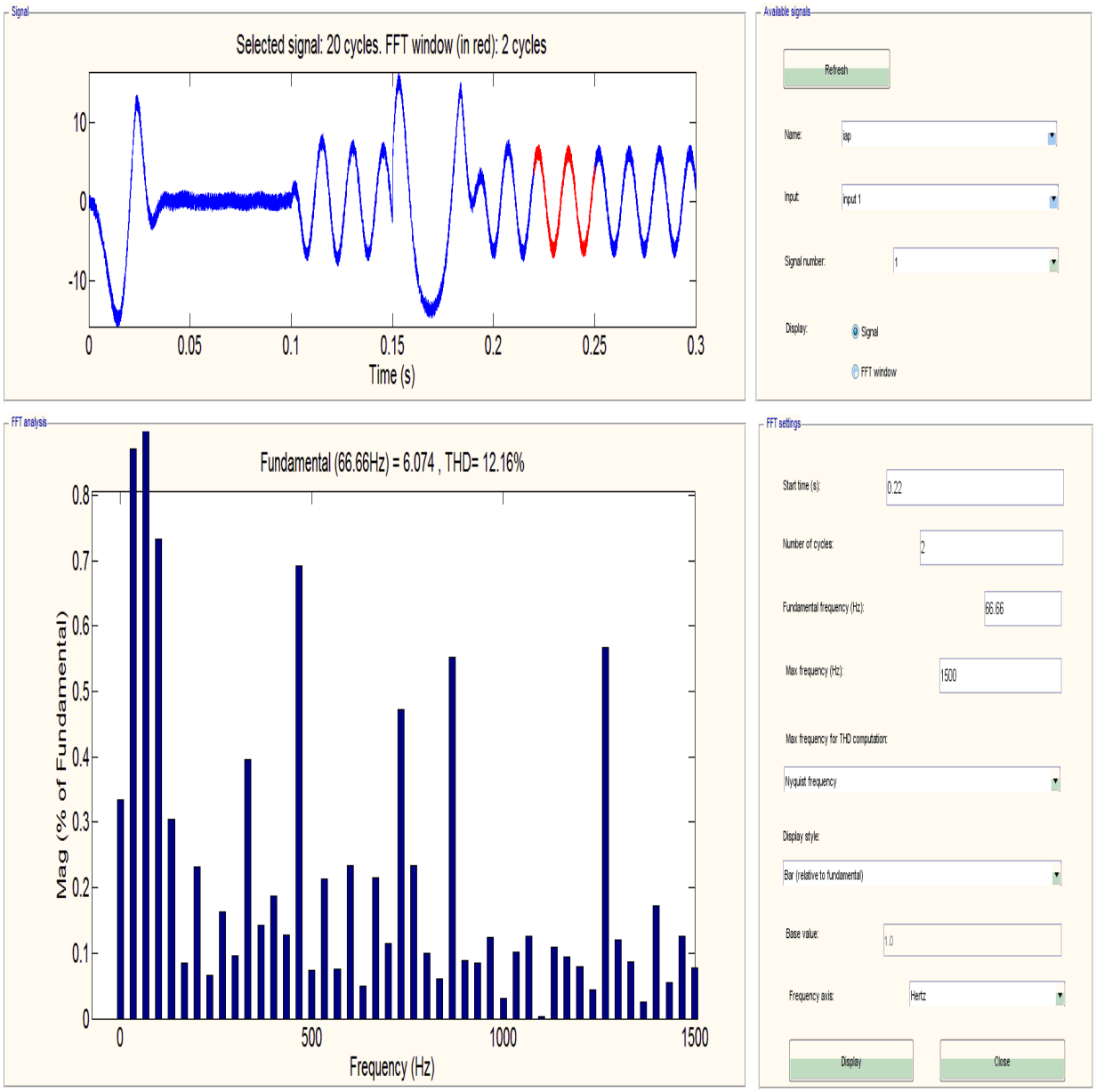

Figure C.3. Analysis of the spectral harmonic behavior of the stator current isa (C-PCC).

C.2.4 Conventional Model Predictive Direct Torque Control (MPDTC)

THD of the stator current

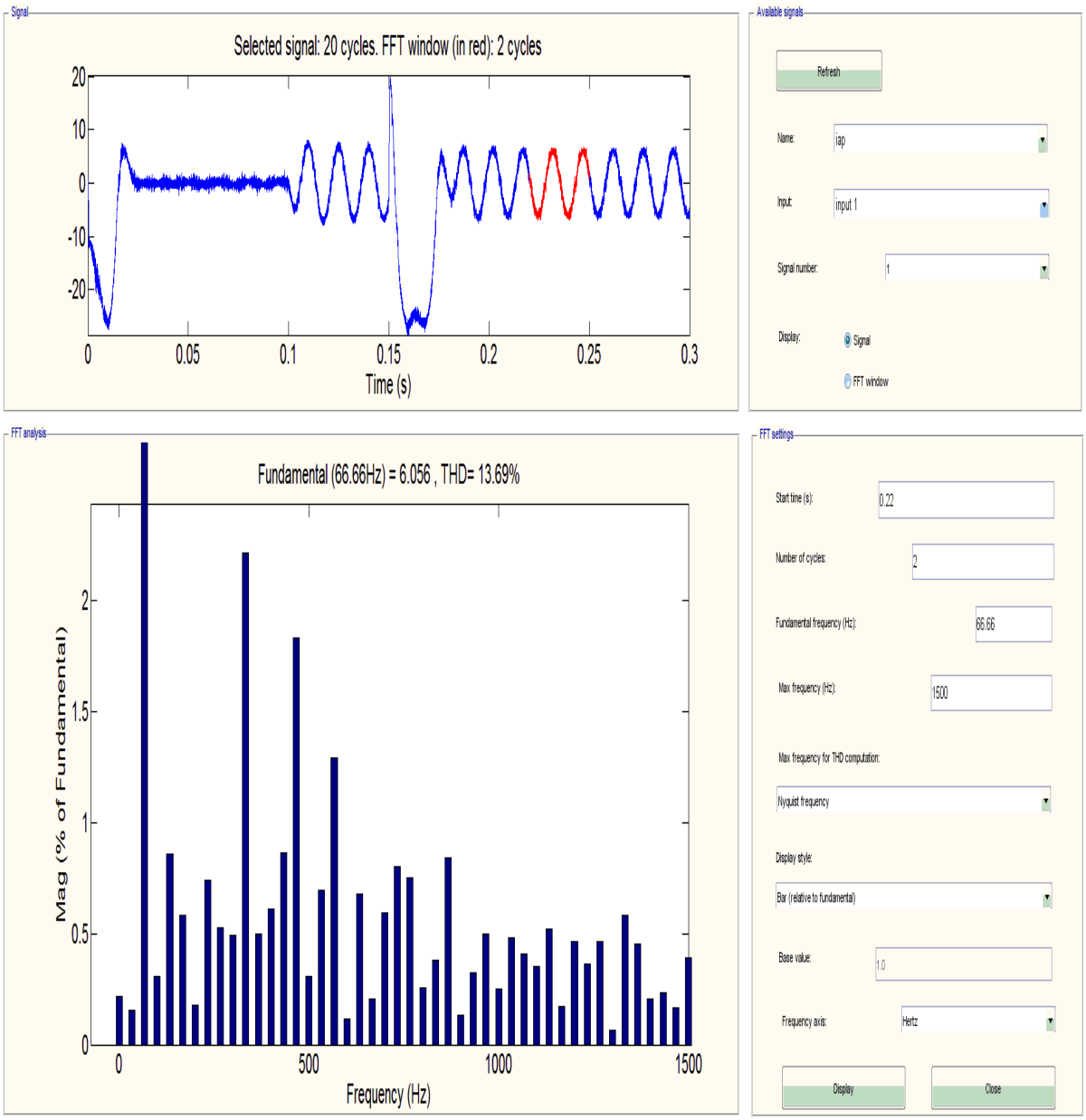

Figure C.4. Analysis of the spectral harmonic behavior of the stator current isa (C-MPDTC) $\lambda = 600$

.

C.2.5 Conventional Predictive Torque Control with external noise applied to the measured currents

THD of the stator current

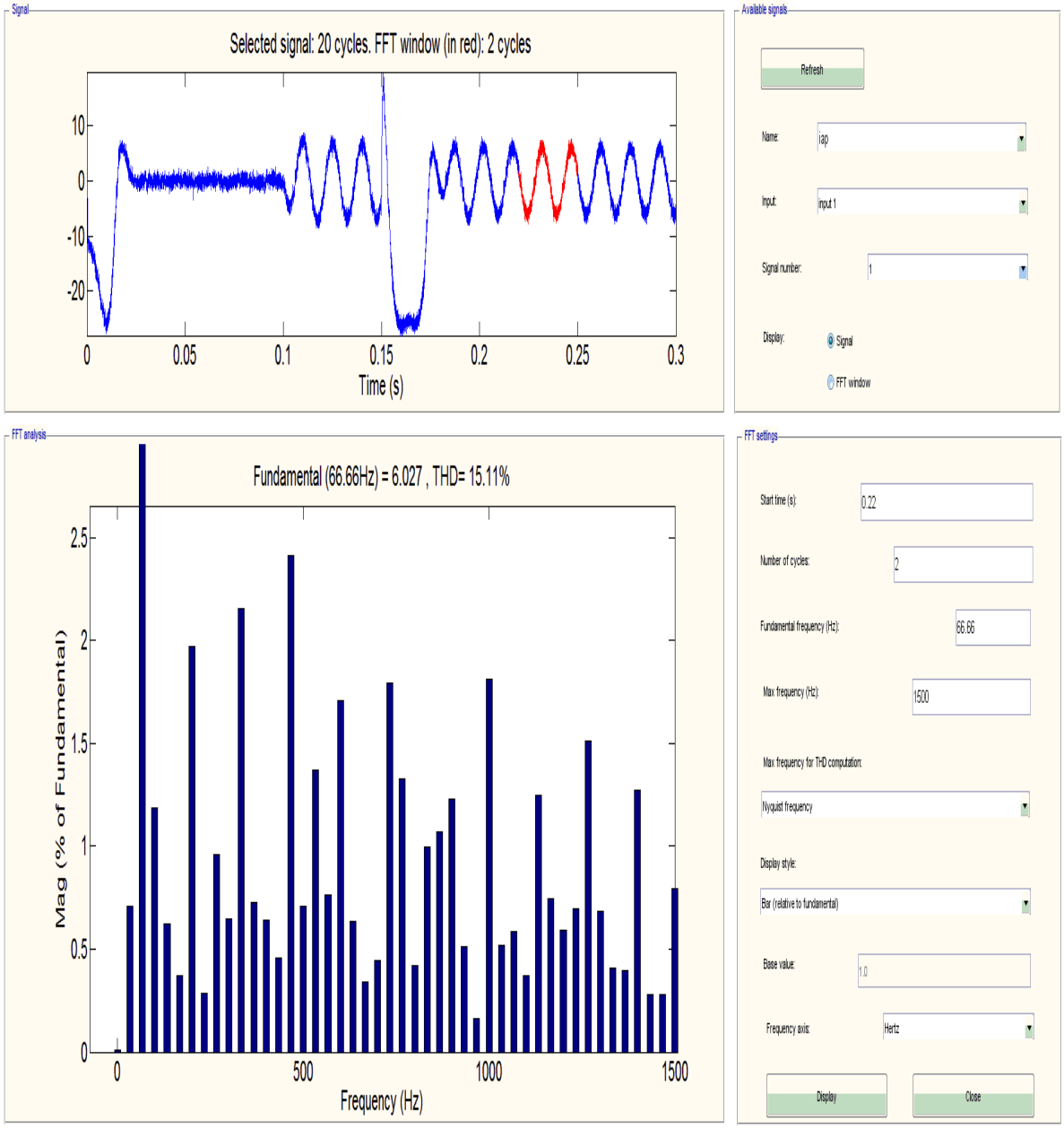

Figure C.5. Analysis of the spectral harmonic behavior of the stator current isa (C-PTC with external noise) $\lambda = 600$

.

C.2.6 Conventional Model Predictive Direct Torque Control + External applied Noises + Optimum Weighting Factor Selection

THD of the stator current

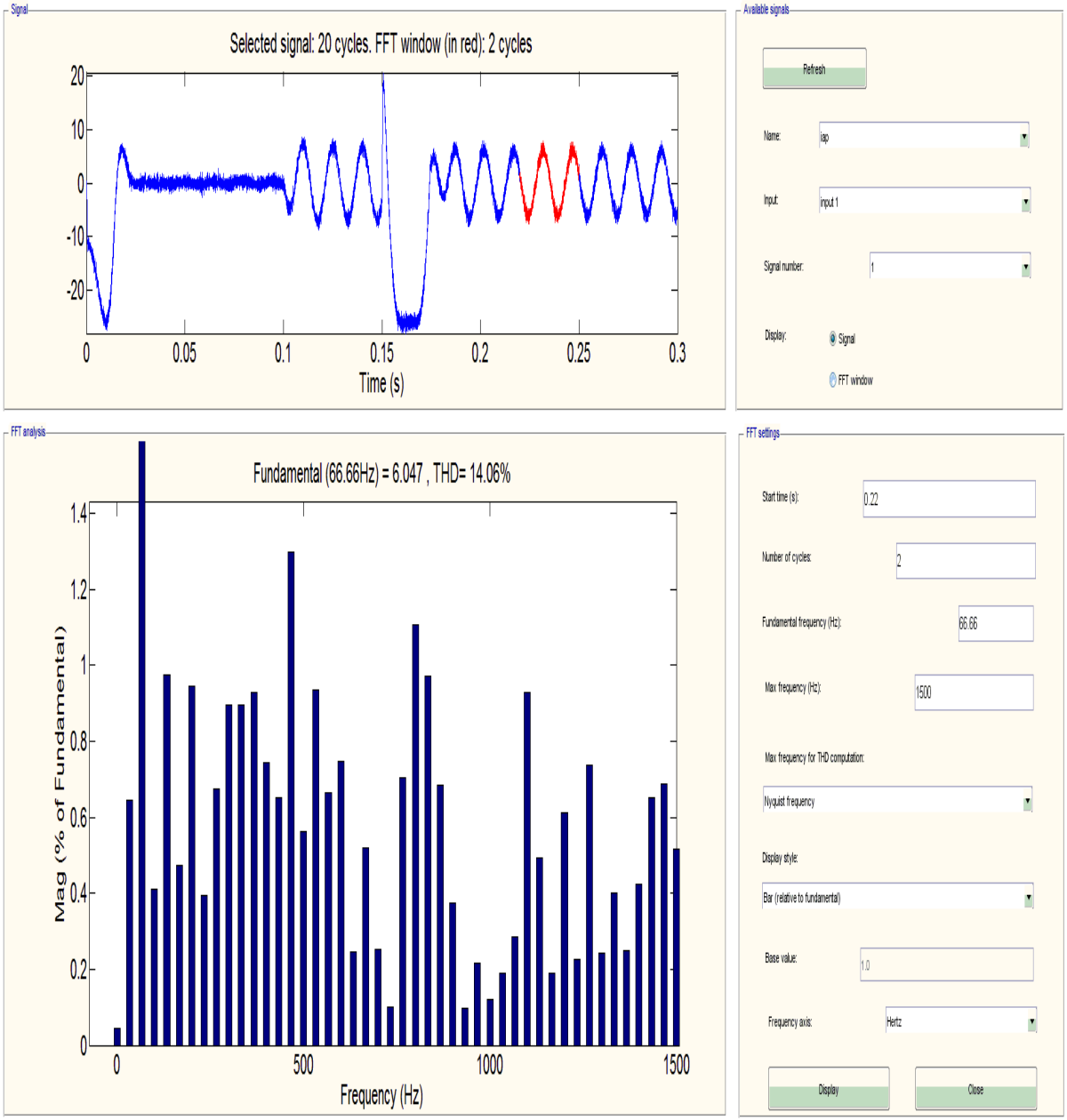

Figure C.6. Analysis of the spectral harmonic behavior of the stator current isa (C-PTC with external noise) $\lambda = 3000$

C.2.7 Improved Model Predictive Direct Torque Control (MPDTC) based on Fuzzy Logic Duty Cycle Controller and EKF Estimator + External applied Noises + Optimum Weighting Factor Selection

THD of the stator current

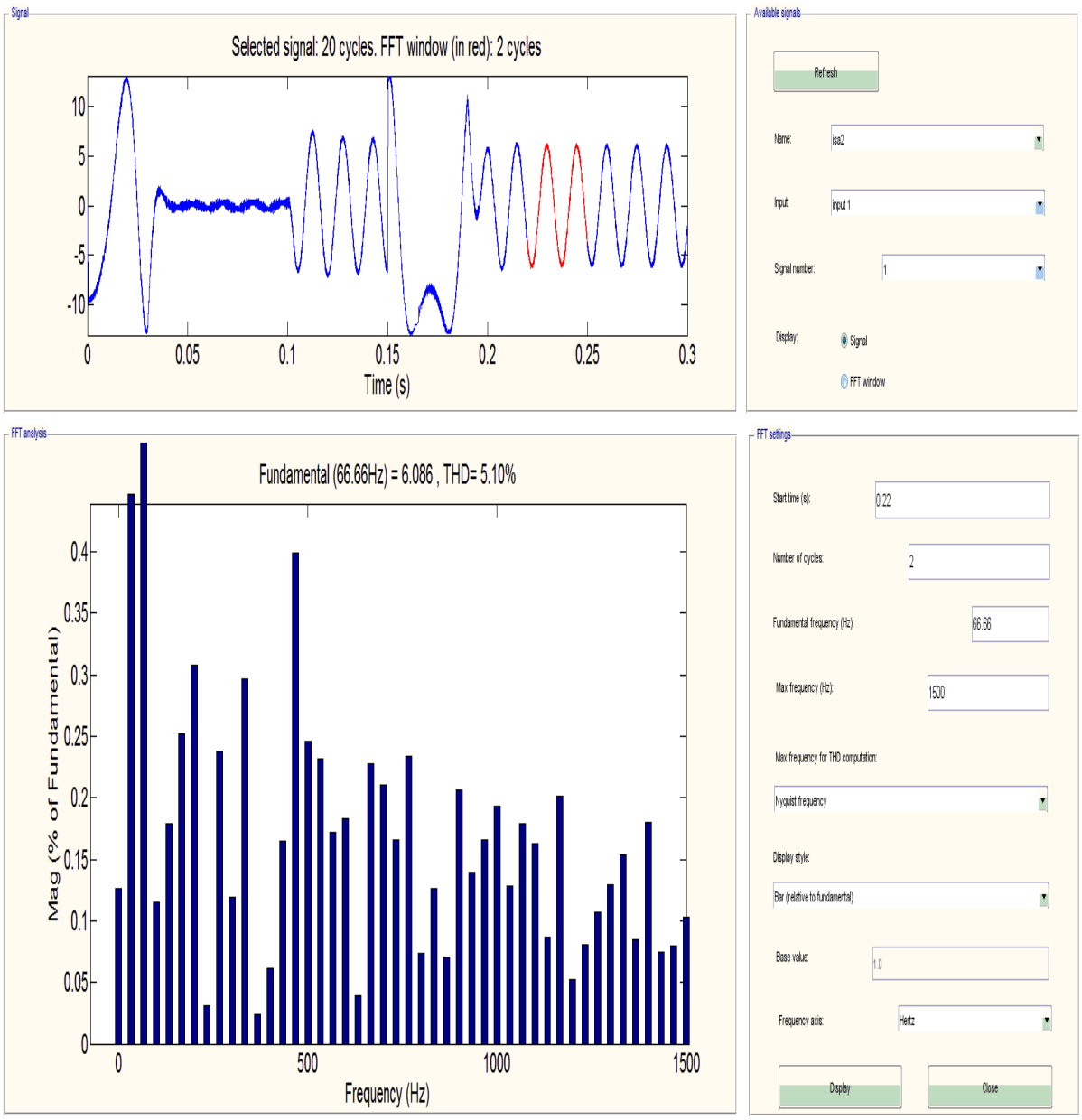

Figure C.7. Analysis of the spectral harmonic behavior of the stator current isa (fuzzy logic modulator MPDTC with external noise and optimum weighting factor selection) $\lambda = 3000$

C.2.8 Improved Predictive Torque Control (PTC) based on Supervised Neural Network Imitator

THD of the stator current

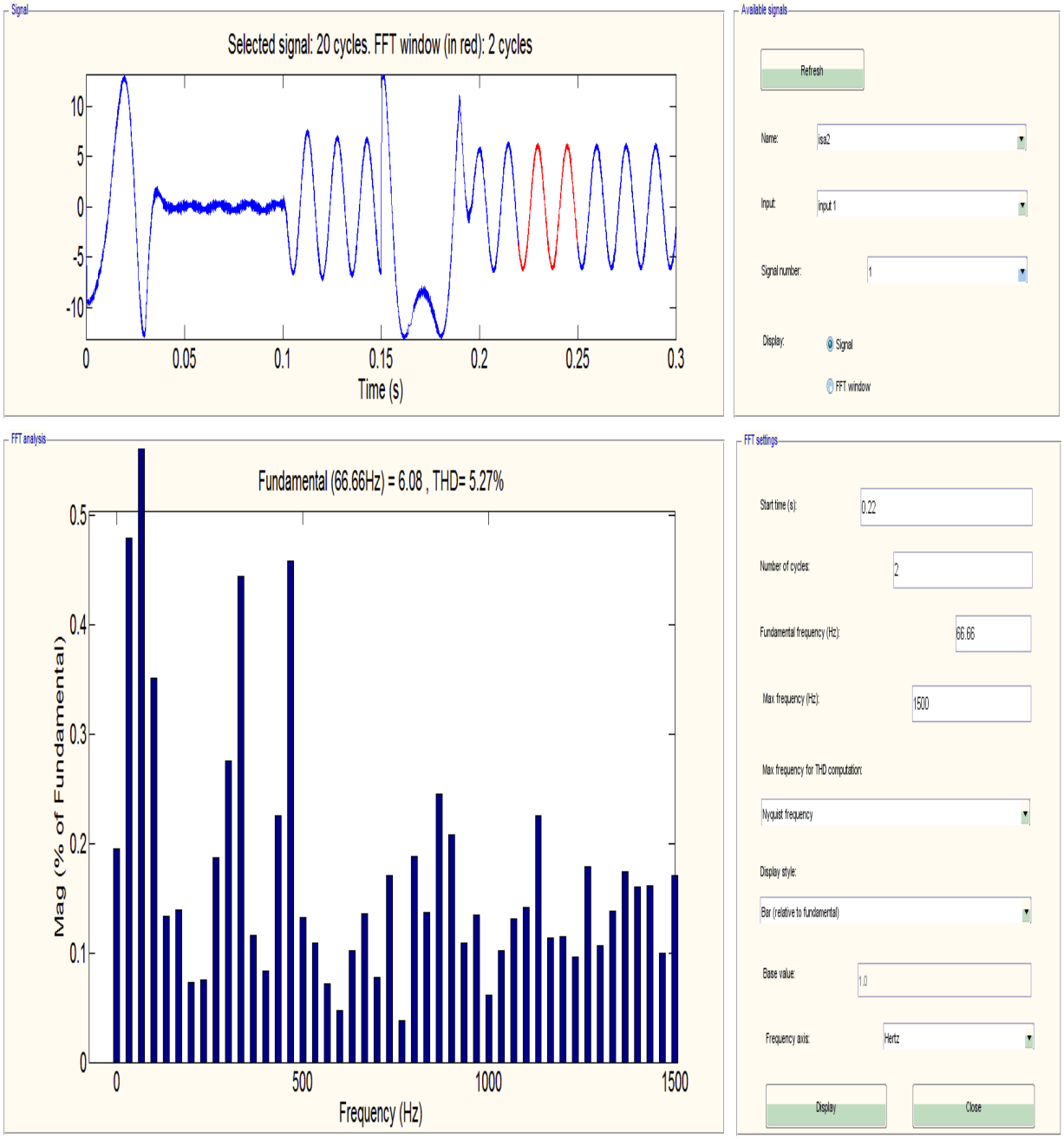

Figure C.8. Analysis of the spectral harmonic behavior of the stator current isa (Neural Network Duty Cycle MPDTC with external noise and optimum weighting factor selection) $\lambda = 3000$

References

References

[1] Shimizu, Y., Morimoto, S., Sanada, M., & Inoue, Y. (2017). Infuence of permanent magnet properties and arrangement on performance of IPMSMs for automotive applications. IEEJ Journal of Industry Applications, 6(6), 401–408.

[2] Dang, D. Q., Vu, N. T. T., Choi, H. H., & Jung, J. W. (2015). Speed control system design and experimentation for interior PMSM drives. International Journal of Electronics, 102(5), 864–885.

[3] Song, Q., Li, Y., & Jia, C. (2018). A novel direct torque control method based on asymmetric boundary layer sliding mode control for PMSM. Energies, 11(3), 657.

[4] Mesloub, H., Boumaaraf, R., Benchouia, M. T., Goléa, A., Goléa, N., & Srairi, K. (2018). Comparative study of conventional DTC and DTC_SVM based control of PMSM motor—Simulation and experimental results. Mathematics and Computers in Simulation, 63, 321–333.

[5] Mesloub, H. (2017). Commande DTC Prédictive D'une Machine Synchrone à Aimants Permanents (Doctoral dissertation, UNIVERSITE MOHAMED KHIDER BISKRA).

[6] Liu, X., Zhang, G., Mei, L., & Wang, D. (2016). Speed estimation with parameters identifcation of PMSM based on MRAS. Journal of Control, Automation and Electrical Systems, 27(5), 527–534.

[7] Merzoug, M. S., & Naceri, F. (2008). Comparison of field-oriented control and direct torque control for permanent magnet synchronous motor (PMSM). World Academy of Science, Engineering and Technology, 45, 299-304.

[8] Rahman, M. F., Zhong, L., Haque, M. E., & Rahman, M. A. (2003). A direct torque-controlled interior permanent-magnet synchronous motor drive without a speed sensor. IEEE Transactions on Energy Conversion, 18(1), 17-22.

[9] Štulrajter, M., Hrabovcova, V., & Franko, M. (2007). Permanent magnets synchronous motor control theory. Journal of electrical engineering, 58(2), 79-84.

[10] Benamor, A., Benchouia, M. T., Srairi, K., & Benbouzid, M. E. H. (2019). A novel rooted tree optimization apply in the high order sliding mode control using super-twisting algorithm based on DTC scheme for DFIG. International Journal of Electrical Power and Energy Systems, 108, 293–302.

[11] Song, Q., Li, Y., & Jia, C. (2018). A novel direct torque control method based on asymmetric boundary layer sliding mode control for PMSM. Energies, 11(3), 657.

[12] Swierczynski, D., & Kazmierkowski, M. P. (2002, November). Direct torque control of permanent magnet synchronous motor (PMSM) using space vector modulation (DTC-SVM)-simulation and experimental results. In IEEE 2002 28th Annual Conference of the Industrial Electronics Society. IECON 02 (Vol. 1, pp. 751-755). IEEE.

[13] Lascu, C., Boldea, I., & Blaabjerg, F. (2000). A modified direct torque control for induction motor sensorless drive. IEEE Transactions on industry applications, 36(1), 122-130.

[14] Ayrir, W., Ourahou, M., El Hassouni, B., & Haddi, A. (2020). Direct torque control improvement of a variable speed DFIG based on a fuzzy inference system. Mathematics and Computers in Simulation, 167, 308-324.

[15] Zhou, J., & Wang, Y. (2002). Adaptive backstepping speed controller design for a permanent magnet synchronous motor. IEE Proceedings-Electric Power Applications, 149(2), 165-172.

[16] Bogani, T., Lidozzi, A., Solero, L., & Di Napoli, A. (2005, May). Synergetic control of PMSM drives for high dynamic applications. In IEEE International Conference on Electric Machines and Drives, 2005. (pp. 710-717). IEEE.

[17] Zhang, X., Sun, L., Zhao, K., & Sun, L. (2012). Nonlinear speed control for PMSM system using sliding-mode control and disturbance compensation techniques. IEEE Transactions on Power Electronics, 28(3), 1358-1365.

[18] Preindl, M., & Bolognani, S. (2012). Model predictive direct speed control with finite control set of PMSM drive systems. IEEE Transactions on Power Electronics, 28(2), 1007-1015.

[19] Vazquez, S., Rodriguez, J., Rivera, M., Franquelo, L. G., & Norambuena, M. (2016). Model predictive control for power converters and drives: Advances and trends. IEEE Transactions on Industrial Electronics, 64(2), 935–947.

[20] Rodriguez, J., Kazmierkowski, M. P., Espinoza, J. R., Zanchetta, P., Abu-Rub, H., Young, H. A., et al. (2012). State of the art of fnite control set model predictive control in power electronics. IEEE Transactions on Industrial Informatics, 9(2), 1003–1016.

[21] Hu, J., & Cheng, K. W. E. (2017). Predictive control of power electronics converters in renewable energy systems. Energies, 10(4), 515.

[22] Kamat, S., & Junnuri, R. K. (2016, July). Model Predictive Control approaches for permanent magnet synchronous motor in virtual environment. In 2016 IEEE 1st International Conference on Power Electronics, Intelligent Control and Energy Systems (ICPEICES) (pp. 1-6). IEEE.

[23] Habibullah, M., Lu, D. D. C., Xiao, D., & Rahman, M. F. (2016). A simplifed fnite-state predictive direct torque control for induction motor drive. IEEE Transactions on Industrial Electronics, 63(6), 3964–3975.

[24] Kakosimos, P., & Abu-Rub, H. (2017). Predictive speed control with short prediction horizon for permanent magnet synchronous motor drives. IEEE Transactions on Power Electronics, 33(3), 2740–2750.

[25] Norambuena, M., Rodriguez, J., Zhang, Z., Wang, F., Garcia, C., & Kennel, R. (2018). A very simple strategy for high-quality performance of ac machines using model predictive control. IEEE Transactions on Power Electronics, 34(1), 794–800.

[26] Ban, F., Lian, G., Zhang, J., Chen, B., & Gu, G. (2019). Study on a novel predictive torque control strategy based on the fnite control set for PMSM. IEEE Transactions on Applied Superconductivity, 29(2), 1–6.

[27] Xu, Y., Shi, T., Yan, Y., & Gu, X. (2019). Dual-vector predictive torque control of permanent magnet synchronous motors based on a candidate vector table. Energies, 12(1), 163.

[28] Rodriguez, J., Kazmierkowski, M. P., Espinoza, J. R., Zanchetta, P., Abu-Rub, H., Young, H. A., & Rojas, C. A. (2012). State of the art of finite control set model predictive control in power electronics. IEEE Transactions on Industrial Informatics, 9(2), 1003-1016.

[29] Sandre-Hernandez, O., de Jesus Rangel-Magdaleno, J., & MoralesCaporal, R. (2019). Modifed model predictive torque control for a PMSM-drive with torque ripple minimisation. IET Power Electronics, 12(5), 1033–1042.

[30] Benhamida, I., Ameur, A., Kouzi, K., & Gaoui, B. (2019). Torque Ripple Minimization in Predictive Torque Control Method of PMSM Drive Using Adaptive Fuzzy Logic Modulator and EKF Estimator. Journal of Control, Automation and Electrical Systems, 30(6), 1007-1018.

[31] Miranda, H., Cortés, P., Yuz, J. I., & Rodríguez, J. (2009). Predictive torque control of induction machines based on state-space models. IEEE Transactions on Industrial Electronics, 56(6), 1916-1924.

[32] Xie, W., Wang, X., Wang, F., Xu, W., Kennel, R. M., Gerling, D., & Lorenz, R. D. (2015). Finite-control-set model predictive torque control with a deadbeat solution for PMSM drives. IEEE Transactions on Industrial Electronics, 62(9), 5402-5410.

[33] Wang, Y., Wang, X., Xie, W., Wang, F., Dou, M., Kennel, R. M., ... & Gerling, D. (2017). Deadbeat model-predictive torque control with discrete space-vector modulation for PMSM drives. IEEE Transactions on Industrial Electronics, 64(5), 3537-3547.

[34] Daouda, M., Lin, C. L., Lee, C. S., Yang, C. C., & Chen, C. A. (2017). Model predictive control of sensorless hybrid stepper motors in auxiliary adjuster for stereotactic frame fixation. Mechatronics, 47, 160-167.

[35] Ilzhöfer, A., Houska, B., & Diehl, M. (2007). Nonlinear MPC of kites under varying wind conditions for a new class of large-scale wind power generators. International Journal of Robust and Nonlinear Control: IFAC-Affiliated Journal, 17(17), 1590-1599.

[36] Babqi, A. J., & Etemadi, A. H. (2017). MPC-based microgrid control with supplementary fault current limitation and smooth transition mechanisms. IET Generation, Transmission & Distribution, 11(9), 2164-2172.

[37] Townsend, C. D., Summers, T. J., Vodden, J., Watson, A. J., Betz, R. E., & Clare, J. C. (2012). Optimization of switching losses and capacitor voltage ripple using model predictive control of a cascaded H-bridge multilevel StatCom. IEEE Transactions on Power Electronics, 28(7), 3077-3087.

[38] Cortés, P., Kouro, S., La Rocca, B., Vargas, R., Rodríguez, J., León, J. I., ... & Franquelo, L. G. (2009, February). Guidelines for weighting factors design in model predictive control of power converters and drives. In 2009 IEEE International Conference on Industrial Technology (pp. 1-7). IEEE.

[39] Kouro, S., Cortés, P., Vargas, R., Ammann, U., & Rodríguez, J. (2008). Model predictive control—A simple and powerful method to control power converters. IEEE Transactions on industrial electronics, 56(6), 1826-1838.

[40] Wang, T., Liu, C., Lei, G., Guo, Y., & Zhu, J. (2017). Model predictive direct torque control of permanent magnet synchronous motors with extended set of voltage space vectors. IET Electric Power Applications, 11(8), 1376–1382.

[41] Berzoy, A., Rengifo, J., & Mohammed, O. (2017). Fuzzy predictive DTC of induction machines with reduced torque ripple and highperformance operation. IEEE Transactions on Power Electronics,33(3), 2580–2587.

[42] Bozorgi, A. M., Farasat, M., & Jafarishiadeh, S. (2017). Model predictive current control of surface-mounted permanent magnet synchronous motor with low torque and current ripple. IET Power Electronics, 10(10), 1120–1128.

[43] Sakunthala, S., Kiranmayi, R., & Mandadi, P. N. (2017, August). A review on artificial intelligence techniques in electrical drives: Neural networks, fuzzy logic, and genetic algorithm. In 2017 International Conference On Smart Technologies For Smart Nation (SmartTechCon) (pp. 11-16). IEEE.

[44] Bose, B. K. (2007). Neural network applications in power electronics and motor drives—An introduction and perspective. IEEE Transactions on Industrial Electronics, 54(1), 14-33.

[45] Joo, D., Cho, J. H., Woo, K., Kim, B. T., & Kim, D. K. (2011). Electromagnetic field and thermal linked analysis of interior permanent-magnet synchronous motor for agricultural electric vehicle. IEEE transactions on magnetics, 47(10), 4242-4245.

[46] Sarala, P., Kodad, S. F., & Sarvesh, B. (2016, March). Analysis of closed loop current controlled BLDC motor drive. In 2016 International Conference on Electrical, Electronics, and Optimization Techniques (ICEEOT) (pp. 1464-1468). IEEE.

[47] Burch, I., & Gilchrist, J. (2018). Survey of global activity to phase out internal combustion engine vehicles. Center of Climate Protection: Santa Rosa, CA, USA.

[48] Nanda, G., & Kar, N. C. (2006, May). A survey and comparison of characteristics of motor drives used in electric vehicles. In 2006 Canadian Conference on Electrical and Computer Engineering (pp. 811-814). IEEE.

[49] Chourasia, R. C., & Bhardwaj, D. A. (2013). Brushless Separately Excited Direct Current Motor Electric Motors: A Survey.

[50] Sakunthala, S., Kiranmayi, R., & Mandadi, P. N. (2017, August). A study on industrial motor drives: Comparison and applications of PMSM and BLDC motor drives. In 2017 International Conference on Energy, Communication, Data Analytics and Soft Computing (ICECDS) (pp. 537-540). IEEE.

[51] Tweney, R. D. (2009). Mathematical representations in science: A cognitive–historical case history. Topics in cognitive science, 1(4), 758-776.

[52] Boldea, I., & Nasar, S. A. (2002). Induction machines: An introduction. In The Induction Machine Handbook (p. 13). CRC Press.

[53] Hatakeyma, S., Yoshino, F., Tsutsui, H., & Tsuji-Iio, S. (2016). Flywheel induction motor-generator for magnet power supply in small fusion device. Review of Scientific Instruments, 87(4), 043509.

[54] Zeb, K., Ali, Z., Saleem, K., Uddin, W., Javed, M. A., & Christofides, N. (2017). Indirect field-oriented control of induction motor drive based on adaptive fuzzy logic controller. Electrical Engineering, 99(3), 803-815.

[55] Boglietti, A., & Pastorelli, M. (2008, November). Induction and synchronous reluctance motors comparison. In 2008 34th annual conference of IEEE industrial electronics (pp. 2041-2044). IEEE.

[56] Krishnan, R. (2001). Electric motor drives: modeling, analysis and control. Prentice Hall.

[57] Bose, B. K. (2002). Modern power electronics and AC drives (Vol. 123). Upper Saddle River, NJ: Prentice hall.

[58] Meier, S. (2002). Theoretical design of surface-mounted permanent magnet motors with field-weakening capability. Master, Departement of Electrical Engineering, Royal Institute of Technology Stockholm, Stockholm.

[59] Ahn, J. B., Jeong, Y. H., Kang, D. H., & Park, J. H. (2004, November). Development of high speed PMSM for distributed generation using microturbine. In 30th Annual Conference of IEEE Industrial Electronics Society, 2004. IECON 2004 (Vol. 3, pp. 2879-2882). IEEE.

[60] Bastiani, P. (2001). Stratégies de commande minimisant les pertes d'un ensemble convertisseur-machine alternative: Application à la traction électrique (Doctoral dissertation, Lyon, INSA).

[61] Łuczak, D., Nowopolski, K., Siembab, K., & Wicher, B. (2014, September). Speed calculation methods in electrical drive with non-ideal position sensor. In 2014 19th International Conference on Methods and Models in Automation and Robotics (MMAR) (pp. 726-731). IEEE.

[62] Hwang, S. H., Kim, H. J., Kim, J. M., Liu, L., & Li, H. (2010). Compensation of amplitude imbalance and imperfect quadrature in resolver signals for PMSM drives. IEEE Transactions on Industry Applications, 47(1), 134-143.

[63] Benammar, M., Ben-Brahim, L., & Alhamadi, M. A. (2005). A high precision resolver-to-DC converter. IEEE Transactions on Instrumentation and Measurement, 54(6), 2289-2296.

[64] Gächter, J., & Hirz, M. (2016). Evaluation of Rotor Position Sensor Characteristics and Impact on Control Quality of Permanent Magnet Synchronous Machines (PMSM).

[65] Resolvers, Optical Encoders and Inductive Encoders. [Online]. Available: https://www.zettlex.com/articles/resolvers-optical-encoders-and-inductiveencoders/.

[66] Perera, P. C., Blaabjerg, F., Pedersen, J. K., & Thogersen, P. (2003). A sensorless, stable V/f control method for permanent-magnet synchronous motor drives. IEEE Transactions on Industry Applications, 39(3), 783-791.

[67] Comanescu, M. (2005). Flux and speed estimation techniques for sensorless control of induction motors (Doctoral dissertation, The Ohio State University).

[68] Morimoto, S., Takeda, Y., Hatanaka, K., Tong, Y. I., & Hirasa, T. (1993). Design and control system of inverter-driven permanent magnet synchronous motors for high torque operation. IEEE transactions on industry applications, 29(6), 1150-1155.

[69] Ameur, A., & Mokrani, L. (2012). Commande sans capteur de vitesse par DTC d'un moteur synchrone à aimants permanents en utilisant des techniques intelligence artificielle (Doctoral dissertation, thèse de Doctorat, Université Batna, Algérie).

[70] Lin, C. K., Liu, T. H., & Yang, S. H. (2008). Nonlinear position controller design with input–output linearisation technique for an interior permanent magnet synchronous motor control system. IET Power Electronics, 1(1), 14-26.

[71] Ozkop, E., & Okumus, H. I. (2008, March). Direct torque control of induction motor using space vector modulation (SVM-DTC). In 2008 12th International Middle-East Power System Conference (pp. 368-372). IEEE.

[72] KI, D. S. (2002). DSP based direct torque control of permanent magnet synchronous motor (PMSM) using space vector modulation (DTC-SVM).

[73] Kumsuwan, Y., Premrudeepreechacharn, S., & Toliyat, H. A. (2008). Modified direct torque control method for induction motor drives based on amplitude and angle control of stator flux. Electric power systems research, 78(10), 1712-1718.

[74] Galvan, C. D., Pacheco, I. T., González, R. G. G., de Jesus Romero-Troncoso, R., Medina, L. C., Alcaraz, M. R., & Almaraz, J. M. (2012). Advantages and disadvantages of control theories applied in greenhouse climate control systems. Spanish Journal of Agricultural Research, (4), 926-938.

[75] Wang, F., Zhang, Z., Mei, X., Rodríguez, J., & Kennel, R. (2018). Advanced control strategies of induction machine: Field oriented control, direct torque control and model predictive control. Energies, 11(1), 120.

[76] Liu, C., & Luo, Y. (2017). Overview of advanced control strategies for electric machines. Chinese Journal of Electrical Engineering, 3(2), 53-61.

[77] Vazquez, S., Leon, J. I., Franquelo, L. G., Rodriguez, J., Young, H. A., Marquez, A., & Zanchetta, P. (2014). Model predictive control: A review of its applications in power electronics. IEEE industrial electronics magazine, 8(1), 16-31.

[78] Garcia, C. E., Prett, D. M., & Morari, M. (1989). Model predictive control: theory and practice—a survey. Automatica, 25(3), 335-348.

[79] Benbrahim, A. (2009). Commande prédictive généralisée d'une machine synchrone à aimants permanents (Doctoral dissertation, Université de Batna 2).

[80] Rodriguez, J. O. S. E., Pontt, J. O. R. G. E., Silva, C. E. S. A. R., Salgado, M., Rees, S., Ammann, U., ... & Cortés, P. (2004). Predictive control of three-phase inverter. Electronics letters, 40(9), 561-563.

[81] Ahmed, A. A., Koh, B. K., & Lee, Y. I. (2017). A comparison of finite control set and continuous control set model predictive control schemes for speed control of induction motors. IEEE Transactions on Industrial Informatics, 14(4), 1334-1346.

[82] Legg, S., & Hutter, M. (2007). A collection of definitions of intelligence. Frontiers in Artificial Intelligence and applications, 157, 17.

[83] Minker, J. (Ed.). (2012). Logic-based artificial intelligence (Vol. 597). Springer Science & Business Media.

[84] Baghli, L. (1999). Contribution à la commande de la machine asynchrone, utilisation de la logique floue, des réseaux de neurones et des algorithmes génétiques (Doctoral dissertation).

[85] Gdaim, S. (2013). Commande directe de couple d'un moteur asynchrone à base de techniques intelligentes (Doctoral dissertation).

[86] Malla, J. M. R., Sahu, M. K., & Subudhi, P. K. (2016, March). DTC-SVM of induction motor by applying two fuzzy logic controllers. In 2016 International Conference on Electrical, Electronics, and Optimization Techniques (ICEEOT) (pp. 4941-4945). IEEE.

[87] Malla, S. G. (2016, March). A review on Direct Torque Control (DTC) of induction motor: With applications of fuzzy. In 2016 International Conference on Electrical, Electronics, and Optimization Techniques (ICEEOT) (pp. 4557-4567). IEEE.

[88] Bendaha, Y., & Benyounes, M. (2015, May). Fuzzy direct torque control of induction motor with sensorless speed control using parameters machine estimation. In 2015 3rd International Conference on Control, Engineering & Information Technology (CEIT) (pp. 1-6). IEEE.

[89] Sung, G. M., Lin, W. S., & Peng, S. K. (2013, October). Reduction of torque and flux variations using fuzzy direct torque control system in motor drive. In 2013 IEEE International Conference on Systems, Man, and Cybernetics (pp. 1456-1460). IEEE.

[90] Gao, Y., Wang, J., & Qiu, X. (2011). The improvement of DTC system performance on fuzzy control. Procedia Environmental Sciences, 10, 589-594.

[91] Xu, D., Wang, B., Zhang, G., Wang, G., & Yu, Y. (2018). A review of sensorless control methods for AC motor drives. CES Transactions on electrical machines and systems, 2(1), 104-115.

[92] Zhao, Y., Wei, C., Zhang, Z., & Qiao, W. (2013). A review on position/speed sensorless control for permanent-magnet synchronous machine-based wind energy conversion systems. IEEE Journal of Emerging and Selected Topics in Power Electronics, 1(4), 203-216.

[93] Bojoi, R., Pastorelli, M., Bottomley, J., Giangrande, P., & Gerada, C. (2013, March). Sensorless control of PM motor drives—A technology status review. In 2013 IEEE Workshop on Electrical Machines Design, Control and Diagnosis (WEMDCD) (pp. 168-182). IEEE.

[94] Abdelrahem, M., Catterfeld, P., Hackl, C., & Kennel, R. (2018, June). A sliding-mode-observer for encoderless direct model predictive control of PMSGs. In PCIM Europe 2018; International Exhibition and Conference for Power Electronics, Intelligent Motion, Renewable Energy and Energy Management (pp. 1-8). VDE.

[95] Liu, X., Yu, H., Yu, J., & Zhao, L. (2018). Combined speed and current terminal sliding mode control with nonlinear disturbance observer for PMSM drive. IEEE Access, 6, 29594-29601.

[96] Ilioudis, V. C., & Margaris, N. I. (2008, June). PMSM sensorless speed estimation based on sliding mode observers. In 2008 IEEE Power Electronics Specialists Conference (pp. 2838-2843). IEEE.

[97] Gao, W., & Guo, Z. (2013). Speed sensorless control of PMSM using model reference adaptive system and RBFN. Journal of networks, 8(1), 213.

[98] Bolognani, S., Tubiana, L., & Zigliotto, M. (2003). Extended Kalman filter tuning in sensorless PMSM drives. IEEE Transactions on Industry Applications, 39(6), 1741-1747.

[99] Zhao, Y., Wei, C., Zhang, Z., & Qiao, W. (2013). A review on position/speed sensorless control for permanent-magnet synchronous machine-based wind energy conversion systems. IEEE Journal of Emerging and Selected Topics in Power Electronics, 1(4), 203-216.

[100] Kim, Y. R., Sul, S. K., & Park, M. H. (1994). Speed sensorless vector control of induction motor using extended Kalman filter. IEEE Transactions on Industry Applications, 30(5), 1225-1233.

[101] Mbukani, M. W. K., & Gule, N. (2019). Comparison of high-order and second-order sliding mode observer based estimators for speed sensorless control of rotor-tied DFIG systems. IET Power Electronics, 12(12), 3231-3241.

[102] Lin, X., Huang, W., Jiang, W., Zhao, Y., Dong, D., & Liu, S. (2019). Position sensorless direct torque control for six-phase permanent magnet synchronous motor under two-phase open circuit. IET Electric Power Applications, 13(11), 1625-1637.

[103] Comanescu, M., & Batzel, T. D. (2009, May). Reduced order observers for rotor position estimation of nonsalient PMSM. In 2009 IEEE International Electric Machines and Drives Conference (pp. 1346-1351). IEEE.

[104] Rashid, M. H. (2004). Power Electronic Circuits, Devices, and Applications. In University of West Florida. Pearson Prentice Hall.

[105] HERNANDEZ, O. S. (2017). Evaluación comparativa de estrategias de control predictivo del par para máquinas síncronas de imanes permanentes usando un FPGA.

[106] Zhang, Z., Wei, C., Qiao, W., & Qu, L. (2015). Adaptive saturation controller-based direct torque control for permanent-magnet synchronous machines. IEEE Transactions on Power Electronics, 31(10), 7112-7122.

[107] Arafa, O. M., Aziz, G. A. A., El-Sebah, M. I. A., & Mansour, A. A. (2016). Observer-based sensorless speed control of PMSM: A focus on drive's startup. Journal of Electrical Systems and Information Technology, 3(2), 181-209.

[108] Yaramasu, V., & Wu, B. (2016). Model predictive control of wind energy conversion systems. John Wiley & Sons.

[109] Justo, J. J., Mwasilu, F., Kim, E. K., Kim, J., Choi, H. H., & Jung, J. W. (2017). Fuzzy model predictive direct torque control of IPMSMs for electric vehicle applications. IEEE/ASME Transactions on Mechatronics, 22(4), 1542-1553.

[110] Elbia, Y. (2009). Commande floue optimisée d'une machine asynchrone à double alimentation et à flux orienté (Doctoral dissertation, Université de Batna 2).

[111] Goguen, J. A. (1973). LA Zadeh. Fuzzy sets. Information and control, vol. 8 (1965), pp. 338–353.-LA Zadeh. Similarity relations and fuzzy orderings. Information sciences, vol. 3 (1971), pp. 177–200. The Journal of Symbolic Logic, 38(4), 656-657.

[112] Baghli, L. (1999). Contribution à la commande de la machine asynchrone, utilisation de la logique floue, des réseaux de neurones et des algorithmes génétiques (Doctoral dissertation).

[113] BENNOUI, H. (2009). Apport de la logique floue et des réseaux de neurones pour la commande avec minimisation des pertes de la machine asynchrone (Doctoral dissertation, Université de Batna 2).

[114] Gherbi, A., & Abbad, A. (2018). Commande d'un moteur asynchrone par la logique floue adartative (Doctoral dissertation, universite de bouira).

[115] Chekroun, S. (2009). commande neuro-floue sans capteur De vitesse d'une machine asynchrone Triphasée. Mémoire magister en Électrotechnique.

[116] Diab, M. O. K. E. D. D. E. M. (2010). Contrôle Flou des Processus Biotechnologiques à Base d'Algorithmes Génétiques (Doctoral dissertation, université de Jijel).

[117] Mendel, J. M. (2001, July). On the importance of interval sets in type-2 fuzzy logic systems. In Proceedings Joint 9th IFSA World Congress and 20th NAFIPS International Conference (Cat. No. 01TH8569) (Vol. 3, pp. 1647-1652). IEEE.

[118] Ramirez, F., & Pacas, M. (2016, May). Finite Control Set Model Based Predictive Control of a PMSM with Variable Switching Frequency and Torque Ripple Optimization. In PCIM Europe 2016; International Exhibition and Conference for Power Electronics, Intelligent Motion, Renewable Energy and Energy Management (pp. 1-8). VDE.

[119] Ramirez, F., & Pacas, M. (2017, September). Enhanced control of the torque ripple in a PMSM drive with variable switching frequency. In 2017 19th European Conference on Power Electronics and Applications (EPE'17 ECCE Europe) (pp. P-1). IEEE.

[120] Zhang, Y., & Yang, H. (2014). Model predictive torque control of induction motor drives with optimal duty cycle control. IEEE Transactions on Power Electronics, 29(12), 6593-6603.

[121] Zeng, Z., Zhu, C., Jin, X., Shi, W., & Zhao, R. (2016). Hybrid space vector modulation strategy for torque ripple minimization in three-phase four-switch inverter-fed PMSM drives. IEEE Transactions on Industrial Electronics, 64(3), 2122-2134.

[122] Sudheer, H., Kodad, S. F., & Sarvesh, B. (2011). Torque ripple reduction in direct torque control of induction motor using fuzzy logic based duty ratio controller. International Journal of Electronic Engineering Research, 3(1), 1-12.

[123] Espejel-García, D., Ortíz-Anchondo, L. R., Alvarez-Herrera, C., Hernandez-López, A., Espejel-García, V. V., & Villalobos-Aragón, A. (2017). An alternative vehicle counting tool using the Kalman filter within MATLAB. Civil engineering journal, 3(11), 1029-1035.

[124] Bolognani, S., Tubiana, L., & Zigliotto, M. (2003). Extended Kalman filter tuning in sensorless PMSM drives. IEEE Transactions on Industry Applications, 39(6), 1741-1747.

[125] Mordjaoui,M.(2008).MODELISATION DES EFFETS ELECTROMAGNETIQUES «Apport de la logique floue et neuro-floue» (Doctoral dissertation, Université de Batna 2).

[126] Lin, F. J., Yu, J. C., & Tzeng, M. S. (2001). Sensorless induction spindle motor drive using fuzzy neural network speed controller. Electric Power Systems Research, 58(3), 187-196.

[127] Suetake, M., da Silva, I. N., & Goedtel, A. (2010). Embedded DSP-based compact fuzzy system and its application for induction-motor $ V/f $ speed control. IEEE Transactions on Industrial Electronics, 58(3), 750-760.

[128] Singh, B., Jain, P., Mittal, A. P., & Gupta, J. R. P. (2006, December). Neural network based DTC IM drive for electric vehicle propulsion system. In 2006 IEEE Conference on Electric and Hybrid Vehicles (pp. 1-6). IEEE.

[129] Sivasubramanian, A., & Jayanand, B. (2009). Application of neural network structure in voltage vector selection of direct torque control induction motor. International Journal of Applied Engineering Research, 4(6), 903-913.

[130] Kumar, R., Gupta, R. A., Bhangale, S. V., & Himanshu, G. (2007). Artificial neural network based direct torque control of induction motor drives.

[131] Abbou, A., & Mahmoudi, H. (2009). Performance of a sensorless speed control for induction motor using DTFC strategy and intelligent techniques. Journal of Electrical Systems, 5(3), 64-81.

[132] GHAYOULA, R. (2008). Contribution à l'Optimisation de la Synthèse des Antennes Intelligentes par les Réseaux de Neurones. Université de Tunis El Manar. Thèse de doctorat, 27.

[133] Cheynet, P. (1999). Etude de la robustesse du contrôle intelligent face aux fautes induites par les radiations (Doctoral dissertation, Institut National Polytechnique de Grenoble-INPG).

[134] Borne, P., Benrejeb, M., & Haggège, J. (2007). Les réseaux de neurones: présentation et applications (Vol. 15). Editions OPHRYS.

[135] Moody, J., & Darken, C. J. (1989). Fast learning in networks of locally-tuned processing units. Neural computation, 1(2), 281-294.

[136] Constant, L. (2000). Modélisation de dispositifs électriques par réseaux de neurones en vue de l'émulation en temps réel (Doctoral dissertation, Toulouse, INPT).

[137] Toufouti, R., Meziane, S., & Benalla, H. (1997). Direct torque control for induction motor using fuzzy logic. Power Electronics, 12(3).

[138] DJERIRI, Y. (2015). Commande directe du couple et des puissances d'une MADA associée à un système éolien par les techniques de l'intelligence artificielle (Doctoral dissertation).

[139] MERABET, Adel. Commande non linéaire à modèle prédictif pour une machine asynchrone. Université du Québec à Chicoutimi, 2007. Thèse De Doctorat. Université Du Québec.

[140] Sobczuk, D. (1999). Application of ANN for control of PWM inverter fed induction motor drives (Doctoral dissertation, The Institute of Control and Industrial Electronics).

[141] Bose, B. K. (2010). Power electronics and motor drives: advances and trends. Elsevier.

[142] Tsagkaris, K., Katidiotis, A., & Demestichas, P. (2008). Neural network-based learning schemes for cognitive radio systems. Computer Communications, 31(14), 3394-3404.

[143] Chaiba, A. (2010). Commande de la machine asynchrone à double alimentation par des techniques de l'intelligence artificielle (Doctoral dissertation, Université de Batna 2).

[144] Jain, A. K., Mao, J., & Mohiuddin, K. M. (1996). Artificial neural networks: A tutorial. Computer, 29(3), 31-44.

[145] Dreyfus, G., Martinez, J. M., Samuelides, M., Gordon, M. B., Badran, F., Thiria, S., & Hérault, L. (2002). Réseaux de neurones-Méthodologie et applications (No. BOOK). Eyrolles.

[146] Moody, J., & Darken, C. J. (1989). Fast learning in networks of locally-tuned processing units. Neural computation, 1(2), 281-294.

[147] RASMUS, Antti, BERGLUND, Mathias, HONKALA, Mikko, et al.Semi-supervised learning with ladder networks. In : Advances in neural information processing systems. 2015. p. 3546-3554.

[148] Cesar, S. "Neural Network Learning by the Levenberg-Marquardt Algorithm with Bayesian Regularization (part 2)", November 18, 2009, http://crsouza.com/2009/11/18.

[149] Nait Seghir, A. (2007). Contribution à la commande adaptative et neuronale d'une machine synchrone à aimants permanents (Doctoral dissertation).